Advanced Engineering Forum *Online: 2013-06-27*
ISSN: 2234-991X, Vols. 8-9, pp 379-386
doi:10.4028/www.scientific.net/AEF.8-9.379

Innovative biocomposite derived from waste materials with applications in electrical domain

Sebastian Teodor ARADOAEI[1, a], Romeo Cristian CIOBANU[1, b], DARIE Raluca Nicoleta[2,c] and MOSNEAGU Mihaela[3,d]

[1]Technical University of Iasi, Department of Electrical Measurements and Materials, Blvd. D. Mangeron 53, 70050 Iasi, Romania

[2]Romanian Academy, “Petru Poni” Institute of Macromolecular Chemistry, 41 A Gr. Ghica Voda Alley, 700487, Iasi, Romania

[3]SC Intelectro Iasi SRL, 3 Iancu Bacalu Street, 700470 Iasi, Romania

[a]asteor@yahoo.com,

Keywords: polypropylene, organic materials, compatibilizing agents, electric insulators

Abstract. The article highlights the possibility of producing biocomposite material from plastic (e.g. polypropylene) and natural organic materials used as fillers (eggplant flour) which have applications in electrical domain. The right amount of material used as filler is evaluated using mechanical tests and dielectric spectroscopy in order to obtain an optimal structure biodegradable, making it suitable as a viable technical solution to partially replace electrical enclosures or different insulators.

Introduction

Continued growth of electrical applications requires materials with increasingly high performance: lighter, more flexible, more resistant to mechanical and thermal stress, with high or low electric conductivity, with greater resistance to environmental actions, with reduced power consumption (both for manufacturing as well for processing and use), with higher reliability, more sustainable and certainly cheaper. These types of materials were developed in short time, in many classes and the materials like composites and nanocomposite have recorded a significant advance, with practical applications in all fields. Obtaining biodegradable materials is an ever-present requirement in the rules on production of new material and especially environmental protection. A method of recovering plastics is by processing of mixtures using natural polymers for reinforcement, namely the production of composite materials with special properties [1]. Use of these materials in electrical and electronics is fully accepted, but their properties are not always appropriate for some applications.

Considering that demand for material in the wood industry is growing and forest resources are continuously decreasing, has led researchers to study and other non-wood lignocellulosic materials. The agricultural sector is the largest provider of lignocellulosic material as waste from cereals processing. The most frequently referred alternative non-wood materials are cereal straws such as rice and wheat straw flax and hemp and reed [2]. The criteria for the evaluation of materials, include general categories of resources, performance and pollution. The resources required for a material may be consumed in extraction, production, and use or disposal process. The performance refers to the energy and resources that can save or squander its use.

The principle of reducing hazardous substances, along with protecting the natural resources by developing alternatives to traditional materials or processes led to new concepts in the design, manufacture and application of such materials by offering an environmental advantage [3]. The interdisciplinarity and complexity of solution is given by designing biocomposite materials used in electrical engineering, obtained from virgin plastic (e.g. polypropylene) and natural organic materials used as fillers (eggplant flour). In different contexts, can be introduced vegetable oils, waxes or additives, or agents of consolidation, homogenization or binding, in order to obtain a biodegradable composite, which makes it suitable as a viable technical solution to replace partially housings of electrical equipments, transformers board in construction of the transformers and electric machineries or a different types of insulators.

Dielectric spectroscopy has proven a powerful tool to investigate in details the dynamical processes of composites materials. The dielectric properties of composite material are affected by several factors, e.g. molecular chain arrangement, amorphous and crystalline phase fraction, molecular weight distribution and temperature. This knowledge is important for the development of new materials and also to understand the eventual degradability of those [4].

Experimental part

Materials. Polypropylene and eggplant stalk residues were used as thermoplastic matrix and organic filler, respectively in order to obtain a homogeneous blend. The thermoplastic polymer polypropylene (PP), used as matrix material, was used as received. It had specific gravity of 0.90–0.91, melting temperatures of 165–171 C and crystallinity of 82%. Maleic anhydride grafted polypropylene (MAPP) was utilized as coupling agent. Eggplant stalk residues were granulated into 60-100 mesh size (149-250μm) flours using Wiley mill. Natural beeswax yellow with temperature melt 63°C was used as is.

Processing. The experimental design of the study is presented in Table 1. During the manufacturing process, depending on the formulation polypropylene (PP), eggplant flour (EF), maleic anhydride grafted polypropylene (MAPP), and wax were mixed in a high intensity mixer to produce homogeneous blend. Then this blend was compounded in a laboratory scale single screw extruder at 40 rpm screw speed and in the temperature range of 170, 180, 185, 190, 200 °C. Extruded samples were collected, cooled and granulated into pellets. Finally, pellets were compression molded in the hot press for 5 minutes at 175°C and cooled for 20 minutes. Panels with thickness of 1 mm and relative homogeneous were produced. See processing steps in figure 1.

Fig.1 Processing steps.
Extruder with single screw (left); Wiley mill (center); Hot press (right)

Table 1. Experimental design used in the study.

Sample	Polypropylene (PP) (%)	Eggplant flour (EPF) (%)	MAPP (%)	Wax (%)
PP	100	0	0	0
88PP/7EF/5MAPP+Wax	87,5	7,5	3	2
80PP/15EF/5MAPP+Wax	80	15	3	2
65PP/30EF/5MAPP+Wax	65	30	3	2

Methods. Mechanical properties like tensile strength, tensile modulus, elongation at break, flexural strength, flexural modulus, impact strength, were carried out with testing machine Zwick Roell z010 and pendulum impact tester Zwick Roell HIT5.5P according to following standards ISO 527-4, ISO 178, ISO 179-1. Broadband dielectric spectroscopy analysis were performed using a

Novocontrol GmbH Concept 80 Broadband Dielectric Spectrometer with an Alpha A analyzer over the frequency range of 10^{-2} Hz to 10^{7} Hz in combination with a Novocontrol Quatro temperature system providing control of the sample temperature with high accuracy, figure 2. The samples were sandwiched between two 20 mm gold plated electrodes and tested within ZGS Alpha Active Sample Cell. The test temperatures were 20°C [5].

Fig. 2 Broadband dielectric analyzer Concept 80 Novocontrol GmbH,

Results and discussion

Tensile properties. The mechanical properties for studied blends are presented in Table 2. In terms of technical difficulties, the thermodynamic mixing of the components may not lead to obtaining truly homogeneous products. A large amount of wax or vegetable oil is not desired because this can reduce the adhesion between fibers and polymer matrix. This can be a problem because it forms a biphasic structure, interactions between the two phases, at the interface, determining the properties of new material. In this case the situation at the interface between the two phases is very important. A high interfacial tension and poor adhesion between phases, associated with high viscosity, specific to macromolecular compounds leads to difficulties in obtaining the desired degree of dispersion, instability in machining operations, phase separation during subsequent processing and use. Poor adhesion between phases leads, on the one hand, to a poor mechanical behaviour and on the other hand makes it impossible to achieve a structured with homogeneous morphologies [6].

Table 2. Mechanical properties for studied blends.

Sample	Tensile Strength (MPa)	Tensile Modulus (MPa)	Elongation at Break (%)	Flexural Strength (MPa)	Flexural Modulus (MPa)	Impact Strength (J/m)
PP	13,83	512,15	3,01	28,79	1567	15,94
88PP/7EF/5MAPP +Wax	10,52	557,02	2,48	14,32	1022,33	14,38
80PP/15EF/5MAPP +Wax	10,74	609,027	2,2	13,03	1110,47	12,41
65PP/30EF/5MAPP +Wax	10,12	629,74	2,15	15,93	1346,25	12,19

The mechanical characteristics (figures) show that for materials with a minimum of added both elongation at break, figure 3 and impact strength, figure 4 has the highest values and decrease with increasing percentage of filler material. This is because by adding eggplant flour composites become more rigid and affinity in amorphous state decreases, even if they entered compatibilizing additives and adhesives. Flexural strength is halved for all mixtures studied because they have lost elasticity through EF mixing, figure 5. A decrease is observed for tensile strength which confirms, once again, brittle behavior due to poor adhesion between PP and EF natural material break, figure 6.

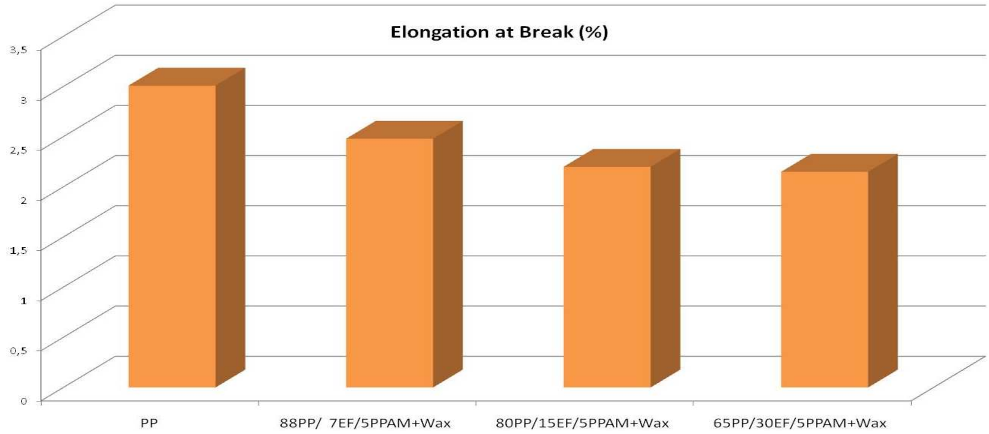

Fig. 3. Elongation at break for studied blends

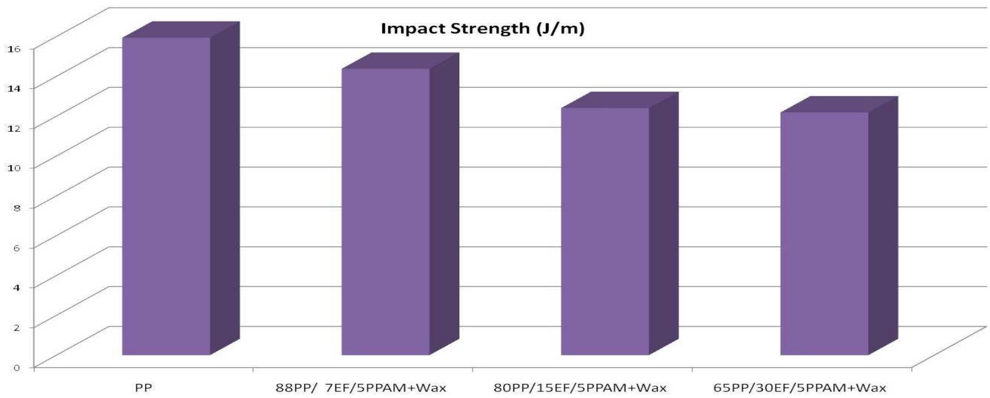

Fig. 4. Impact strength for studied blends

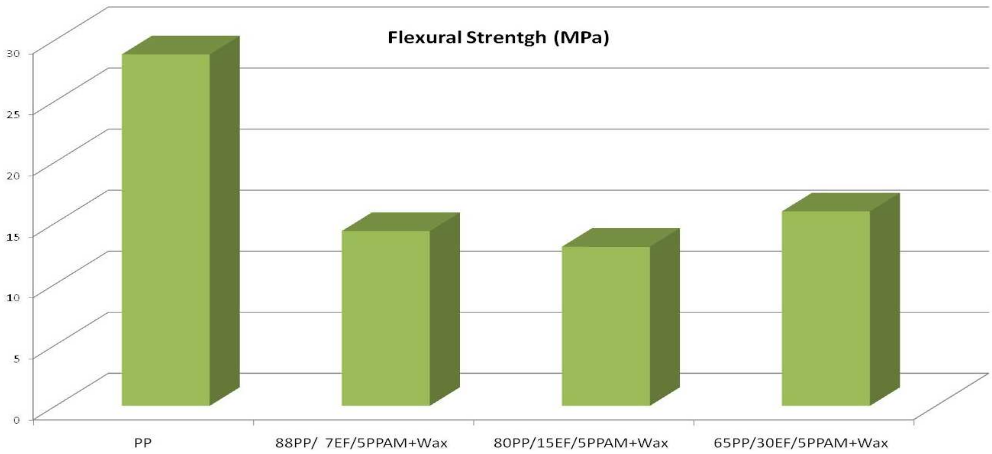

Fig. 5. Flexural strength for studied blends

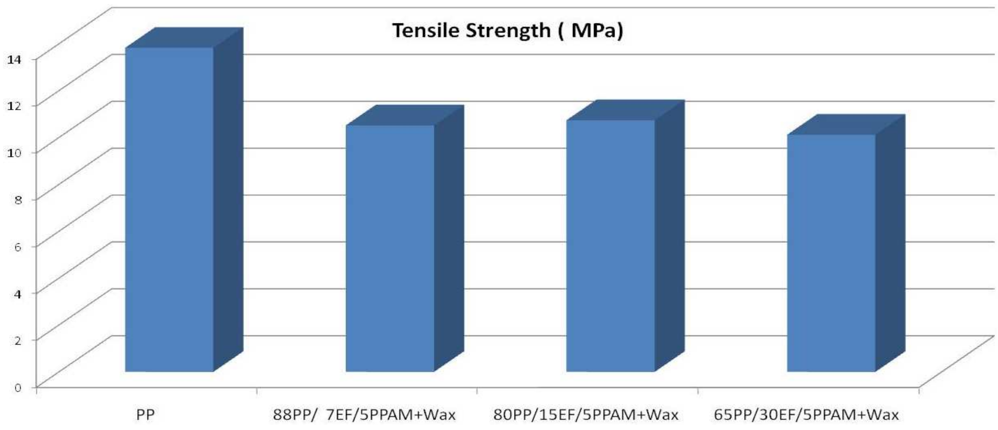

Fig. 6. Tensile strength for studied blends

Broadband Dielectric spectroscopy analysis. Dielectric characteristics analysis indicates that the composite material with 65PP/30%EF/5MAPP + Wax has remarkably high dielectric constant, being at industrial frequencies with 100% higher than the compound with 88PP/ 7EF/5MAPP+Wax. As expected, the highest values, both for dielectric constant and loss are recorded if the maximum addition of eggplant flour, figure 7.

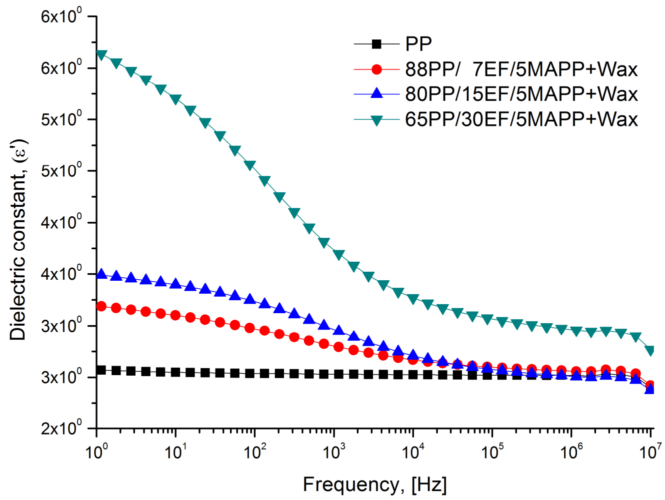

Fig. 7. Variation of dielectric constant (ε’) function of frequency for studied blends

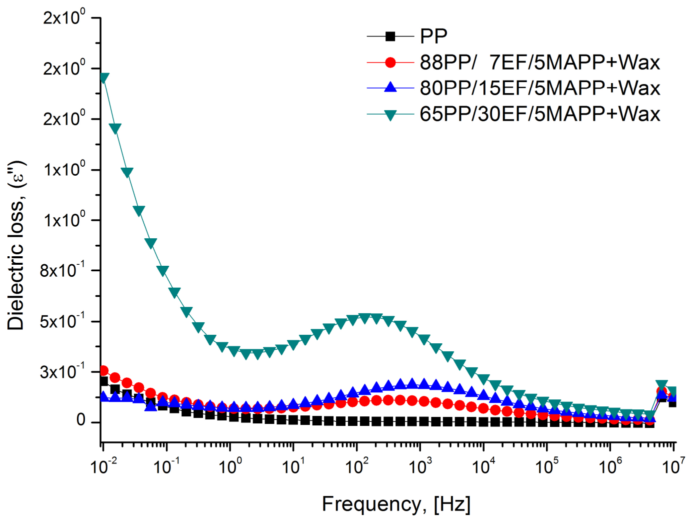

Fig. 8. Variation of dielectric loss (ε") function of frequency for studied blends

Specific dielectric losses due to polar character of eggplant have a high value at 1 kHz due to increasing percentage of eggplant flour. A novel aspect is that the hygroscopicity of the material which makes flour with increasing percentage of eggplant to identify significant losses by conduction phenomena, figure 8.

The tan δ curves follow the shape of the correspondent loss factor for this biocomposite. Significant increase of tan δ was found especially for the frequency 1 kHz. For 65PP/30%EF/5MAPP + Wax, there is a sudden jump in tan δ just like in the case of loss factor, figure 9.

Besides permitivity, loss factor and tangent (tan δ), real conductivity of the dielectric materials was also analyzed, figure 10. The conductivity increases with increasing frequency and was found to be strongly dependent on EF content as is observed in range of frequency between 1kHz up to 1MHz, and the weakest conductive effect composite was registered for 88PP /7%EF/5MAPP + Wax. Like conductivity, the specific resistance was found to be strongly dependent on EF content and decreases with increasing frequency, figure 11.

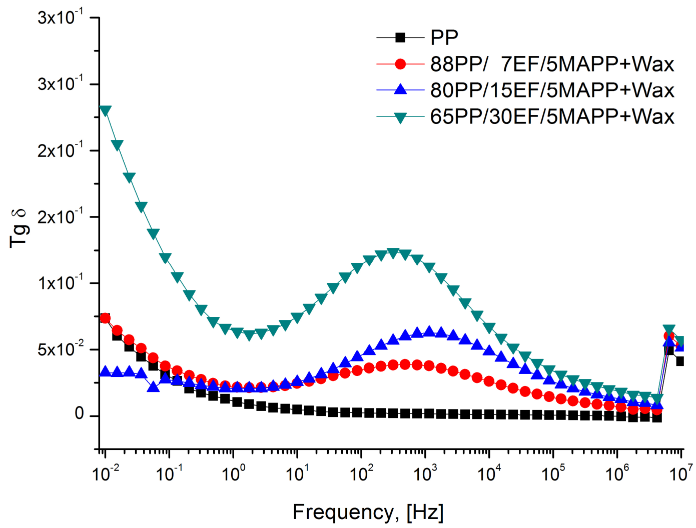

Fig. 9. Variation of tg(δ) function of frequency for studied blends

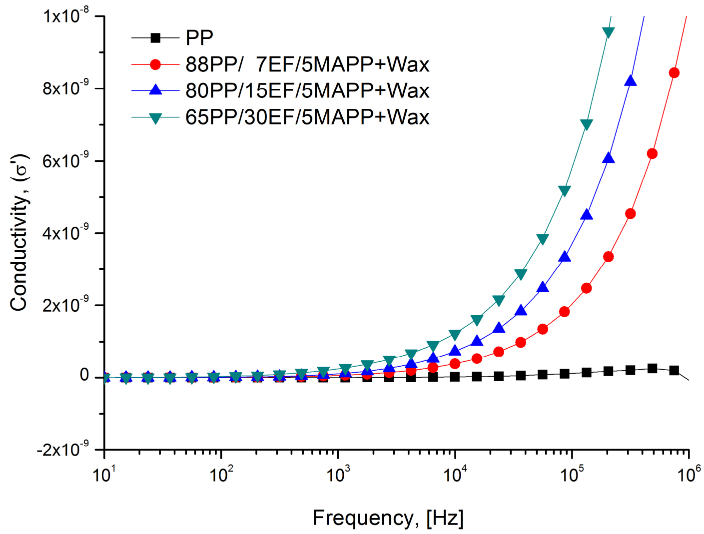

Fig. 10. Variation conductivity (σ') function of frequency for studied blends

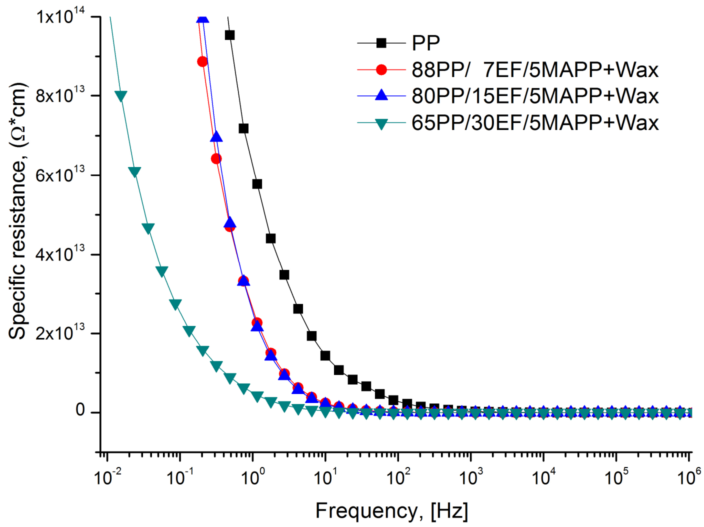

Fig. 11. Variation of specific resistance function of frequency for studied blends

Conclusions

Obtaining biodegradable materials is an ever-present requirement in norms of production of new material and especially environmental protection. Biocomposite materials were obtained from virgin plastic (e.g. polypropylene), natural organic materials used as fillers (eggplant flour) and waxes with potential application in electrical engineering like housings of electrical equipments, transformers board or a different types of insulators.

The results of mechanical test show a different behavior of blends function of amount of filler used in the system. As long as the amounts of filler increase the biocomposites become more rigid and amorphous affinity decreases. Also a large amount of wax is not desired because this can reduce the adhesion between fibbers and polymer matrix.

Taking into account both dielectric and mechanical properties, it seems that the biocomposite material with 65PP/30%EF/5MAPP + Wax has a remarkably high dielectric constant value, being at industrial frequency with 100% higher than the compound with 88PP /7%EF/5MAPP + Wax. From dielectric analyze can see that these materials can be tested for electrical applications like insulation capacitor, especially at industrial frequencies.

The physical-mechanical properties and biodegradability of the biocomposites depend both on the filler type component introduced, as well as its proportion. If the proportion of natural polymer, incorporated in the synthetic polymer matrix, exceeds 10%, the physical and mechanical properties will change, and induction period of biodegradation will be smaller and once the natural component disappear, will disappear in time and synthetic polymer that which will decay in very small fragments.

Increasing the proportion of natural ingredients to 40-60%, physical and mechanical properties are maintained within acceptable limits, and with the introduction in composite of vegetable oils and natural waxes biodegradation rate will increase significantly.

The potential reserves by plant materials are provided by woody plants and annual form cereal straw, crops, textiles and agricultural, and the main polymers of biomass (cellulose, hemicelluloses and lignin). Cellulosic material impregnated with waxes, are used because of excellent dielectric properties.

Acknowledgment

This paper was supported by the project "Development and support of multidisciplinary postdoctoral programmes in major technical areas of national strategy of Research - Development - Innovation" 4D-POSTDOC, contract no. POSDRU/89/1.5/S/52603, project co-funded by the European Social Fund through Sectoral Operational Programme Human Resources Development 2007-2013.

References

[1] G. Constantinescu, G. Cazacu, V.I. Popa, Contributions to the Modification of Lignocellulosics by Epoxydation and Estherification, Cellulose Chemistry and Technology, 2005, 39(3-4), pp.201-210.

[2] E. Guuntekin, B. Uner B. Karakus, Chemical composition of tomato (Solanum lycopersicum) stalk and suitability in the particleboard production, Journal of Environmental Biology, 2009, 30(5) pp.731-734.

[3] C. Vasile, A. Iwanczuk, S. Frackowiak, G. Cazacu, G. Constantinescu, M. Kozlowski, Modified lignin /polyethylene blends, Cellulose Chem. Technol., (2006), 40 (5), 345-351

[4] S. Aradoaei, R. Ciobanu, A. Trandabat, G. Constantinescu "Technological analysis via dielectric spectroscopy of materials obtained by recycled PET and wood derivates, 8th IEEE International Conference on Solid Dielectrics ICSD Toulouse France, 2004, Topic 4, pp. 462-465.

[5] S. Aradoaei, R Darie, M Mosneagu, S Ursache, Technological analysis of materials derived from recycled PET and LDPE via dielectric spectroscopy method, 7th International Conference on Management of Technological Changes, Alexandroupolis, Grecia, 2011, pp. 449-452.

[6] S. Aradoaei, R. Darie, G. Constantinescu, M. Olariu, R. Ciobanu, Modified lignin effectiveness as compatibilizer for PET/LDPE blends containing secondary materials, Journal of Non-Crystalline Solids, Article Number: 14511, Vol.356, 2010, pp.768-771.

Interdisciplinary Research in Engineering: Steps towards Breakthrough Innovation for Sustainable Development

10.4028/www.scientific.net/AEF.8-9

Innovative Biocomposite Derived from Waste Materials with Applications in Electrical Domain

10.4028/www.scientific.net/AEF.8-9.379

Advanced Materials Research Vol. 649 (2013) pp 231-235
Online available since 2013/Jan/25 at www.scientific.net

doi:10.4028/www.scientific.net/AMR.649.231

Development of new materials for construction sector obtained from renewable resources

Sebastian Teodor Aradoaei[1, a], Mihaela Mosneagu[2,b] , Raluca Darie[3,c] and Gabriela Constantinescu[4,d]

[1]"Gheorghe Asachi" Technical University of Iasi, Department of Electrical Measurements and Materials, 53, Blvd. Prof. D. Mangeron, 70050 Iasi, Romania

[2]S.c. AllGreen s.r.l., 53, Blvd. Prof. D. Mangeron, 70050 Iasi, Romania

[3]Romanian Academy, "Petru Poni" Institute of Macromolecular Chemistry, 41 A Gr. Ghica Voda Alley, 700487, Iasi, Romania

[4]Institute of Legal Medicine, Forensic Toxicology Department, 4 Buna Vestire Street, 700455, Iasi, Romania

[a]asteor@yahoo.com, [b]mosneagum@yahoo.com, [c]ucadarie@yahoo.com, [d]gabison32@yahoo.com

Keywords: recycling, composite material, mechanical characterization, dielectric spectroscopy analysis

Abstract. Article tries to highlight the advantages of using in construction area of composites materials obtained from recycled polyethylene and wood dust in the presence of compatibilizing agents. The composite materials have been evaluated in terms of dielectric properties and mechanical characteristics to take into account for the optimum materials structure. The advantage of composite materials made of plastic is that those can be designed in accordance with the formulas of composite plastic and technology to achieve high performance properties in a wide variety of commercial and residential construction applications.

Introduction

Plastics are a crucial part of twenty-first century life. Not only do they provide us with useful, lightweight and durable products, but they play a key role in the sustainable development of our world [1]. Lighter plastic components enable safety and resource efficiency solutions for cars and aircraft. It helps to insulate buildings and save lives in healthcare applications. 12% to 15% of a modern car is made of plastic to help to reduce weight, save fuel and reduce emissions.

Plastics can even help reduce energy consumption and greenhouse gas emissions in many circumstances. Nearly 40% of all energy consumed is used in buildings. Plastic insulation helps our homes to stay warm or cool in a sustainable, eco-efficient way.

The continuously increasing demand for plastic materials for different societal sectors, figure 1, correlated with the continuously decreasing of supplies, determined the scientists to consider any possibility of superior recycling of plastic waste.

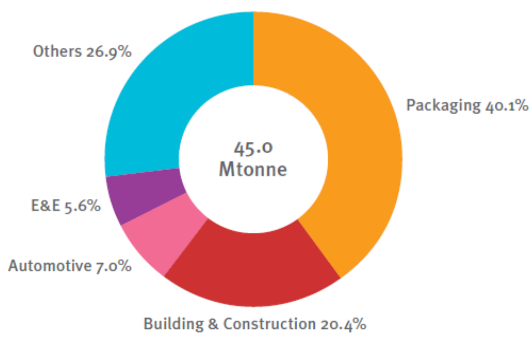

Fig. 1: Europe Plastics Demand by Resin Types 2009, Source APME 2009

As with all materials, once plastics are sorted and prepared ready for recycling they are available for the recycling market. This market has, as with other recycled raw material, developed into a global market. A significant amount of secondary raw materials are recycled within Europe [2]. This is due to a well developed recycling industry and the fact that many recycled materials are used in the production of new products.

Experimental Part

Materials. As a polymer matrix it was used recycled polyethylene (RPE) in the powder shape with 0.17 g/min. flow index (at the 190°C temperature and with the 2.16 kg. Weight) and 0.94 g/cm^3 density obtained by recycling the packages for bottle drinks; As filling material it was use wood dust (WD).

For improve the compatibility between components, three compatibilizing agents have been used (supplied by Exxon Chemical): Copolymer ethylene-propylene modified with 0.7% maleic anhydride (C 1803); Copolymer ethylene-propylene modified with 0.3% maleic anhydride (C 1820); Copolymer ethylene-propylene unmodified with 77% ethylene (C 805).

Composites were obtained by mixing RPE with lignin and the compatibilizing agent. The extruder temperature profile was over to 130°C-145°C.

Investigation method. Mechanical characteristics of composites were determined with a testing machine Tiratest 2200 Germany according to STAS 6642-73. Measurements were made to a 100 mm/min. pulling speed. Before analyzing the samples, these were conditioned by maintaining then into a vacuum oven for three hours to 50°C and 0.98 kPa pressures. For each sample a number of 5 determinations were made, and their mean was considered the final result. The impact strength has been evaluated on notched samples in Izod mode using a testing machine Complete Izod Pendulum 540/228062 Germany according to STAS 7310-87.

In order to obtain more information about composite materials dielectric investigations were carried out. These investigations were made using a Novocontrol Concept C 80 system, with dielectric analyzer running in a large broadband (frequency range from 10^{-2} to 10^{6} Hz) equipped with specialized software towards identifying charge migration and dipole orientation mechanism, with focus on interfacial effects [3].

Results and Discussions

Mechanical Properties. The mechanical properties, elastic modulus (E), breaking strength (σ) and elongation at break (ε) of the plastic/natural polymers mixture reprocessed in the single screw extruder are reported in Figures 2 and 3.

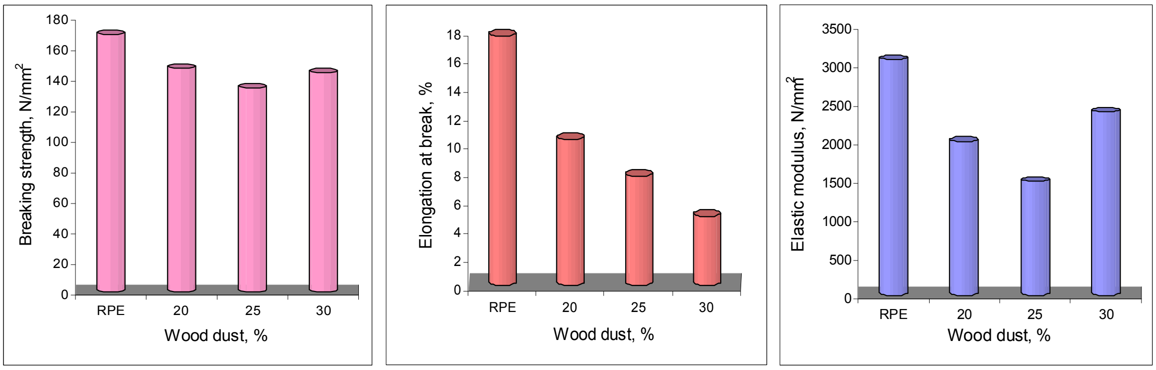

Fig. 2: The influence of wood dust percent on the breaking strength, elongation at break and modulus of elasticity

The optimum filling material percentage to which the elongation at break value is higher that the matrix value, is 20 %, at a higher than that percentage both the elongation at break and breaking strength are diminished.

The modulus of elasticity is improved at the same time, with the wood dust quantity increase; at a 30 % wood dust addition the composite material elasticity modulus is nearest with the recycled polyethylene matrix elasticity modulus.

By the wood dust addition in composite materials, some properties are going to be diminished comparatively to the polyethylene waste properties, such as breaking strength. The breaking strength stays approximately constant at 20-30 % lignin addition (148.45 N/mm^2).

It seems that by introducing mixtures compatibilizing agents in all mechanical properties are improved compared to mixtures without compatibilizing agents. The influence of three agents on breaking strength is about the same. Significant changes are recorded for the composite modulus is achieved with C1803 maximum of 1988.9 N/mm2 as maleic anhydride, present in made compatible, react with OH groups of lignin causing plasticization phenomenon.

In case of elongation at break the new created materials presents higher values than those determined for the recycled polyethylene, but from three compatibilizing agents the C 1820 offers the lower values. The 0.7 % maleic anhydride grafted ethylene-propylene copolymer has a positive influence on the composite materials elasticity modulus.

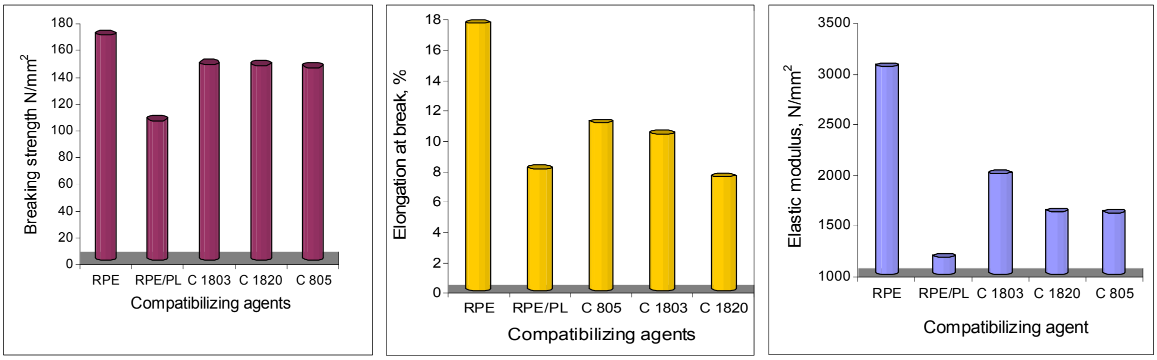

Fig. 3: The influence of compatibilizing agent type on the on the breaking strength, elongation at break and modulus of elasticity

Dielectric Analysis. The inclusion of wood dust in the matrix polyolefin dielectric characteristics lead to changes in a wide range and because this evaluation is absolutely necessary dielectric properties.

The experimental values are correlated and discussed in relation to the dielectric characteristics of recycled polyethylene high density matrix (RPE). The permittivity (ε') and tg (δ) of recycled polyethylene blends/wood dust/compatibilizing agents with variable addition function of frequency is illustrated graphically in figure 4 and 5.

Dielectric properties show a significant change only in the frequency range 0-100 Hz. After the value of 100 Hz, tan δ takes very small values - electric dipoles are unable to track rapid variations of the electric field [4]. The addition of wood dust influences both permittivity and tan (δ), observing that by increasing the percentage of filler from 20% to 25% dielectric constant increases from 4.5 to 5.8, and compared with RPE is about two times higher. This behavior is mainly due to the structure of amorphous/crystalline polymer material and natural structural discontinuities that allows migration of electrical charges in the interfacial area.

By introducing compatibilizing agent in blends, the permittivity decreases, unless that use compatibilizing agent C1803 which has permittivity value is 4.2 compared to 2.3 for recycled PE.

The agents increase conductivity and the maximum value is recorded for compatibilizing agent with 0.3% maleic anhydride [5].

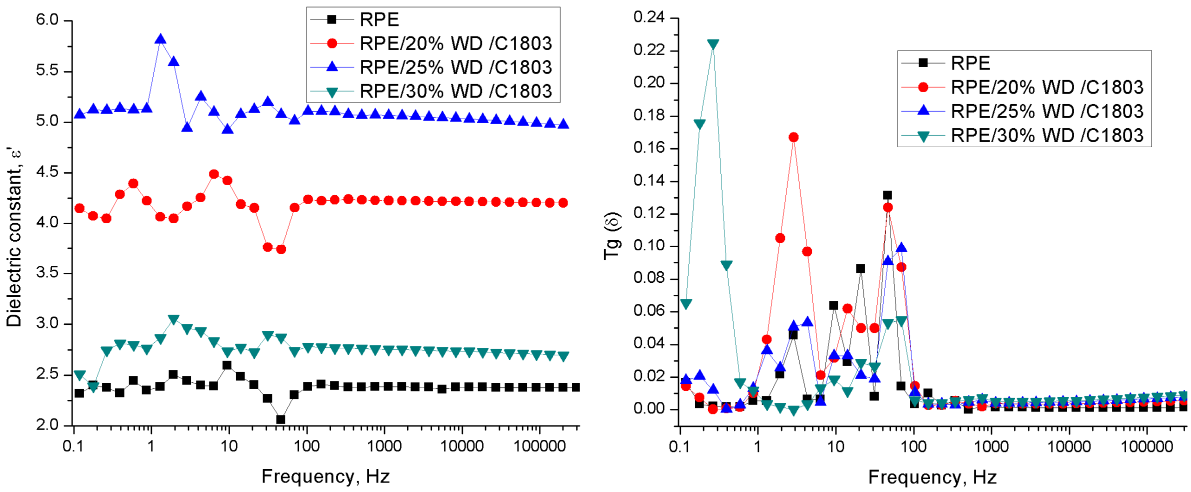

Fig. 4: Variation of permittivity and Tg(δ) vs. frequency for RPE/WD/C1803 blends

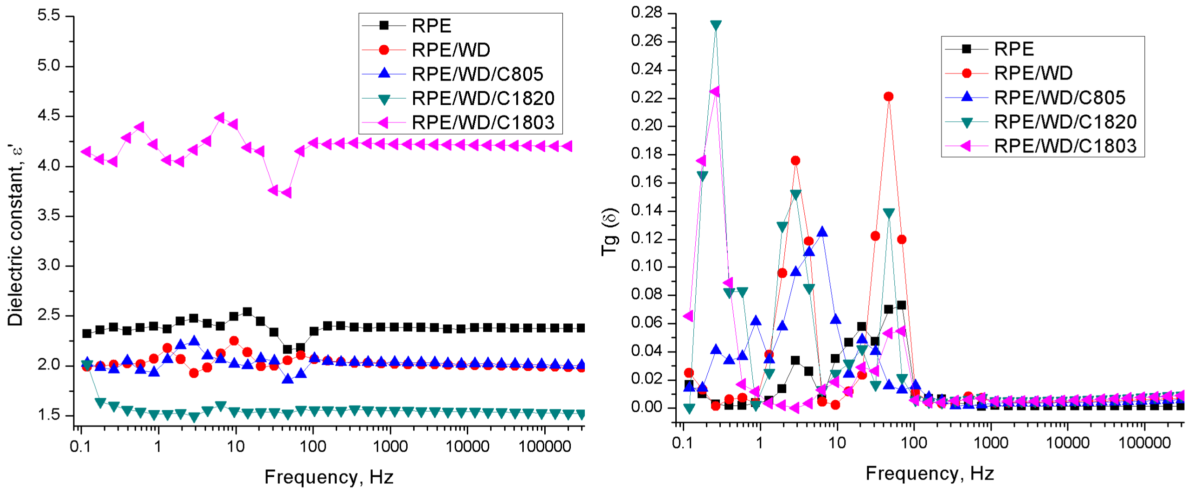

Fig. 5: Variation of permittivity and Tg(δ) vs. frequency for RPE/20%WD/compatibilizing agents blends

The introduction of wood dust the conductivity increase when is compared with matrix polymer mixtures of polyethylene, as natural polymer contains some moisture which increases the electrical conduction and reducing the volume resistance of the surface, and the blends become more rigid.

Conclusions

Introducing natural polymer causes significant changes in physical and mechanical properties, such elongation at break decreases with increasing proportion of filler in the mixture. A different situation is found for the modulus showing a maximum addition of 30% wood dust.

By introducing the filling material, elongation is reduced greatly compared with modulus and breaking strength that varies less.

The addition of wood dust in RPE matrix does not influence the mechanical properties of the material. In case of RPE/wood dust mixtures, wood dust increases the blends elastic modulus; Introduction of the ethylene-propylene modified with 0.7 % maleic anhydride copolymer as a compatibilizing agent increases the physical-mechanical properties;

For composite materials obtained from RPE and compatibilizing agents improve mechanical properties. The influence of compatibilizing agents on the breaking strength of composites is about the same, significant changes recorded for the modulus of the structures where the use compatibilizing agents C1803 0.7% maleic anhydride leads to a maximum value it - 1988.9 N/mm2.

Dielectric properties are characterized by significant changes only in the frequency range 0-100 Hz. During this time the addition of wood dust affects the permittivity and tan (δ), which is mainly due to biphasic amorphous structure/crystalline polymer of natural structure that allows migration of electrical charges.

This materials can be used in various field (electrical industry, construction, car industry, family use). The greatest growth potential for wood plastic composites is in building products that have limited structural requirements. Products include decking, roof cover, fencing, industrial flooring, landscape timbers, railings, and moldings figure 6.

Fig. 6: Application in construction of wood plastic composites as roof cover, wall cladding and wall panel

Although wood plastic composites is more expensive than treated wood its have lower maintenance, lack of cracking or splintering, and high durability. New research efforts will be concentrated in future towards realizing more tests, for a better structure of composite.

Acknowledgment

This paper was supported by the project "Development and support of multidisciplinary postdoctoral programmes in major technical areas of national strategy of Research - Development - Innovation" 4D-POSTDOC, contract no. POSDRU/89/1.5/S/52603, project co-funded by the European Social Fund through Sectoral Operational Programme Human Resources Development 2007-2013.

References

[1] Information on http://www.plasticseurope.org.

[2] Ciobanu R, Aradoaei S, Trandabat A, et al Knowledge-based bio-compounds from recycled PE/PET and wood derivates: Technological analysis, properties, perspectives, 10th International conference on optimization of electrical and electronic equipments, Vol I – Electrotechnics, Brasov, Romania, 2006, pp.117-122.

[3] S. Aradoaei, R. Ciobanu, A. Trandabat and G. Constantinescu, Technological Analysis via Dielectric Spectroscopy of Materials Containing Recycled PET and Wood Derivates, 8th IEEE International Conference on Solid Dielectrics, Toulouse, Vol. 1, 2004, pp 462-465.

[4] S. Aradoaei, R. Darie, G. Constantinescu, M. Olariu, R. Ciobanu, Modified lignin effectiveness as compatibilizer for PET/LDPE blends containing secondary materials, Journal of Non-Crystalline Solids, Article Number: 14511, Vol.356, 2010, pp.768-771.

[5] S. Aradoaei, R. Darie, C. Vasile, M. Mosneagu, M. Olariu, Morphology and dielectric properties of some LDPE/PA blends in presence of compatibilizers, Solid State Phenomena Vol. 188, 2012, pp 268-274.

enviBUILD 2012

10.4028/www.scientific.net/AMR.649

Development of New Materials for Construction Sector Obtained from Renewable Resources

10.4028/www.scientific.net/AMR.649.231

Journal of Non-Crystalline Solids 356 (2010) 768–771

Contents lists available at ScienceDirect

Journal of Non-Crystalline Solids

journal homepage: www.elsevier.com/locate/jnoncrysol

Modified lignin effectiveness as compatibilizer for PET/LDPE blends containing secondary materials

S. Aradoaei [a,*], R. Darie [b], G. Constantinescu [b], M. Olariu [a], R. Ciobanu [a]

[a] *Technical University of Iasi, Department of Electrical Measurements and Materials, Blvd. D. Mangeron 53, 700050 Iasi, Romania*
[b] *"Petru Poni" Institute of Macromolecular Chemistry, 41A Gr. Ghica Voda Alley, 700047 Iasi, Romania*

ARTICLE INFO

Article history:
Available online 10 February 2010

Keyword:
Polymers and organics

ABSTRACT

The compatibilizing efficiency of poly(ethylene terephthalate)/low density polyethylene (PET/LDPE) blends has been evaluated by following the rheological behavior during processing, dynamic testing as well as tensile characteristics and dielectric properties to account for the optimum materials structure. The binary and compatibilized blends containing secondary PET (PETr) and LDPE (PEr) and reactive compatibilizing agent as commercial maleated ethylene–propylene rubber (EP–MA) or esterified lignin have been processed by melt mixing in a counter-rotating twin rotors HAAKE RHEOCORD 9000 mixer. The experimental results highlight the possibility of producing materials with modulated and new properties from secondary PET and LDPE by overcoming the lack of interfacial adhesion of polyolefin–PET blends, typical of an immiscible system. Lignin can be efficiently used as compatibilizing agent in PETr/PEr blends.

1. Introduction

Blends of poly(ethylene terephthalate) (PET) and polyolefins (POs) have recently attracted considerable research activity since both materials are among the most frequently used thermoplastics, especially as packaging materials. Owing to their broad-scale applications, PET/PO mixtures represent a significant part of post-consumer waste.

Poly(ethylene terephthalate) and polypropylene (PP) are incompatible due to differences in chemical nature and polarity; therefore, their blends exhibit a clear two-phase morphology, where the dispersed phase forms relatively large spherical droplets, and no particular adhesion between the phases exists [1]. Generally, the strength and stiffness of their blends increase with raised PET content almost linearly, but owing to the incompatibility, the blends exhibit very poor impact strength. Hence, appropriate compatibilization is needed to achieve better adhesion between the two phases and to overcome the brittleness [1].

In earlier studies, it was found that PO-based compatibilizers containing maleic anhydride (MA) or epoxy functionalities are effective in improving the properties of blends of polar engineering polymers like polyamides, polyesters, or polyester-type liquid-crystal polymers with non-polar polymers like POs [2]. Thanks to its various properties, lignin can be used for different technical purposes.

Lignin, the most abundant substance in plant kingdom after cellulose, is an aromatic biopolymer, which can be separated from almost all types of woody resources [3]. It results mainly as a by-product from pulp and paper industry and is conventionally treated as a waste material with low practical usage.

Unmodified lignin possesses a poor solubility in common solvents and its thermoplastic melt flow characteristics are like those of cellulose. Similar to the thermoplastic ester derivatives of cellulose, one method to improve the thermoplastic behavior of lignin polymer is etherification [4]. Etherification of lignin has been in practice from the late forties when it was found to be useful as a mold lubricant, possessing characteristics of softening point and solubility [5].

Enhanced solubility and melt characteristics along with a reduction in glass transition temperature and improved thermal decomposition behavior were reported for lignin alkanoates.

However, lignin and its derivatives are biodegradable polymers, which can be used in combination with other biodegradable materials. The use of lignin as a modifier for biopolymers would certainly be advantageous from the viewpoint of new potential applications as well as the economical recovery of this waste material resulted from biomass processing [6].

In this study, the reactive blending of post-consumer poly(ethylene terephthalate) (PET) with LDPE in presence of different compatibilizers as EP–MA or modified lignin was studied in an attempt to obtain new materials with enhanced properties with respect to the starting materials. Rheological behavior during melt processing, dynamic testing, as well as tensile characteristics has been followed.

* Corresponding author. Tel.: +40 723 394 392; fax: +40 232 237 627.
E-mail address: asteor@yahoo.com (S. Aradoaei).

0022-3093/$ - see front matter
doi:10.1016/j.jnoncrysol.2009.11.046

Dielectric spectroscopy method represents an interesting pursuit for studying molding resins, compounds and composites, by two declared aims: one related to the potential application of such materials for electrical domain, other accounting for the optimum structure and technology via derived dielectric parameters [7].

2. Experimental part

2.1. Materials

Poly(ethylene-terephtalate) (PETr), waste originating from bottle scraps having melt temperature 260 °C and density = 1.26 g/cm^3.

Low density polyethylene (LDPEr) stretch type E, waste originating from film scraps having density = 0.92 g/cm^3.

Ethylene–propylene rubber grafted with maleic anhydride (EP–MA) with trade name Exxelor VA 1803 was supplied by Exxon Chemical. The EP–MA compound contained 0.7% of MA, composition by weight: 43% ethylene, 57% propylene. Other characteristics: melt flow rate (230 °C/10 kg) of 22 g/10 min, density: 0.86 g/ cm^3, glass transition temperature −57 °C.

Lignin was esterified with stearoyl chloride in pyridine medium at a molar ratio of 1:1.2, for 2 h at 80 °C. The reaction product (esterified lignin – LER) was neutralized with diluted sulfuric acid solution and successively washed with hot and cold water [8]. The main characteristics of lignin are: C = 50.15%, H = 5.97%, O = 42.02%, N = 1.65%, Cl = 0.21, OCH_3 = 14.8%, OH_{total} = 11.07%.

2.2. Processing

Blends containing secondary PET, LDPE, modified lignin, or/and EP–MA have been obtained by means of a HAAKE RHEOCORD 9000 mixer with a mixing chamber of 50 cm^3 in the following conditions: temperature of mixing of 260 °C, mixing time of 10 min, the rotational speed of 60 rpm. The amount of LER or EP–MA was 5 and 7 wt% with respect to the initial amount of LDPE in the blend. The composition of the prepared mixtures has been shown in Table 1. The components were dried before mixing in a vacuum oven as follows: PET for 12 h at 150 °C, LDPE and EP–MA for 12 h at 80 °C and LER at 40 °C for 12 h. The samples obtained by injection molding are relatively homogeneous and compact [9].

3. Investigation methods

Processing behavior was evaluated from the torque–time curves recorded during the blending on a HAAKE Rheocord 9000 mixer.

Melt dynamic rheological tests were conducted in a HAAKE RT 20 Rotovisco-Oscillatory Rheometer in parallel plate oscillatory mode.

The tensile behavior of the studied systems was followed by uniaxial tension tests using a Lloyd LR 10 K tensile tester according to Standard Testing Method ISO 527. Tensile speed was 10 mm/min, gauge length 40.0 mm. Ten characteristic parameters for the relationship stress–strain in a sample were registered until its break.

Broadband dielectric spectroscopy analysis was submitted to a Novocontrol dielectric analyzer (frequency range from 10^{-2} to 10^7 Hz), equipped with specialized software towards identifying charge migration, dipole orientation mechanisms, and derived dielectric parameters, which can be related to the bonding mechanisms of micro-components.

3.1. Processing behavior

The processing behavior of the obtained blends was appreciated from the following characteristics: torque at different mixing time and at the end of mixing and the specific energy after 1 min of mixing (energy required to process a unit mass of material). The specific energy is calculated from total shear energy (that is energy introduced in polymer material by motor drive during processing) and it is obtained by multiplying torque with rotor speed and 9.087×10^{-3} and divided by processed mass of material [10]. These characteristics are presented in Table 1.

At a first sight, the torque curves of the studied blends lay between the curves of the neat secondary polymers, depending on the mixing ratios used as can be observed in Fig. 1.

The studied processing characteristics demonstrated an increase in the blend viscosity compared to binary PETr/LDPEr blend at the beginning of processing by using the commercial EP–MA, following a constant line until the end of processing. While using esterified lignin, the processing viscosity decreases due to the plasticizing role of this natural polymer.

3.2. Dynamic rheology

Viscoelastic properties as shear modulus (G') and loss modulus (G'') have been analyzed at a temperature of 260 °C both for the pure polymers and blend systems in melt state. The results of

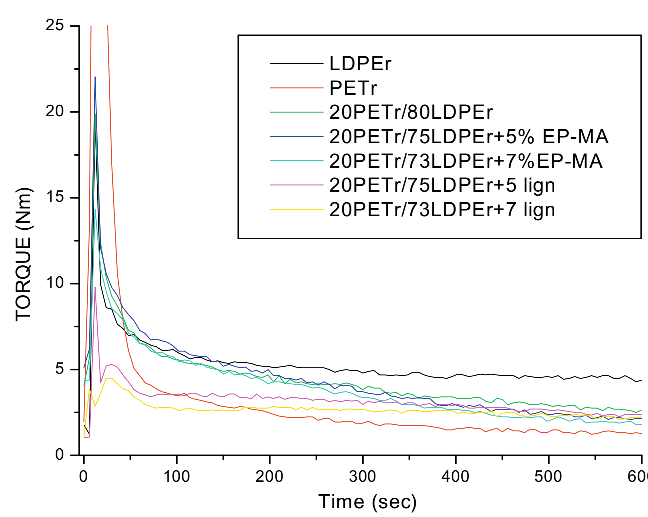

Fig. 1. Torque–time curves for studied blends.

Table 1
Processing characteristics for studied blends.

Sample	TQ_{max} (N m)	$TQ_{1\ min}$ (N m)	TQ_{fin} (N m)	$E_{mix\ 1\ min}$ (J/g)
PETr	55.93	4.64	1.28	37.42
LDPEr	19.56	6.72	4.38	82.46
20PETr/80LDPEr	19.86	6.52	2.65	72.46
20PETr/75LDPEr/5EP–MA	22.06	7.28	2.14	80.01
20PETr/73LDPEr/7EP–MA	14.32	6.88	1.78	76.44
20PETr/75LDPEr/5LER	9.79	3.62	2.39	39.22
20PETr/73LDPEr/7LER	4.49	3.21	2.24	34.42

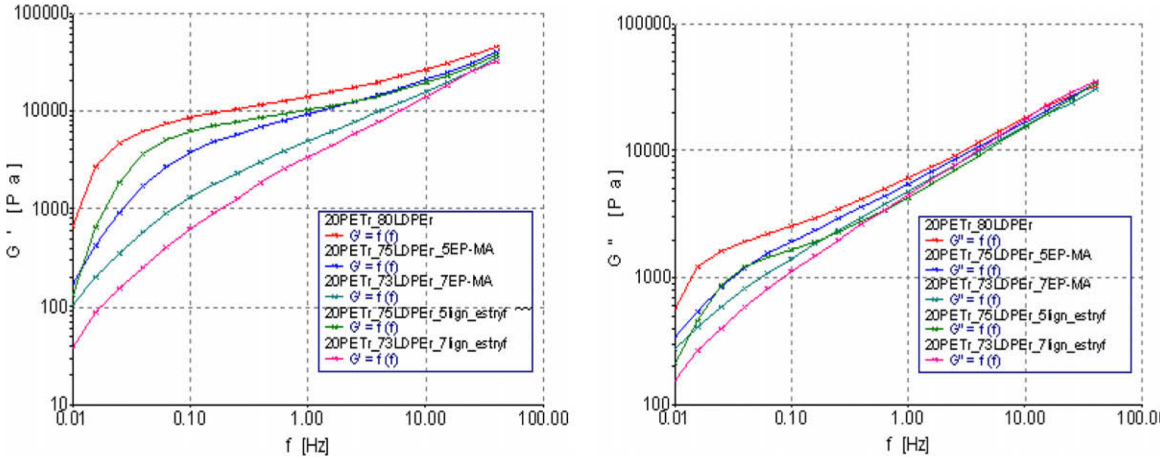

Fig. 2. Variation of shear modulus (G') and loss modulus (G'') function of oscillation frequency for studied blends.

dynamic rheological test show a different behavior of blend function of compatibilizing agent used in the system – Fig. 2.

In presence of 5 wt% esterified lignin, the system rigidity increase with respect to the same blend containing 5 wt% EP–MA and so higher shear modulus has been recorded due to the complex reactions in the system between the functional groups of lignin and PET [11]. A higher amount (7 wt%) leads to the increase of system's elasticity due to the plasticizing role of lignin. For G'' a similar evolution has been recorded, for 5 wt% lignin, G'' values increase at low frequencies (up to 0.1 Hz) due to an increase of dissipated energy as released heat.

When EP–MA was added in the binary 20PETr/80LDPEr blend, G' values decrease because the absorbed energy during testing increase, this behavior being more intense at higher amounts of EP–MA.

The differences are more obvious at low frequencies, whereas the dynamic rheology presents similar behavior as higher oscillatory frequencies where the chain mobility is increased in melt.

The rheological characterization indicates that the addition of modified lignin and functionalized EP promotes the compatibilization of the two main phases of the studied blends.

3.3. Tensile properties

The uncompatibilized blends of PETr/LDPEr were found to have mechanical properties typical of immiscible blends. The mechanical properties of injection-molded specimens are reported in Table 2 for 20PETr/80LDPEr blends.

It is readily observed that blending the two components causes the elongations at break to fall to very low values. The pronounced fragility of the blend is clearly due to the lack of interface adhesion. The used compatibilizers introduces generally enhanced tensile characteristics of the systems compared with binary blend, the highest stress at break as well as Young Modulus being recorded for 5 wt% modified lignin used, while the best elongation at break was found for the blend containing 7 wt% lignin due to its plasticizing role. These mechanical results are in concordance with the previous presented processing and rheological behavior of the studied systems.

Table 2
Tensile parameters for studied blends.

Sample	Young Modulus (MPa)	Stress at break (MPa)	Strain at break (%)
20PETr/80LDPEr	422.64	12.06	68.47
20PETr/75LDPEr/5EP–MA	521.33	12.89	80.51
20PETr/73LDPEr/7EP–MA	501.87	12.30	73.14
20PETr/75LDPEr/5LER	552.60	13.36	71.13
20PETr/73LDPEr/7LER	509.29	12.36	82.35

3.4. Broadband dielectric spectroscopy analysis

One of the most important applications of dielectric spectroscopy is the investigation of relaxation processes which are due to rotational fluctuation of molecular dipoles. As they are related to characteristic parts of a molecule (functional group) or the molecule as whole, information about the dynamics of a molecular ensemble can be obtained by analyzing the dielectric function [12].

The experimental dielectric domain boundaries are represented by PETr with greatest permittivity value and significant dipolar losses, and LDPEr with minimum permittivity value and an increased value of dielectric losses at low frequencies, explained by some conductive effects due to the low mineral purity of the recycling process, Fig. 3. The characteristics of PET/LDPE compound without mass additives occupy, as expected, a middle position within these domains, without significant dipolar or interfacial effects, being a consistent proof of an optimum coupling process of PET/LDPE.

The recycling process of PET (even if expected with a similar residual mineral content in polymer mass) looks more professional and leads obviously to a more mineral purity. The lower dielectric losses at low frequencies of PETr compared to LDPEr are shown in Fig. 3.

The technological coupling process to PET/LDPE with lignin/EP–MA mass additives and related effects upon the structure of materials represented another important research direction towards optimizing the PET/LDPE derived compounds.

Some influence of lignin/EP–MA mass additives was noticed only for dielectric permittivity of LDPEr/PETr composites, Fig. 3. As regards the dielectric losses in Fig. 3, negligible dipolar or interfacial effects of composites with lignin/EP–MA mass additives are noticed, in spite of, e.g. a strong dipolar effect expected for lignin. This is an important proof of a very homogenous structure and a successful coupling process in amorphous state. Only the composites with 7% EP–MA and with 5% lignin provided a superior value of permittivity when compared with PET/LDPE compound without mass additives, considering optimum receipts of polymers coupling technology with lignin/EP–MA. On the other hand, a

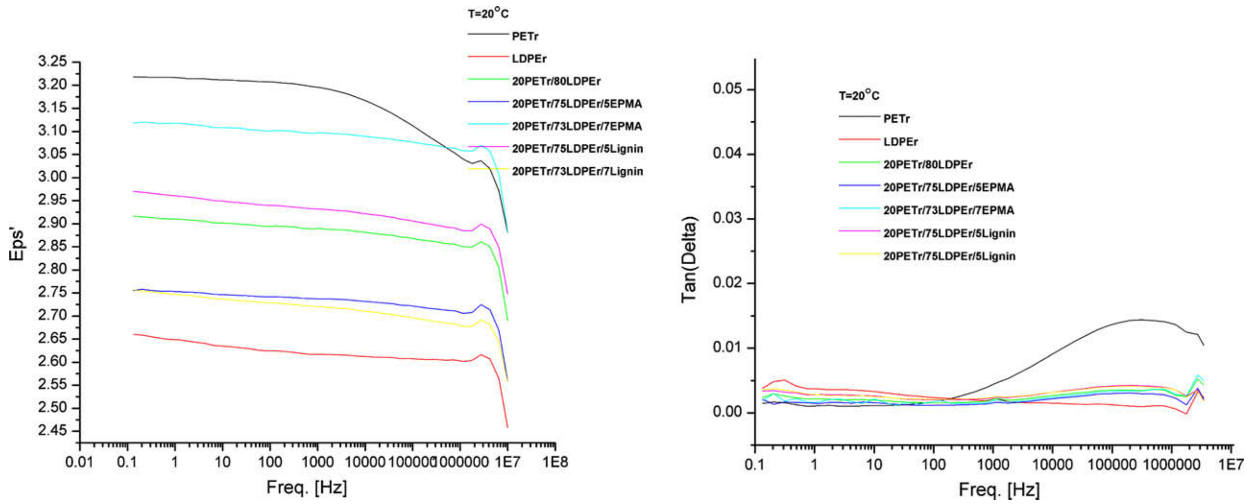

Fig. 3. Variation of permittivity (ε') and tan(δ) function of frequency for studied blends.

significant stability of permittivity (lowest decease versus frequency) was noted only for the compounds with EP–MA.

Accordingly, and taking into account also the mechanical properties, the compound with 7% EP–MA is considered the most convenient material for potential applications in electrical domain (insulating system/capacitor).

4. Conclusions

The studied processing characteristics demonstrated an increasing in the blend viscosity compared to binary PETr/PEr blend at the beginning of processing by using the commercial EP–MA, following a constant line until the end of processing. While using esterified lignin, the processing viscosity decreases due to the plasticizing role of this natural polymer.

The results of dynamic rheological test show a different behavior of blend function of compatibilizing agent used in the system. The presence of esterified lignin leads to an increase of dissipated energy at 5 wt% used.

Overall, the experimental results highlight the possibility of producing materials with modulated and new properties from secondary PET and LDPE by overcoming the lack of interfacial adhesion of polyolefin–PET blends typical of an immiscible system. Lignin and EP–MA can be efficiently used as compatibilizing agents in PETr/PEr blends.

To obtain an optimum coupling process and a homogenous structure of PET/LDPE compounds with lignin/EP–MA, a content up to 7% EP–MA and/or up to 5% lignin provided to be optimum.

Taking into account both dielectric and mechanical properties, the PETr/PEr compound with 7% EP–MA is considered the most convenient material for potential applications in electrical domain (insulating system/capacitor).

Acknowledgment

The present paper was developed with financial support of CNCSIS through PNII Idei 320 project.

References

[1] M. Xanthos, M.W. Young, J.A. Bieseberger, Polym. Eng. Sci. 30 (1990) 355.
[2] Hsien-Tang Chiu, Yao-Kuei Hsiao, J. Polym. Res. 13 (2006) 153.
[3] W.G. Glasser, S.S. Kennedy, in: H.F. Mark, N.M. Bikales, G. Menges (Eds.), Encyclopedia of Polymer Science and Engineering, vol. 8, Wiley, New York, 1987, p. 795.
[4] G. Constantinescu, G. Cazacu, V.I. Popa, Cellulose Chem. Technol. 39 (3–4) (2005) 201.
[5] W.G. Glasser, R.K. Jain, Holzforschung 47 (1993) 225.
[6] C. Vasile, A. Iwanczuk, S. Frackowiak, G. Cazacu, G. Constantinescu, M. Kozlowski, Cellulose Chem. Technol. 40 (5) (2006) 345.
[7] S. Aradoaiei, R. Ciobanu, A. Trandabat, G. Constantinescu, Technological analysis via dielectric spectroscopy of materials obtained by recycled PET and wood derivates, in: 8th IEEE International Conference on Solid Dielectrics ICSD, Toulouse, France, July 5–9, 2004, Topic 4 – Materials and Insulation Systems, pp. 462–465, IEEE Cat. No. 04CH37539, ISBN 0-7803-8348-6.
[8] G. Constantinescu, G. Cazacu, V.I. Popa, Cellulose Chem. Technol. 39 (3–4) (2005) 201.
[9] M. Canetti, F. Bertini, Composites Sci. Technol. 67 (15–16) (2007) 3151.
[10] C. Vasile, R.D. Deanin, M. Mihaes, C. Roy, A. Chaala, W. Ma, Int. J. Polym. Mater. 37 (1997) 173.
[11] C. Vladuta, M. Voinea, E. Purghel, A. Duta, Correlations between the structure and the morphology of PET-rubber nanocomposites with different additives, Mater. Sci. Eng. B, in press (corrected proof, available online 23 July 2009; doi:10.1016/j.mseb.2009.07.004).
[12] F. Kremer, A. Schonhals, Broadband Dielectric Spectroscopy, Springer, Berlin, 2002.

Green Materials Derived from Renewable Resource for Electrical Applications

SEBASTIAN ARADOAEI[1], ROMEO CRISTIAN CIOBANU[1], RALUCA DARIE[2], TRAIAN ZAHARESCU[3]*, ALINA CARAMITU[3]*

[1] "Gheorghe Asachi" Technical University of Iasi, Department of Electrical Measurements and Materials, 53 D. Mangeron Blv., 70050 Iasi, Romania

[2] Romanian Academy, "Petru Poni" Institute of Macromolecular Chemistry, 41A Gr. Ghica Voda Alley, 700487, Iasi, Romania

[3] Institutul National de cercetare Dezvoltare pentru Inginerie Electrica ICPE CA, 313 Splaiul Unirii, Bucuresti, Romania

Nowadays, the growing environmental awareness throughout the world has triggered a paradigm shift towards designing environmentally friendly materials. The interest in cellulose fibers as reinforcement agents in composite materials with polymer matrices has increased dramatically in the last decades, the main reasons associated with this upsurge being their renewable and ubiquitous character, good mechanical properties, low density, low cost and recyclability. Focus on dielectric spectroscopy technique, the article makes a comparison between the dielectric properties of transformer board and composite materials obtained by mixing recycled polyethylene with wood powder or lignin in different percentages.

Keywords: recycled polyethylene, transformer board, dielectric spectroscopy analysis

Thanks to plastics, fewer resources are required to satisfy our daily needs. Fewer valuable goods are wasted when protected by plastic packaging, improvements in crops productivity are made possible and renewable energy solutions are unveiled. The plastics industry plays an important role in enabling growth through innovation in a wide range of industries key such as automotive, electrical and electronic, building and construction and food and beverage sectors.

Plastics are the true resource champions by saving more resources. For example substituting plastics with alternative materials would result in a 46% increase in energy consumption, a 46% increase in CO_2 emissions and generate 100 million t more of waste every year across the EU. The success story for plastics is expected to continue as its unique properties lend to more and more innovation applications. The global demand per capita is expected to grow by 4% each year.

Demand from European converters increased by 1.1% from 2010 to 47 million t in 2011. The market share of end use applications remained stable with packaging the largest segment representing 39.4% of overall demand. This is followed by Building and Construction (20.5%), Automotive (8.3%) and Electrical and Electronic equipment (5.4%). Others include different small segments like sport, leisure, agriculture, etc. (fig. 1).

Plastic products can contribute to sustainable development after their use phase if they are disposed of responsibly and processed for recycling and recovery. All plastics are recyclable – mechanically or chemically - but not all plastics are beneficial to recycle from an environmental and economic perspective.

Recycling is often perceived as sustainable development. It all starts with appropriately designed products. Once the functional needs are safeguarded the designer should factor in sustainability through material selection, manufacturing methods, reuse and recyclability. Sorting, reprocessing and marketing recycled materials back into applications as a complement to virgin plastics require a quality approach throughout the recycling operation and include quality systems and market knowledge. The European recycling value chain must continue to drive a quality focus so their products can complement virgin plastics and other materials. Global trade in plastics waste would still be a necessary complement to maximize the recycling opportunities [1].

The growing environmental awareness throughout the world has triggered a paradigm shift towards designing environmentally friendly materials. The composites or moulding resins based on recycled polyethylene (RPE) and wood derivates - used as fillers, are also examples in this direction.

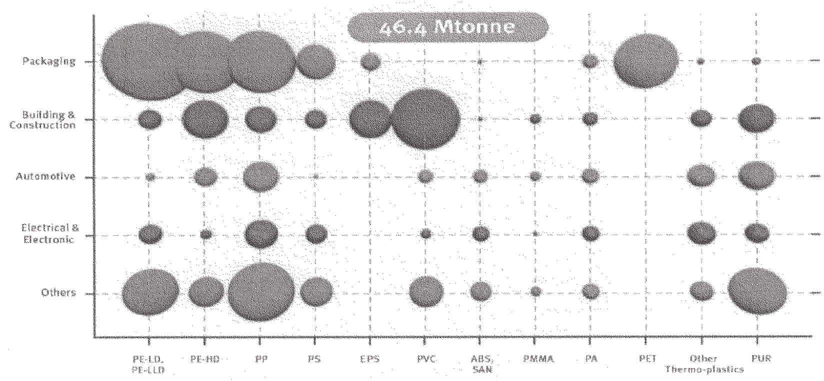

Fig. 1. Europe Plastics Demand by European Plastics Demand* by Segment and Resin type 2011

* email: traian_zaharescu@yahoo.com, alina.caramitu@icpe-ca.ro.

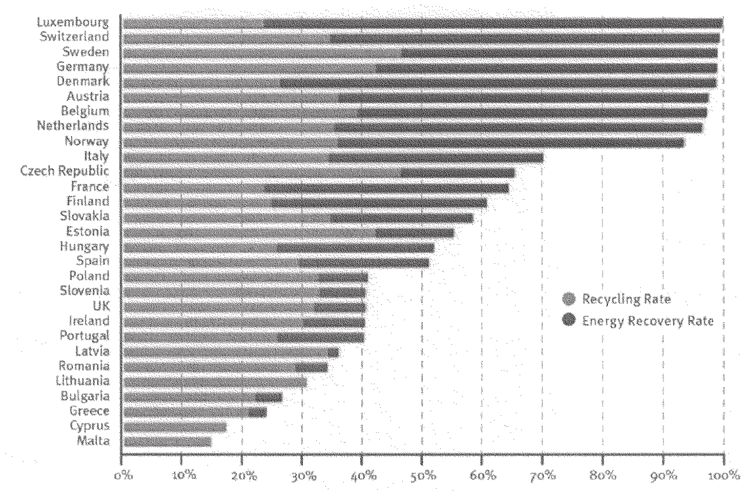

Fig. 2. Total Recovery Rate by Country 2011

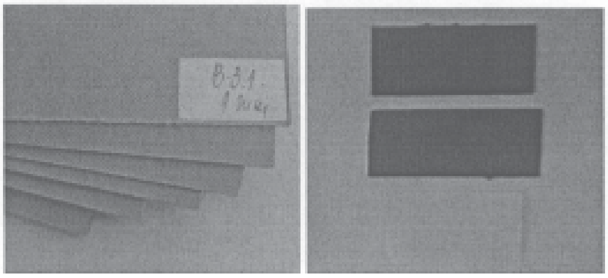

Fig. 3. Transformer board 1 mm thickness made by S.C. Petrocart S.A. Piatra Neamt, Romania (left) and composites obtained from recycled polyethylene with wood powder or lignin (right)

Such materials can provide a large domain of characteristics in accordance with the exploitation requirements and potential appliances, due to the possibility of varying the state components and their percentages, for example, by modifying the polymer structure by adding wood powder and / or lignin, or by including appropriate mass additives or short fibers [2].

The interest in cellulose fibers as reinforcement agents in composite materials with polymer matrices has increased dramatically in the last decades, the main reasons associated with this upsurge being their renewable and ubiquitous character, good mechanical properties, low density, low cost and recyclability [3].

There are few reports in the literature dealing with dielectric analysis of polymer reinforced with cellulose fibbers. Dielectric analysis provides information about important dielectric parameters such as dielectric constant, dielectric loss, loss tangent, conductivity and specific resistance [4].

Experimental part

In the present work, several blends containing different types of polyethylene and wood powder or lignin have been obtained by melt processing [5]. It was evaluated the influence of the amount of natural component during processing, on dielectric behaviour of biocomposites studied.

The transformer board (TB) was offered by the company S.C. Petrocart S.A. Piatra Neamt, Romania, in plate form, with 1 mm thickness figure 3. The transformerboard is manufactured according to the type B.3.1. of the CEI 641-3-1 standard and has a density by 1.0-1.3 g/cm^3. This International Standard gives the requirements for pressboard for electrical purposes comprised of 100 % sulphate wood pulp or a mixture of sulphate wood pulp and cotton.

Composite materials were obtained by mixing recycled PE with natural polymers and compatibility agents. The raw materials used in making composites are recycled high density polyethylene (RPE) as powder derived from recycling crates for soft drinks [3], wood powder (WP) used as filler obtained from grinding wood, commercial lignin powder. All compositions were made in collaboration with one type of modifying reagent C1803, based on modified maleic anhydride which, added in mass led to obtain some improved parameters and optimal structure [6]. Compatibility agent C1803 contains 0.7% of maleic anhydride and is grafted with ethylene-propylene copolymer.

Before mixing, the natural polymers and compatibility agents were subject to conditioning treatment in the oven for 24 h at a temperature of 105°C and 50°C. Then, the mixture was placed in an extruder with a single screw and was processed into test specimens with 1 mm thickness. Two formulations were produced with RPE as matrix and various content (20 wt% and 30 wt%) of wood powder (WP) or lignin (L).

This paper represents a part of an extended study about the use of dielectric spectroscopy analysis on composite materials, with target on their potential appliances as insulating systems. The polyethylene is a main chain semicrystalline polymer, providing dielectrically active α- and β-relaxation processes. Generally speaking, semicrystalline polymers are at least biphasic materials consisting of amorphous and crystalline regions, with important implication for dielectric measurements.

Dielectric spectroscopy has proven a powerful tool to investigate in details the dynamical processes of composites materials. The dielectric properties of composite material are affected by several factors, e.g. molecular chain arrangement, amorphous and crystalline phase fraction, molecular weight distribution, temperature and measuring frequency [3].

Broadband dielectric spectroscopy analysis were performed using a Novocontrol GmbH Concept 80 Broadband Dielectric Spectrometer with an Alpha A analyzer over the frequency range of 0.01 Hz to 20 MHz in combination with a Novocontrol Quatro temperature system providing control of the sample temperature with high accuracy [4]. The samples were sandwiched between two 20 mm gold plated electrodes and tested within ZGS Alpha Active Sample Cell, figure 4. The test temperatures were 20°C.

The experiments were conducted towards analyzing standard compounds obtained from recycled polyethylene, wood powder or commercial lignin and powder and compatibility agent in different percentages 77/20/3 or 67/

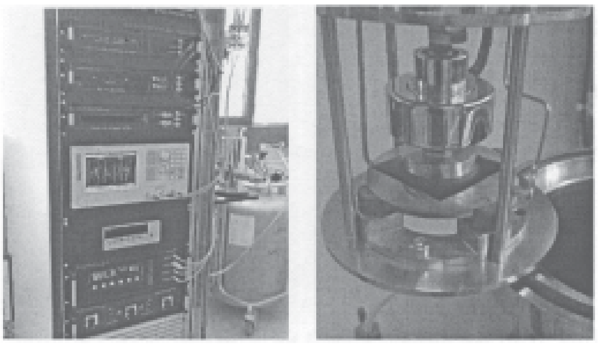

Fig. 4. Broadband dielectric analyzer Concept 80 Novocontrol GmbH, Germany and sample of material sandwiched between two 20 mm gold plated electrodes tested within Active Sample Cell 30/3.

Results and discussions

Including wood powder and lignin in the polyolefin matrix lead to changes in a wide range of dielectric characteristics and because of that dielectric properties evaluation is absolutely necessary.

The experimentally results are correlated and discussed in connection with dielectric characteristics of recycled polyethylene matrix (RPE) and board transformer characteristics (TB). Features permittivity (ε') and dielectric loss (tan δ) for mixtures of recycled polyethylene / wood powder or lignin and C1803 compatibility agent, added as filler, the frequency of applied field are presented graphically in figures 5 and 6.

Applying an electric field on probes is observed as the most significant variation is found in transformer board frequency, especially at frequencies below 50Hz. In absolute values, the dielectric constant for samples with 20% wood powder is about. 50% higher than for samples obtained from RPE without addition or with addition of lignin.

The influence of chemical structure of natural polymers in wood powder, highly polar, is close to the values determined homologous transformer board. By comparison

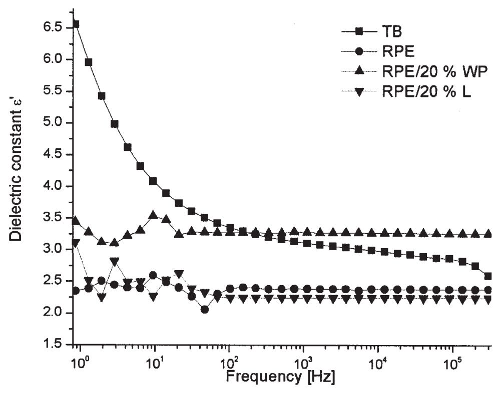

Fig. 5. Variation of dielectric constant ε' vs. frequency for studied blends

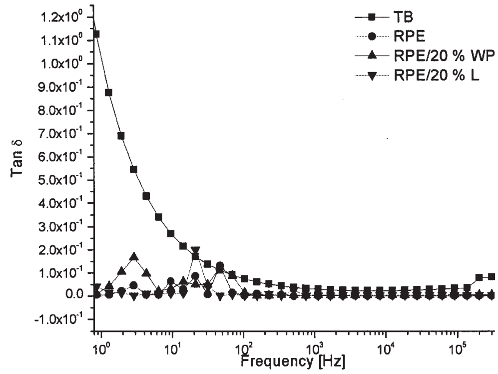

Fig. 6. Variation of tan (δ) vs. frequency for studied blends

with cardboard transformer characteristics obtained for composite materials have higher frequency stability.

Overall, it is anticipated that materials made from 20% RPE wood powder can be used for transformers as transformer board. Further considering the composite material with 30% wood powder/lignin to identify possible applications in the electrical industry, figure 7.

The characteristic of dielectric constant with 30% WP shown a slight increase compared with recycled polymeric matrix. Also, characteristics of dielectric loss tan (δ) for these materials are comparable with those of composite materials containing 20% filler, the effect of interfacial exchange is diminished, figure 8.

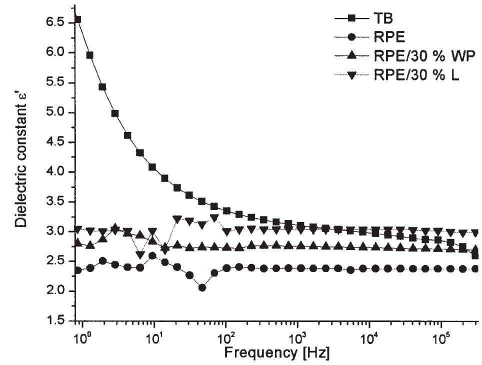

Fig. 7 Variation of dielectric constant ε' vs. frequency for studied blends

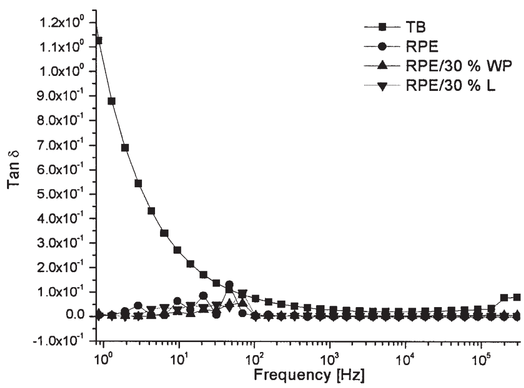

Fig. 8 Variation of tan (δ) function of frequency for studied blends

Tabel 1
DIELECTRIC PARAMETERS FOR TRANSFORMER BOARD (TB), RECYCLED POLYETHYLENE AND RECYCLED POLYETHYLENE WITH 20% WOOD POWDER

Dielectric properties	Frequency [Hz]	Transformer board (TB)	RPE	RPE/20% WP
Conductivity σ, S × cm	60 Hz	$2,506 \cdot 10^{-10}$	$1.27 \cdot 10^{-12}$	$4.132 \cdot 10^{-8}$
	100 Hz	$3.268 \cdot 10^{-10}$	$4.72 \cdot 10^{-13}$	$7.341 \cdot 10^{-9}$
	1000 Hz	$8.508 \cdot 10^{-10}$	$2.29 \cdot 10^{-12}$	$9.744 \cdot 10^{-8}$
Resistivity ρ_v, Ohm × cm	60 Hz	$3.987 \cdot 10^{9}$	$7.87 \cdot 10^{11}$	$2.419 \cdot 10^{15}$
	100 Hz	$3.059 \cdot 10^{9}$	$2.11 \cdot 10^{12}$	$1.362 \cdot 10^{15}$
	1000 Hz	$1.175 \cdot 10^{9}$	$4.35 \cdot 10^{11}$	$1.026 \cdot 10^{15}$
Impedance Z_p, Ohm	60 Hz	$1.270 \cdot 10^{8}$	$6.26 \cdot 10^{9}$	$3.851 \cdot 10^{13}$
	100 Hz	$9.738 \cdot 10^{7}$	$1.68 \cdot 10^{10}$	$2.167 \cdot 10^{14}$
	1000 Hz	$3.740 \cdot 10^{7}$	$3.46 \cdot 10^{9}$	$1.633 \cdot 10^{13}$
Capacity C_p, F	60 Hz	$2.627 \cdot 10^{-11}$	$2.56 * 10^{-11}$	$2.256 \cdot 10^{-7}$
	100 Hz	$2.252 \cdot 10^{-11}$	$2.65 \cdot 10^{-11}$	$2.363 \cdot 10^{-7}$
	1000 Hz	$1.683 \cdot 10^{-11}$	$2.65 \cdot 10^{-11}$	$2.349 \cdot 10^{-7}$

It can be concluded that composite material with 20% wood powder is closest to the values of transformer board. In these conditions and other dielectric properties were investigated for composite material containing 20% of wood powder, which are presented in table 1.

Dielectric characteristic values for composites with 20% wood powder, which are comparable to those of transformer board, but because European law requires the use of recycled materials in various sectors, these materials can be a viable technical solution to cardboard partially replace transformers and transformer design electric cars, given that TB technology, which is very selective with the timber used has implications on the environment and biodiversity [7].

Conclusions

Increased demand for plastics in various sectors, coupled with continuous decrease of resources, lead researchers to consider any possibility of recycling waste plastic top.

Dielectric spectroscopy is a very powerful method to investigate in detail the dynamic processes of composite materials and development of new materials. Dielectric properties have significant changes in the frequency range 0-100 Hz. Additions RPE matrix materials having strong polar (wood powder min. Lignin 20% or min. 30%), significantly influence the permittivity and dielectric loss of composites. Noteworthy is that in the frequency range between 10 and 10^5 Hz dielectric constant is compared with the values of transformer board.

Dielectric characteristics obtained for composite materials studied by 20% wood powder have similar values, but also high stability frequency to TB, which indicates that a viable technical solution to partially replace the transformer cartoon transformers and electrical machines construction, given that TB technology, which is very selective with the timber used has implications on the environment and biodiversity.

Acknowledgment: This paper was supported by the project "Development and support of multidisciplinary postdoctoral programmes in major technical areas of national strategy of Research - Development - Innovation" 4D-POSTDOC, contract no. POSDRU/89/ 1.5/S/52603, project co-funded by the European Social Fund through Sectoral Operational Programme Human Resources Development 2007-2013.

Reference

1. *** www.plasticseurope.org, Plastics – the Facts 2012 - PlasticsEurope
2. VASILE C., IWANCZUK A.., FRACKOWIAK S., CAZACU G., CONSTANTINESCU G., KOZLOWSKI M., Modified lignin /polyethylene blends, Cellulose Chem. Technol., (2006), 40 (5), pp.345-351.
3. ARADOAEI S., CIOBANU R., TRANDABAT A.., CONSTANTINESCU G., 8th IEEE ICSD, Toulouse, France, (2004), pp. 462–465.
4. CIOBANU R., ARADOAEI S., TRANDABAT A., CONSTANTINESCU G., Knowledge-based Bio-Compounds from Recycled PE/PET and Wood Derivates: Technological Analysis, Properties, and Perspectives, Proceedings of 10th OPTIM, Brasov, Romania, (2006) vol. 1, pp. 117-122.
5. ARADOAEI S., DARIE R., CONSTANTINESCU G., OLARIU M., CIOBANU R., Journal of Non-Crystalline Solids, Article Number: 14511, 2010.
6. ZHAO J., RU-MIN W., NING L., Advance in apllication of vegetable cellulose in biodegradable composite – Suliao Gongye, China (2004), 32(11), pag.1-3, 18
7. LABUZEK S., BOZENA N., Biodegradation of an aged composite of polyethylene with a synthetic polyester. Poland Polimery, (2006), 51(1), 27-32

Manuscript received: 24.04.2013

Solid State Phenomena Vol. 188 (2012) pp 268-274
Online available since 2012/May/14 at www.scientific.net

doi:10.4028/www.scientific.net/SSP.188.268

Morphology and dielectric properties of some LDPE/PA blends in presence of compatibilizers

ARADOAEI Sebastian Teodor[1, a], DARIE Raluca Nicoleta[2,b], VASILE Cornelia[3,c], MOSNEAGU Mihaela[1,d] and OLARIU Marius Andrei[1,e]

[1]Technical University of Iasi, Department of Electrical Measurements and Materials, Blvd. D. Mangeron 53, 70050 Iasi, Romania

[2]Romanian Academy, "Petru Poni" Institute of Macromolecular Chemistry, 41 A Gr. Ghica Voda Alley, 700487, Iasi, Romania

[a]asteor@yahoo.com

Keywords: low density polyethylene, polyamide, compatibilizing agents, scanning electron microscopy tests, dielectric spectroscopy analysis.

Abstract. The article emphasizes the improvement of compatibility in a polymer blend composed of two normally incompatible constituents as LDPE and PA6. The effect of amount and type of compatibilizing agents is evaluated using electronic microscopy and dielectric spectroscopy, to obtain the optimum materials structure.

Introduction

Interest in blending polyethylene with polyamide is due to the differences in their properties, mainly the barrier properties. Polyethylene transmits oxygen and hydrocarbons but it is resistant to moisture. Polyamide is highly sensitive to moisture but a good oxygen barrier. Thus, the main applications of the two polymers are in packaging films and containers requiring low permeability. Another disadvantage of polyamides is their low resistance to stress in the presence of sharp notches or cracks, commonly evaluated as notched impact strength. To overcome this deficiency, polyamides have been blended with several types of impact modifiers, typically elastomeric or low modulus type olefinic polymers. Compatibilizers, which reduce the interfacial tension and stabilize the dispersed structure, can be added to improve the properties of polyethylene/polyamide blends [1].

In order to improve the compatibility in a polymer blend composed of two normally incompatible constituents as LDPE and PA6, a small amount of rubbery phase and different types of compatibilizers have been added, in other words, applying reactive compatibilization cumulated with the impact modification, because LDPE presents poor reactivity and PA contains carboxyl and amino- end groups as well as amidic bonds. In a previous study the efficiency of some compatibilizers upon thermal and impact properties has been proved [2]. In this work, the compatibilization effect was evaluated by analyzing the melt processing, morphology and dielectric properties.

Experimental Part

Materials. Low density polyethylene (LDPE) offered by Petrochemia Plock S.A., Poland, MALEN-E type, FABS, 23-D022, granules. This type includes antioxidant, antiblock and slip additives and has been foreseen for thin packaging films (30 micrometer thickness), possible injection molding applications and has the following characteristics: MFI 1,6-2,5 g/10 min; density 0,919-0,923 g/cm^3; Vicat min. 90^{o}C, swelling index max. 160%; tensile stress at break min. 11MPa; Mn 10.580; Mw 66.000.

Polyamide 6 (PA6*)* STILAMID S type, supplied by STILON, Gorzow, Poland, having melting temperature T_m = 221 ^oC, decomposition temperature range of 297-492 ^oC, tensile strength at yield of 78±4 MPa, Charpy impact strength with notch of 5.0±0.1 kJ/m^2, hardness HK = 122±3 MPa, moisture content at 20 ^oC was max. 0.1 wt%, free amino groups of 45-47 mval/kg, density of 1.14 g/cm^3.

Ethylene-propylene-1, 4 hexadiene terpolimer (EPDM) Buna EP 5450G type from BAYER AG Germany has a decomposition temperature range of 223-487 ^oC, Money viscosity of 46±5 (MS 1+4; 121 ^oC) (DIN 53523), ash content < 0.2 wt% (DIN 53568), volatiles = 0.5 wt% (DIN 53526), density = 0.86g/cm^3.

LDPE melt functionalization was performed in a laboratory installation, according to the procedure previously described [3]. Low density polyethylene was functionalized with either acrylic acid (LDPE/AA), maleic anhydride (LDPE/MA) or bismaleimide (LDPE/BMI). The comonomer content was determined by the titration method. In respective samples it accounted to 1.05 •10^{-4} mole of grafted acrylic acid/100 g sample, 2.3 •10^{-4} mole of maleic anhydride/100 g sample or 0.7 •10^{-4} mole of grafted bismaleimide/ 100 g sample.

Blending procedure. All main polymers used for this study in their neat form were processed in the similar manner as that of a blend. This was to ensure that the neat polymers and the blends had similar thermal history, so as to minimize any possible effects on the subsequent tests due to processing discrepancy in the upstream preparation work.

The binary, ternary and compatibilized blends containing LDPE, PA6, EPDM and reactive compatibilizing agent as functionalized LDPE have been processed by melt mixing in a counter-rotating twin rotor HAAKE RHEOCORD 9000 mixer. The following operational conditions have been used for blending: temperature of mixing of 220^{o}C, mixing time of 10 minutes, and the rotational speed of 60 rpm. The blends with the mixing ratios presented in the first column of the Table 1. have been obtained. The LDPE/PA6 ratio used was of 66.7/33.3 and 10 wt% of EPDM were added in ternary blends.

The content of functionalized LDPE (LDPE-MA, LDPE-BMI and LDPE-AA) in the ternary blend was 3 and 5 wt% in respect with initial amount of LDPE used in the blends. Before mixing, the components were dried in a vacuum oven for 24 hours at a temperature of 80^{o}C to remove most of the absorbed humidity.

Investigation method. Processing behavior was evaluated from the torque-time curves recorded during the blending on a HAAKE Rheocord 9000 mixer.

Scanning Electron Microscopy (SEM) test – blend's morphology has been analyzed by means of an electronic microscope VEGA. The samples have been obtained by fracture in liquid nitrogen and etched with gold before the morphological examination. The coated surface had a thickness of ~ 18 nm.

Broadband Dielectric Spectroscopy measurements were carried out with a Novocontrol Concept 80 [4].Dielectric Spectroscopy it's a powerful technique to evaluate the different molecular mobility's of nanostructured complex systems.

Processing behavior. The processing behavior was evaluated from the torque-time curves recorded during previously described blend preparation. The following characteristics were evaluated: torque at 1 min mixing time (TQ_{1min}) and at the end of mixing (TQ_{end}) as well as the specific energy after one minute of mixing ($Emix_{1min}$ - energy required to process a unit mass of material) [4]. At a constant speed of mixing, variation in torque among samples at the same temperature is indicative the viscosity differences, since viscosity is proportional to the torque.

The processing characteristics depend on blend composition (Table 1). Increase in the viscosity is more obvious in the presence of the functionalized LDPE. It can observe that the presence of EPDM in ternary LDPE/PA/EPDM blends led to the increase of viscosity and further to a finer dispersion of the components (as it is shown also in SEM results – see below).

Table 1. Processing behavior for binary, ternary and compatibilizer blends

Sample[a]	$TQ_{1\ min}$ [Nm]	TQ_{fin} [Nm]	E_{mix} [J/g]
67LDPE/33PA6	8.2	3.2	92
60LDPE/30PA6/10EPDM	9.4	4.6	107
60LDPE/30PA6/10EPDM+3%LDPE-BMI	10.0	4.4	113
60LDPE/30PA6/10EPDM+3%LDPE-AM	9.6	4.4	105
60LDPE/30PA6/10EPDM+3%LDPE-AA	9.2	3.6	104
60LDPE/30PA6/10EPDM+5%LDPE-BMI	9.4	4.5	106
60LDPE/30PA6/10EPDM+5%LDPE-AM	11.0	5.4	124
60LDPE/30PA6/10EPDM+5%LDPE-AA	9.8	4.6	110

[a] The symbol of the samples includes weight percentage followed by respective polymer abbreviation

When LDPE-MA and LDPE-BMI compatibilizing agents were introduced in ternary systems, higher values of torques and specific energy after one minute of mixing have been recorded. The increase of the melt viscosity could be explained by the chemical reactions appearing in the systems between the functional groups of modified LDPE and amino or amide groups of PA leading to "in situ" formation of LDPE-g-PA grafted copolymer placed at the interface between the main components. Due to the low amount of acrylic acid grafted in LDPE-AA, the best processing characteristics have been observed for 5 wt% LDPE-AA used in the ternary blends instead of 3 wt%. The evolution of specific energy of mixing depending on the blend's type is similar with the explanations for torque variation.

Results and discussions

SEM results. The examination of the fractured surfaces by electronic microscopy (SEM) offers some information's on the effect of the EPDM and compatibilizing agents presence over the studied blends morphology. The morphology of LDPE/PA blends is illustrated by the micrographs shown in figure 1-5.

An ordered distribution of the dispersed phase is observed even for the binary blend, the difference between binary and compatibilized blends being the particles dimensions. Nevertheless, the biphasic nature of these blends is revealed quite clearly by the granularity of the fracture surfaces of the specimens. The distribution width has a value of 7.6 µm for binary 67LDPE/33PA6 blend (Table 2). In the compatibilized blends, the morphology is changed, the average size of the droplets is reduced considerably and the dispersion of the minor phase is improved, the finest distribution (from 4.1 µm for binary 67LDPE/33PA6 blend to 2.2 µm in compatibilized blend) being obtained when LDPE-MA is incorporated it being the most efficient compatibilizing agent for all the compositions of the studied blends.

Table 2. Morphological characteristics of LDPE/PA6/EPDM blends

Sample	Average particle size [µm]	Distribution width [µm]
67LDPE/33PA6	4.1	7.6
60LDPE/30PA6/10EPDM	3.8	4.8
60LDPE/30PA6/10EPDM + 3 PP-BMI	3.9	4.4
60LDPE/30PA6/10EPDM + 3 PP-MA	2.2	1.9
60LDPE/30PA6/10EPDM + 3 PP-AA	4.0	4.5

The explanation could be that the presence of compatibilizing agents resulted in reduction of interfacial tension between blend components and this behavior could be due to the interfacial reactions of the carboxyl or imide groups of the functionalized LDPEs with the polar groups of polyamide forming "in situ" copolymers placed at the interphase of LDPE and PA6.

The compatibilizing effect doesn't lead to the total disappearance of the phase separation, but to an enhancement of the phase's dispersion and adhesion, the dimensions of the dispersed particles representing in these systems a critical factor in mechanical properties controlling, especially for impact strength.

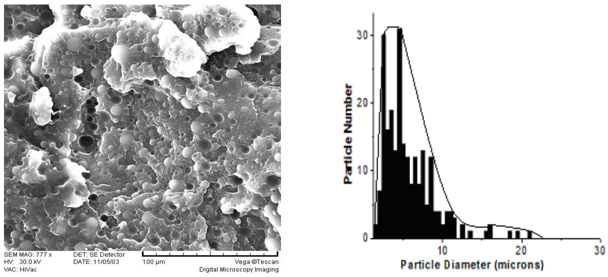

Fig.1 SEM micrographs for 66.67LDPE/33.33PA6 blend

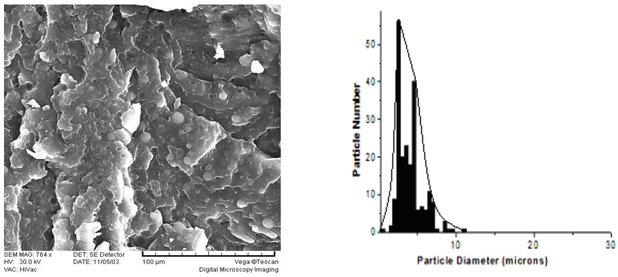

Fig.2 SEM micrographs for 60LDPE/30PA6/10EPDM blend

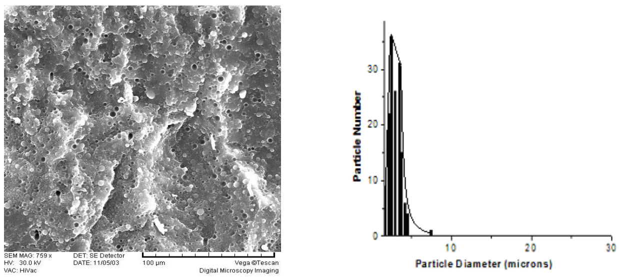

Fig.3 SEM micrographs for 60LDPE/30PA6/10EPDM + 3wt% LDPE-AM blend

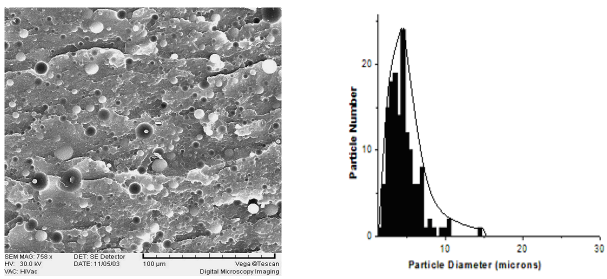

Fig.4 SEM micrographs for 60LDPE/30PA6/10EPDM + 3wt% LDPE-BMI blend

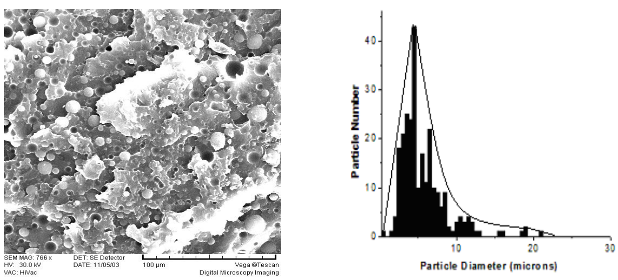

Fig.5 SEM micrographs for 60LDPE/30PA6/10EPDM + 3wt% LDPE-AA blend

Broadband dielectric spectroscopy analysis. Spectra were collected using a Novocontrol GmbH Concept 80 Broadband Dielectric Spectrometer with an Alpha A analyzer over the frequency range of 0.01 Hz to 20 MHz. Samples of the PA6/LDPE blend with a thickness of 0.8 mm were sandwiched between two gold plated electrodes, with 20 mm diameter.

Dielectric spectroscopy method was used to investigate relaxation processes in the blends. Using this method was obtained important dielectric characteristics like dielectric constant and dielectric loss which give valuable information about molecular dipole fluctuations.

From figure 6 is observed clear differences between LDPE and PA6, and 67LDPE/33PA6 blend seems to be the most optimal to achieve good compatibility between the two materials and occupies the middle position in the dielectric characteristics.

From characteristic of dielectric constant is obvious that by introducing EPDM in PA6/LDPE blend, the dielectric constant of the material decreases to 5.5, compared with 67LDPE/33PA6 blend which is 6.3, figure 6. This can be explained by a more homogeneous structure of the mixture.

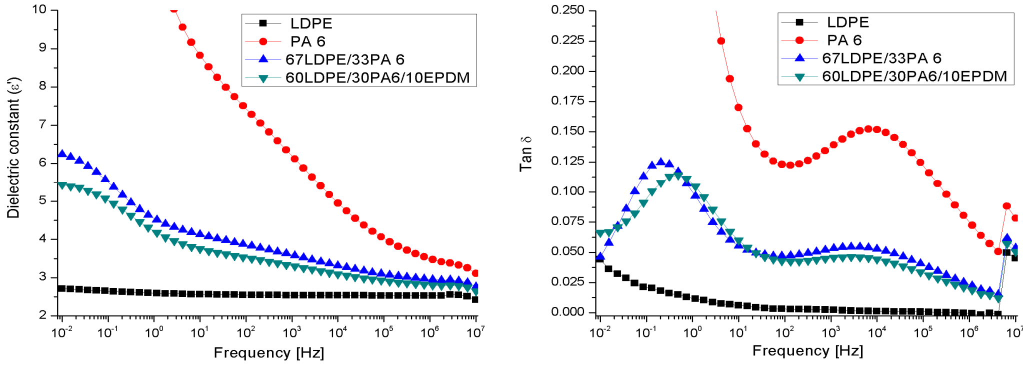

Fig. 6 Variation of dielectric constant ε ’ and tan (δ) function of frequency for studied blends.

By introducing functionalized LDPE, the dielectric characteristics curves decrease in terms of percentage added. Therefore, its observed that by introducing a 3% of functionalized LDPE there is a decrease of dielectric constant values when is compared with the 67LDPE/33PA6 blend, the most pronounced being recorded for the dielectric constants of LDPE–BMI and LDPE–AM blends, which reach the value 4.2, figure 7. Also, can be observed that the dielectric losses are the lowest for LDPE-AM blend.

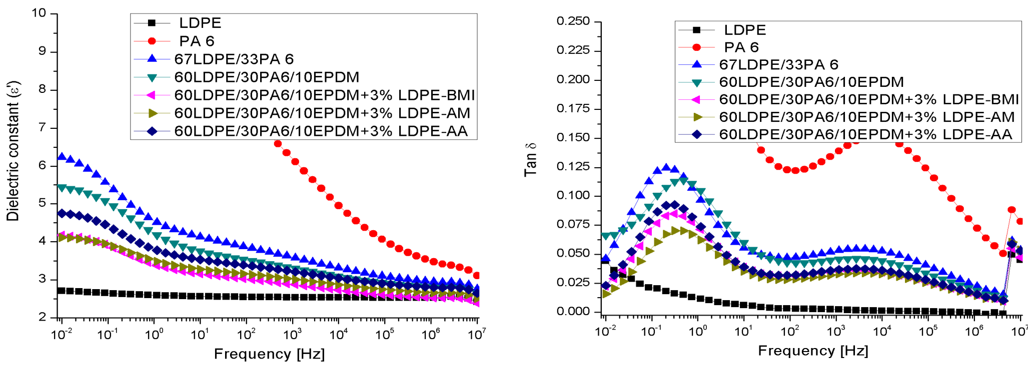

Fig. 7 Variation of dielectric constant ε ’ and tan (δ) function of frequency for studied blends with 3% of compatibilizing agents.

When the percentage of functionalized LDPE increases the amount of 5% decrease observed for LDPE (MA, AA, BMI) is more pronounced compared with 67LDPE/33PA6 blend, the dielectric characteristic values for these mixtures is in the range 3.8-3.9, figure 8.

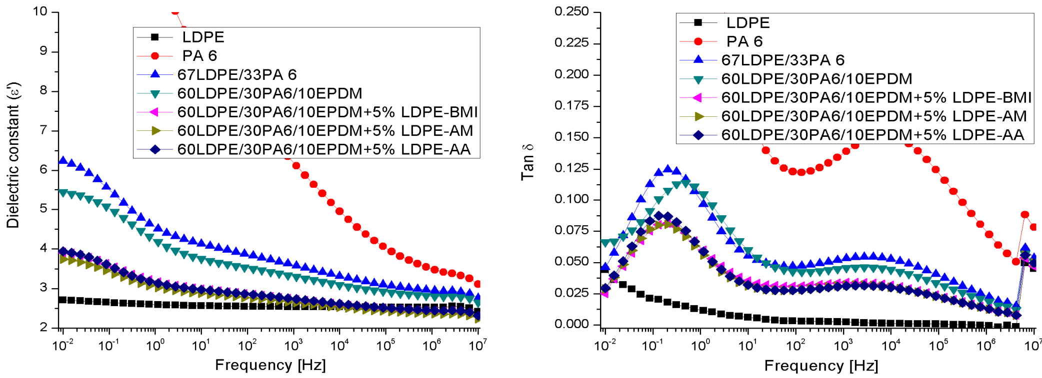

Fig. 8 Variation of dielectric constant ε ’ and tan (δ) function of frequency for studied blends with 5% of compatibilizing agents.

The dielectric characteristics provide conclusive information on the effects of quantity and type of compatibility agents as AA, AM, BMI on the obtained blend structure. From the dielectric characteristics it is observed that 3% of LDPE is the most recommended and the dielectric characteristics of functionalized LDPE with BMI and AM are placed between of LDPE and 67LDPE/33PA6 curves.

Analyzing the dielectric characteristics dielectric constant ε ’ and tan δ and taking into account the morphological characteristics obtained under an electronic microscop can be considered as LDPE-AM is the best compatibility between LDPE agent and PA6.

Conclusions

A new method consisting in reactive compatibilization correlated with the impact modification has been performed in order to realize a better compatibility between LDPE and PA phases and consequently obtaining enhanced properties.

The binary PP/PA6 and LDPE/PA6 blends are incompatible due to the structural difference of the components, presenting an obvious phase separation. The general improvement of the morphology for the compatibilized blends has been explained by the chemical reactions between the polar groups of the functionalized LDPE and the functional end or inner groups of PA, when the copolymer LDPE-g-PA is formed at the interface between the two separated phases and reduces the phase dimensions, producing a more stable morphology by reducing the rate of coalescence during melt processing, in addition to strengthening the interface between the two phases.

Spectra collected using dielectric spectroscopy provides valuable information about the structure of mixtures. The effect produced by the quantity and type of compatibilizing agents are obvious and it seems that reduce interfacial tension and led to a better adhesion between blend components.

Thus, it was noted that to achieve optimal coupling process and a homogenous structure of LDPE/PA mixture, containing 3% of functionalized LDPE MA appears to be most suitable.

Acknowledgment

This paper was supported by the project "Development and support of multidisciplinary postdoctoral programmes in major technical areas of national strategy of Research - Development - Innovation" 4D-POSTDOC, contract no. POSDRU/89/1.5/S/52603, project co-funded by the European Social Fund through Sectoral Operational Programme Human Resources Development 2007-2013 and the project PERFORM-ERA "Postdoctoral Performance for Integration in the European Research Area" (ID-57649), financed by the European Social Fund and the Romanian Government.

References

[1] M.K. Akkapeddi, Commercial polymer blends, in Polymer Blends Handbook, Vol 2, Utracki, L.A. (Eds.), Kluwer Academic Publishers, Dordrecht, 2002, pp.1023-1115.

[2] R.N. Darie, C. Vasile, M. Kozlowski, The effect of compatibilization in the reactive processing of the low density polyethylene/polyamide 6/EPDM blends, Polimery, 51 (9), (2006) 656-661.

[3] R. Darie N, C. Vasile, H. Darie, Chemical modification of PE-LD by using polar monomers, in: Global Symposium on Recycling, Waste Treatment and Clean Technology, REWAS'04, Vol. III, Gaballah I., Mishra R., Solozabal R., Tanaka M (Eds.), 2004, pp. 2923.

[4] S. Aradoaei, R. Darie, G. Constantinescu, M. Olariu, R. Ciobanu, Modified lignin effectiveness as compatibilizer for PET/LDPE blends containing secondary materials, Journal of Non-Crystalline Solids, Vol.356, 2010, pp.768-771.

Advanced Materials and Structures IV
10.4028/www.scientific.net/SSP.188

Morphology and Dielectric Properties of some LDPE/PA Blends in Presence of Compatibilizers

10.4028/www.scientific.net/SSP.188.268

BULETINUL INSTITUTULUI POLITEHNIC DIN IAŞI
Publicat de
Universitatea Tehnică „Gheorghe Asachi” din Iaşi
Volumul 63 (67), Numărul 2, 2017
Secţia
ELECTROTEHNICĂ. ENERGETICĂ. ELECTRONICĂ

SYMMERICAL COMPONENTS EVALUATION IN REAL-TIME

BY

SEBASTIAN ARADOAEI and OLGA PLOPA*

Technical University “Gheorghe Asachi” of Iaşi,
Faculty of Electrical Engineering, Energetics
and Applied Informatics

Received: April 25, 2017
Accepted for publication: May 26, 2017

Abstract. Using Symmetrical components methodology, unbalanced system conditions, like those caused by common fault types may be visualized and analyzed. In order to calculate direct and inverse components, the phasors must be multiplied by the phasor rotation operator $\underline{a}=e^{j2\pi/3}$. The classical mathematical expressions associated with this issue are well-suited especially in phasic calculus. However, in the time domain, the authors do not offer practical solutions. The paper presents concrete ways to solve the problem of rotating a sinusoidal size in real-time using PSpice and Matlab Simulink software. Based on these, the real and the inverse components of an unbalanced three-phase system are determined in real time.

Key words: symmetrical components; PSpice; Simulink; electrical machines.

1. Introduction

Symmetrical components is a methodology discovered by Charles Legeyt Fortescue. He demonstrated that any set of unbalanced three-phase quantities could be expressed as the sum of three symmetrical sets of balanced phasors (Fortescue, 1918). Using this tool, unbalanced system conditions, like

*Corresponding author: *e-mail*: asteor@yahoo.com

those caused by common fault types may be visualized and analyzed. The method of symmetrical components is usually used in power systems to simplify the analysis of unbalanced three-phase systems. In the most common case of three-phase system, the resulting symmetrical components are referred as direct (or positive), inverse (or negative) and homopolar (or zero). The resulting transform equations are mutually linearly independent.

The basic idea is that an asymmetrical set of three phasors can be expressed as a linear combination of three symmetrical sets of phasors by means of a complex linear transformation.

The first application of the symmetrical components to the electrical machines was described by Lyon (1954). In addition, other authors have developed studies on the use of symmetrical components in the study of electric machines (White & Woodson, 1959; Harris *et al.*, 1970; Paap, 2000).

A study on the possibility of using symmetrical components method in the analysis of induction machine behavior is presented in (Cociu & Cociu, 2014). Starting from the observation that induction machine is described by a system generally of nonlinear equations, the authors try to determine the circumstances in which this method can be used in studying the behavior of the induction machine.

Consider a three-phase (asymmetric) system of sinusoidal quantities with the same pulse ω, the amplitude and the initial phase having an arbitrary value, generally different for each voltage:

$$\begin{aligned} v_a(t) &= \sqrt{2}V_a \sin(\omega t + \gamma_a) \\ v_b(t) &= \sqrt{2}V_b \sin(\omega t + \gamma_b) \\ v_c(t) &= \sqrt{2}V_c \sin(\omega t + \gamma_c) \end{aligned} \tag{1}$$

These quantities can be mapped to their corresponding complex phasors:

$$\begin{aligned} \underline{V}_a &= V_a e^{j\gamma_a} \\ \underline{V}_b &= V_b e^{j\gamma_b} \\ \underline{V}_c &= V_c e^{j\gamma_c} \end{aligned} \tag{2}$$

According to symmetrical components method, they can be expressed as:

$$\begin{aligned} \underline{V}_a &= \underline{V}_{ad} + \underline{V}_{ai} + \underline{V}_0 \\ \underline{V}_b &= \underline{V}_{bd} + \underline{V}_{bi} + \underline{V}_0 \\ \underline{V}_c &= \underline{V}_{cd} + \underline{V}_{ci} + \underline{V}_0 \end{aligned} \tag{3}$$

The system is uniquely determined by the origin vectors:

$$\begin{aligned}\underline{V}_d &= (\underline{V}_a + \underline{a} \cdot \underline{V}_b + \underline{a}^2 \cdot \underline{V}_c)/3 = \underline{V}_{ad} \\ \underline{V}_i &= (\underline{V}_a + \underline{a}^2 \cdot \underline{V}_b + \underline{a} \cdot \underline{V}_c)/3 = \underline{V}_{ai}\end{aligned} \tag{4}$$

$$\underline{V}_0 = (\underline{V}_a + \underline{V}_b + \underline{V}_c)/3 \tag{5}$$

where: $\underline{a}$ is a phasor rotation operator which rotates a phasor vector counterclockwise by 120 degree.

From eq. (4), for the determination of the direct and inverse phase component of the three voltages we must multiply with $\underline{a}$ and $\underline{a}^2$. In the time domain it corresponds to phasing sinusoidal quantities $v_x(t)$ with $2\pi/3$ or $4\pi/3$ radians respectively. The same problem applied to two-dimensional sizes requires shifting.

2. Theoretical Part

The paper aims is to solve in real time the problem of determining a sinusoidal quantities with the angle θ, fig. 1.

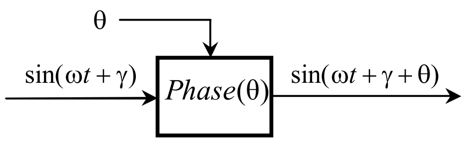

Fig. 1 – Phase modifying of a sinusoidal quantity.

Consider a sinusoidal quantity (voltage) with amplitude value equal to 1, pulse ω, and initial phase γ:

$$v_x(t) = \sin(\omega t + \gamma) \tag{6}$$

The quantity to be determined has the expression:

$$v_y(t) = \sin(\omega t + \gamma + \theta) \tag{7}$$

Applying trigonometric formulas:

$$v_y(t) = \sin(\omega t + \gamma + \theta) = \sin(\omega t + \gamma)\cos(\theta) + \sin(\theta)\cos(\omega t + \gamma) \tag{8}$$

On the other hand,

$$\cos(\omega t+\gamma)=\frac{1}{\omega}\cdot\frac{\mathrm{d}[\sin(\omega t+\gamma)]}{\mathrm{d}t}=\frac{1}{\omega}\cdot\frac{\mathrm{d}[v_x(t)]}{\mathrm{d}t}, \tag{9}$$

resulting:

$$v_y(t)=v_x\cos(\theta)+\sin(\theta)\frac{1}{\omega}\cdot\frac{\mathrm{d}(v_x)}{\mathrm{d}t}. \tag{10}$$

Eq. (10) allows the sinusoidal quantities to be determined for the angle θ starting from any sinusoidal size. Note that, pulse ω must be known. Otherwise it should be determined. When a machine is supplied from the network, the fundamental frequency is constant over time or over large time intervals. In the worst case, the frequency can be measured for a large interval of time and its value used as an input constant. This gives $\omega(t)$ = const = ω. (Cociu & Cociu, 2017).

3. Pspice Implementation of the Derivative

The starting point is to evaluate the possibility of determining the sinusoidal quantities using eq. (10). As it turns out, it is necessary to determine the derivative of a quantities variable in time. Consider an ordinary first order differential equation:

$$y(t)=a\frac{\mathrm{d}x}{\mathrm{d}t}. \tag{11}$$

which in Simulink does not raise problems to compute because there is a specialized block for this mathematical operation (Fig. 2).

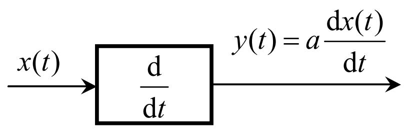

Fig. 2 – Derivative block in Simulink

PSpice integration of differential equations is usually performed by means of generic integrators that are obtained by implementing electric circuits comprising controlled voltage – E (or current – G) sources, capacitors and inductors (Justus, 1993). The sources allow describing the forcing terms, the inductors and capacitors accomplish the derivative terms. The result is obviously a voltage or current whose value is numerically equal to the desired quantity.

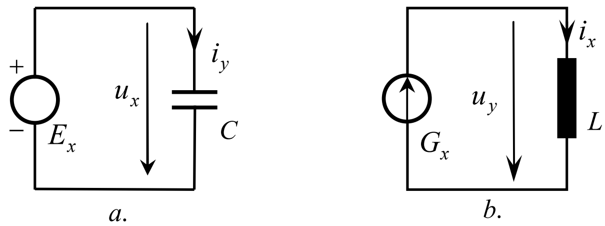

Fig. 3 – Generic integrators.

As show in Fig. 3 *a*, the relationship among currents and voltages:

$$i_y(t) = C\frac{\mathrm{d}u_x(t)}{\mathrm{d}t} \leftrightarrow y(t) = a\frac{\mathrm{d}x(t)}{\mathrm{d}t} \tag{12}$$

Identifying terms gives correspondence between the variables and parameters.

$$\begin{array}{ccc} y & \leftrightarrow & i_y \\ x & \leftrightarrow & u_x \end{array}, \quad a \leftrightarrow C \tag{13}$$

For the circuit in Fig. 3 *b*:

$$u_y(t) = L\frac{\mathrm{d}i_x(t)}{\mathrm{d}t} \quad \leftrightarrow \quad y(t) = a\frac{\mathrm{d}x(t)}{\mathrm{d}t} \tag{14}$$

$$\begin{array}{ccc} y & \leftrightarrow & u_y \\ x & \leftrightarrow & i_x \end{array}, \quad a \leftrightarrow L \tag{15}$$

Based on both the correspondences, of variables and parameters, above mentioned, in order to solve eq. (8) two possible integrator configurations can be used, as shown in Fig. 3.

The PSpice code for the two integrators to be used in practice are comparatively given below:

case a.

```
.param w=10
Ex 0 x Value={sin(w*time)}
C x 0 {1/w}
Rx 0 x 1meg
.probe
.tran 0.1 10 0 0.1m
.end
```

case b.

```
.param w=10
Gx 0 y Value={sin(w*time)}
Lj  y 0 {Ljj}
Ry g y {1/w}
.probe
.tran 0.1 10 0 0.1m
.end
```

The case *a* is superior from both points of view, of integration time and data output file size. This is due to the circuit topology description in PSpice where, even if the two electrical circuits contain the same number of nodes, PSpice description of case a comprises only two nodes where as the description in case b has three nodes.

This method of solving differential equations have been widely used for modeling and simulating the motion mass equation (Cociu & Cociu, 2011), (Cociu & Cociu, 2014).

In Fig. 4 are presented the results obtained using an input signal $v_x(t) = 324\sin(\omega t - 2\pi/3)$ and $\theta = 3\pi/4$.

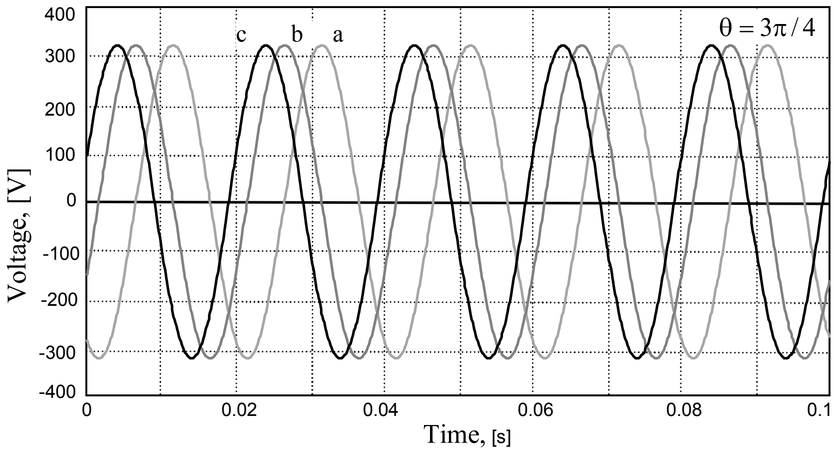

Fig. 4 – Input and output signal waveform;
a – $v_x(t)$; b – $\mathrm{d}/\mathrm{d}t[v_x(t)]/\omega$; c – $v_y(t)$

4. Symmetrical Components Evaluation in Real-Time Using Pspice and Simulink

The calculation of symmetric components v_d, v_i, v_0 of an unbalanced three-phase voltage system v_a, v_b, v_c is performed based on the block diagram in Fig. 5.

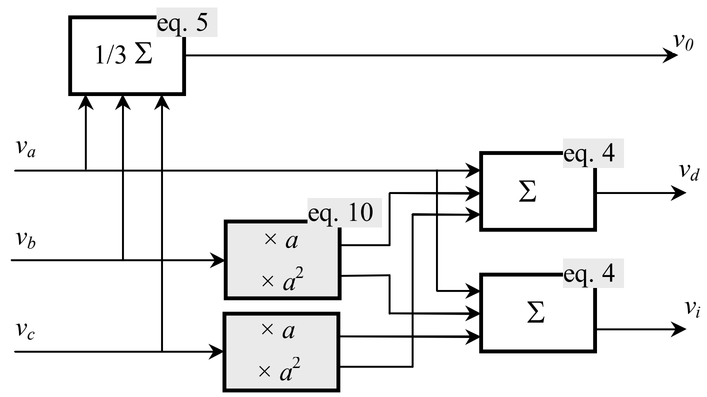

Fig. 5 – Unbalanced three-phase voltage system block diagram.

The implementation of component blocks in PSpice leads to the text-based source program presented below:

```
Symmetrical components calculus
** Parameters
.param w={100*pi}
.param Vam=324, ga=0
.param Vbm=324, gb={-2*pi/3}
.param Vcm=162, gc={+2*pi/3}
.param a1=(2*pi/3)
.param a2=(-2*pi/3)
** Unbalanced three-phase voltage system
Ea a 0 Value={Vam*sin(w*time+ga)}
Eb b 0 Value={Vbm*sin(w*time+gb)}
Ec c 0 Value={Vcm*sin(w*time+gc)}
Ra a 0 1
Rb b 0 1
Rc c 0 1
**Homopolar component calculus "0"
Eh h 0 Value={(V(a)+V(b)+V(c))/3}
Rh h 0 1
** Rotation: a1 and a2 *
Eba1 ba1 0 Value={V(b)*cos(a1)+sin(a1)*V(bder)}
Eba2 ba2 0 Value={V(b)*cos(a2)+sin(a2)*V(bder)}
Eca1 ca1 0 Value={V(c)*cos(a1)+sin(a1)*V(cder)}
Eca2 ca2 0 Value={V(c)*cos(a2)+sin(a2)*V(cder)}
Gb  0 bder Value={V(b)}
Gc  0 cder Value={V(c)}
Lb  bder 0 {1/w}
Lc  cder 0 {1/w}
```

```
** Direct component calculus "d"*
Ead ad 0 Value={(V(a)+V(ba1)+V(ca2))/3}
Rad ad 0 1
** indirect component calculus "i"*
Eai ai 0 Value={(V(a)+V(ba2)+V(ca1))/3}
Rai ai 0 1
**
.probe
.tran 0.01 0.1 0.1m 0.1m uic
.end
```

In Fig. 6 is an unbalanced three-phase voltage system characterized by V_a=324 V with γ_a=0 rad, V_b=324 V with γ_b=–2π/3 rad, V_c=162 V, γ_c=2π/3 rad and the results obtained following the determination of the symmetrical components.

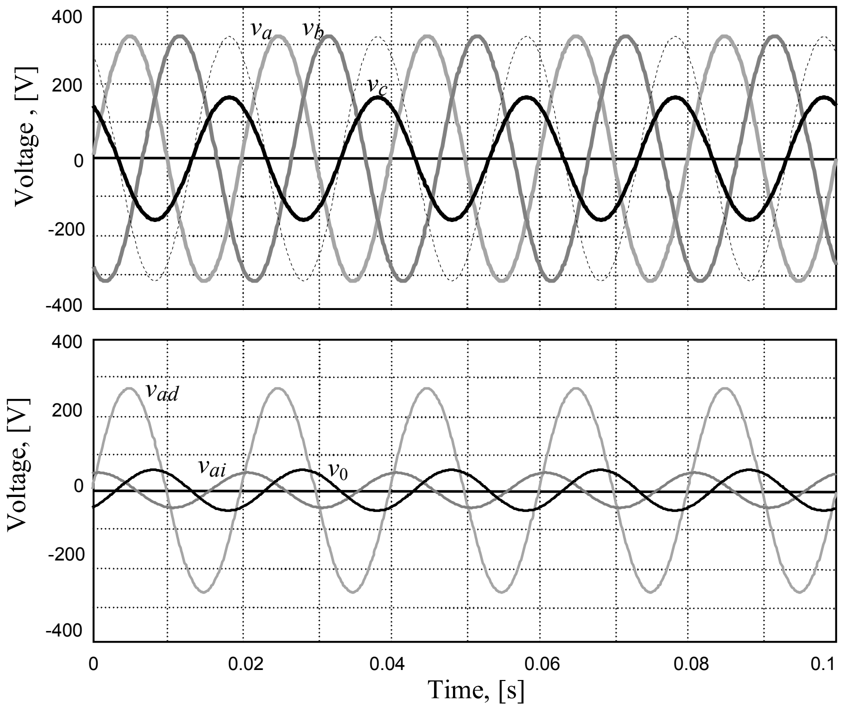

Fig. 6 − Unbalanced three-phase voltage system curves.

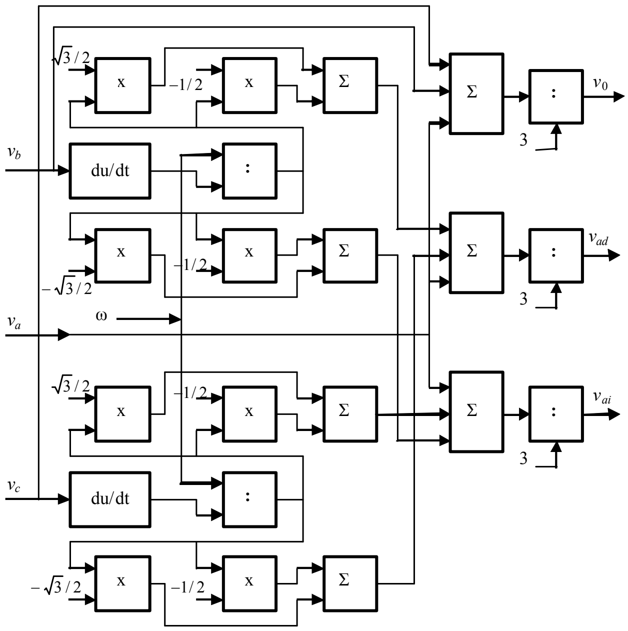

Fig. 7 − Block diagram implemented in Simulink.

The block diagram of Fig. 5 was implemented also in Simulink using the specific blocks and is presented in Fig. 7.

In Fig. 8 is an unbalanced three-phase voltage system characterized by $V_a = 324$ V with $\gamma_a = 0$ rad, $V_b = 324$ V with $\gamma_b = -2\pi/3$ rad, $V_c = 324$ V, $\gamma_c = \pi/2$ rad and the results obtained following the determination of the symmetrical components.

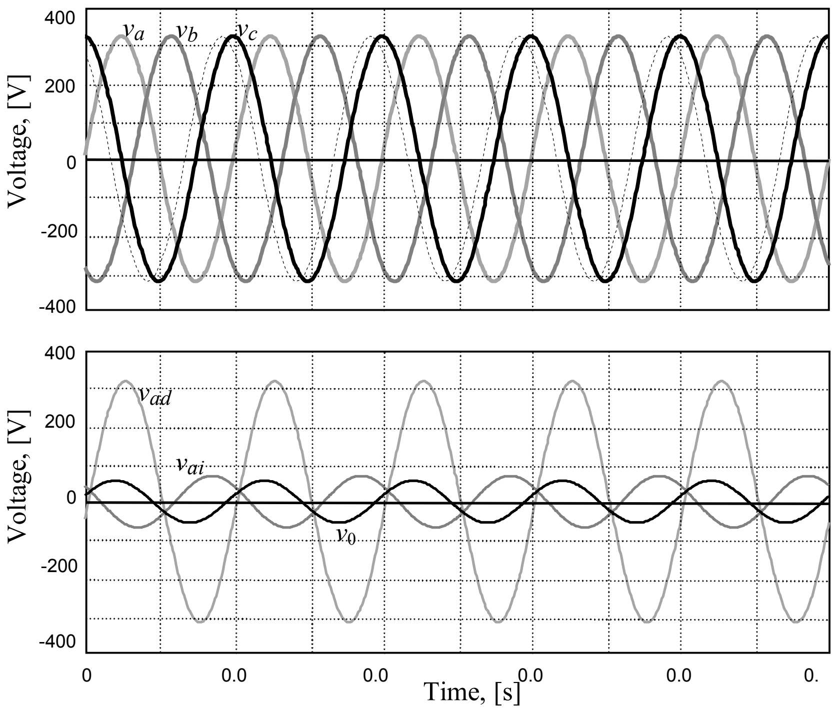

Fig. 8 − Unbalanced three-phase voltage system curves.

5. Conclusions

For the determination of the direct and inverse phase component of the three voltages the corresponding equations are multiplied with $\underline{a}$ and $\underline{a}^2$. In the time domain thic corresponds to phasing sinusoidal quantities $v_x(t)$ with $2\pi/3$ or $4\pi/3$ respectively. The sinusoidal quantities are determined for a phasing with the angle θ starting from any sinusoidal size with pulse ω known by modelling in PSpice and differential equations are solved by Matlab Simulink.

REFERENCES

Cociu V.R., Cociu L., *Analysis of Transient Short Circuit Currents and Fluxes Expressions of Induction Machines*, Electrical and Power Engineering (EPE), 2014 Internat. Conf. and Exposition, pp.386-391, 16-18 Oct., 2014.

Cociu V.R., Cociu L., Haba C.G., *On Asynchronous Motor Transient for Sudden Modification of the Load Torque*, Advanced Topics in Electrical Engineering (ATEE), 2011 7th Internat. Symp., pp.1-6, 12-14 May 2011.

Cociu V.R., Cociu L., *Optimization of a Method to Evaluate the Fundamental Frequency in Real Time*, 2017 Internat. Conf. on Electromechanical and Power Syst. (SIELMEN), Chişinău, pp. 157-162, oct. 2017.

Cociu V.R., Cociu L., *Symmetrical Components Method in Induction Machine Behavior*

Analisis. Bul. Inst. Politehnic, Iaşi, **LX(LXIV)**, *4*, s. Electrot., Energ., Electron., 23-38 (2014).
Fortescue C.L., *Method of Symmetrical Coordinates Applied to the Solution of Polyphase Networks*, Trans. AIEE, pt. II, vol. **37**, pp. 1027-1140 (1918).
Harris M.R., Lawrenson P.J., Stephenson J.M., *Per-Unit Systems with Special References to Electrical Machines*, London: IEE Monograph, Cambridge University Press, 1970.
Justus O., *Dynamisches Verhalten elektrischer Maschinen. Eine Einfuhrung in die numerische Modellierung mit PSPICE*, Vieweg & Sohn Verlagsges, Braunschweig/Wiesbaden, 1993.
Lyon W.V., *Transient Analysis of Alternating-Current Machinery*, Cambridge, and John Wiley, New York: Technology Press, 1954.
Paap G.C., *Symmetrical Components in the Time Domain and Their Application to Power Network Calculations*, IEEE Transactions on Power Systems, **15**, *2* (2000).
White D.C., Woodson H., *Electro Mechanical Energy Conversion*, New York and Chapman & Hall, London: John Wiley & Sons, 1959.

EVALUAREA COMPONENTELOR SIMMETRICE ÎN TIMP REAL

(Rezumat)

Folosind metodologia componentelor simetrice, pot fi vizualizate și analizate condițiile de sistem dezechilibrat, cum ar fi cele cauzate de defecțiuni comune. Pentru a calcula componentele directe și inverse, fazorii trebuie înmulțiți cu operatorul de rotație a fazorului $a = e^{j2\pi/3}$. Expresiile matematice clasice asociate cu această problemă sunt potrivite în special în calculul fazorilor. Cu toate acestea, în domeniul timpului, autorii nu oferă soluții practice. Lucrarea prezintă modalități concrete de a rezolva problema rotirii unei mărimi sinusoidale în timp real folosind software-ul PSpice și Matlab Simulink. Pe baza acestora sunt determinate în timp real componentele reale și inverse ale unui sistem trifazat dezechilibrat.

Blended Learning Approach Applied to Electrical Engineering Courses

Arădoaei Sebastian Teodor [1], Adăscăliței Adrian[1]

(1) "Gheorghe Asachi" Technical University of Iași,
55 Prof. D. Mangeron Blvd. Iași, 700050, ROMANIA
E-mail: asteor[at]yahoo.com; adrian.adascalitei[at]yahoo.com

Abstract

The review paper is about how to Using Blended Learning Resources in Electrical and Computer Engineering Programs on the Moodle Platform of "Gheorghe Asachi" Technical University of Iași. Virtual environments for training and learning process based on Blended Learning methodology are highlighted. This paper presents elearning instruction materials for electrical engineering undergraduates developed on the Virtual Learning Environment http://moodle.ee.tuiasi.ro.

Keywords: Blended Learning, Engineering Education, e-Pedagogy, Moodle

1 Introduction

Traditional models of teaching (one-to-many communication supported with one-to-few encounters) do not sustain the quality of learning and teaching. e-Learning used creatively and effectively can offer support, maintain and enhance learning process. For training and learning process improvement dedicated to engineering students as one of the components in the foundation technological program has been a challenging task to engineering lecturers.

The article presents the concept of using current pedagogical methods based on the analysis of the advantages of teaching model in the network environment (Christiansen and Weber, 2017). The instructor's role in a networked learning environment changes: From lecturer to consultant, guide, and resource provider; Teachers become expert questioners, rather than providers of answers; Instructors become designers of student learning experiences rather than just providers of content; Instructors provide only the initial structure to student work, encouraging increasing self-direction; Instructors present multiple perspectives on topics, emphasizing the salient points; From a solitary instructor to a member of a learning team(reduces isolation sometimes experienced by instructors); From instructors having total autonomy to activities that can be broadly assessed; From total control of the teaching environment to sharing with the student as fellow learner; More emphasis on sensitivity to student learning styles. Also, the student's role in a networked learning environment changes: From passive receptacles for hand-me-down knowledge to constructors of their own knowledge; Students become complex problem-solvers rather than just memorizing of facts; Students see topics from multiple perspectives; Students refine their own questions and search for their own answers; Students work as group members on more collaborative/cooperative assignments; group interaction significantly increased; Increased multi-cultural awareness; Students work toward fluency with the same tools as professionals in their field; More emphasis on students as autonomous, independent, self-motivated managers of their own time and learning process; Discussion of students' own work in the classroom; Emphasis on knowledge use rather than only observation of the instructor's expert performance or just learning to "pass the test";

Emphasis on acquiring learning strategies (both individually and collaboratively); Access to resources is significantly expanded

As in all courses, the quality of the instructional planning maximizes the learning for all students. In the Web environment, the components of a course website, which enhance teaching and learning and save time by being posted for students to access online, are especially valuable. At the most basic level, instructors can post content and announcements at a course website. However, course planning usually begins with a course map – an outline of topics, weeks, objectives, activities, assignments, and assessments to show alignment of course components with each other in a weekly calendar format. Planning also includes the purposeful design of activities to create a student learning community – supportive student groups in a course that develop with the students' active access, pursuit, generation, and evaluation of information and learning in their discussion, chats, and e-mail communications.

2 Blended-Learning Concept for Basic Lectures in Electrical Engineering

From a didactical perspective lectures with such large number of participants have particular shortcomings: differences in prior knowledge, in types of learning or in speeds of comprehension cannot be accounted for. Only minimal or at least no interaction related to the subject matter is taking place during each session in the lecture hall and students are driven into a consuming attitude. Usually no timely feedback to individual problems in comprehension or learning performance is available to the students. (Winterstein, T.,et. al. , 2012). So, to achieve a good learning performance and learning outcomes, students had to be highly intrinsically motivated. Yet, in this case, the contrary is the truth for the majority of lecture attendees, since students are coming from other disciplines than electrical engineering and attending the lecture mostly for the single reason that it is prescribed by their study plans.

These problems were addressed by four main aspects for the new concept.

1) All-time accessible material that follows the curriculum and can be autonomously as well as repeatedly used allows self-study according to the individual skills and background knowledge

2) Elements with direct feedback shall allow control of the personal learning progress on a regular basis.

3) New and different learning elements shall create an incentive to continuously stick to the lecture and lower the inhibition threshold to electrical engineering.

4) The material has to be transparently organized, but administration effort needs to be kept low enough for one person to manage the lecture.

To increase the flexibility of learning time and place, provide individual learning opportunities and thus support more self regulated learning on the one hand, and to address typical difficulties in comprehension, raise motivation and improve the learning experience on the other hand, e-Learning elements were chosen to complement the traditional lecture.

Amendatory material was added to give background knowledge and motivation, addressing incentive aspects as well as direct feedback. The educational material as well as organizational aspects of the lecture is administrated in on central online platform.

3 Planning the Components of a Website

As in all courses, the quality of the instructional planning maximizes the learning for all students. In the Web environment, the components of a course website, which enhance teaching and learning and save time by being posted for students to access online, are especially valuable (Jiménez-Castañeda et al., 2018).

Course planning usually begins with a course map – an outline of topics, weeks, objectives, activities, assignments, and assessments to show alignment of course components with each other in a weekly calendar format, Figure 1.

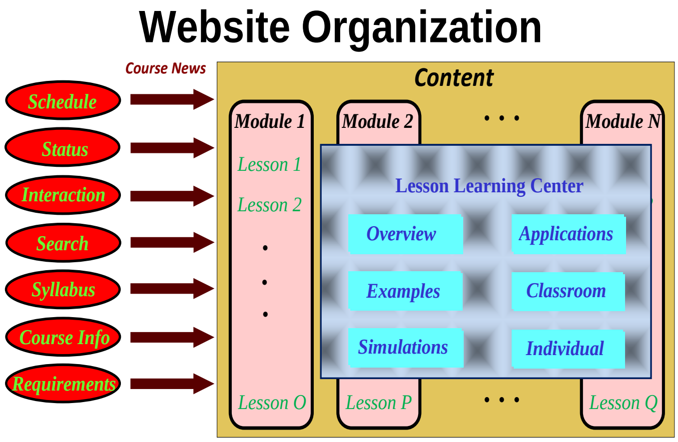

Fig. 1. Web site organization diagram

Planning also includes the purposeful design of activities to create a student learning community – supportive student groups in a course that develop with the students' active access, pursuit, generation, and evaluation of information and learning in their discussion, chats, and e-mail communications.

Course content is aligned with curriculum standards, objectives, assignments, assessments (Adascalitei, A. A., 2006).

• Course Syllabus. The course contains a syllabus and supporting documents. The course includes items such as: course title; correct course semester; course description; course contact and credit hours; course prerequisites; course objectives; course assignment; course test schedule; required course materials; grading criteria; testing information; library resources; any on-campus requirements; work ethics information.

• Staff Information. The course contains staff information: instructor name; appropriate picture (optional); e-mail address; telephone and fax numbers; office hours

• Student Information. The course contains a student orientation and explains: how to get started; technical equipment requirements; technology competency requirements; browser recommendations; drop deadlines; format for assignments; requirements for chat room and/or e-mail; instructor response time; troubleshooting advice.

• Course Calendar – Due dates for readings, activities, assignments, quizzes, and exams

• Assignments and Activities, including directions and due dates. Course assignments are designed: to be interactive and requires students to interact with: each other and their instructor via e-mail, chat room, and/or discussion board; and to address a variety of learning styles through: written assignments; reading activities; discussions; simulations; case studies; and give students the opportunity to engage in critical and abstract thinking.

• Course Documents – Additional documents for reference or study or answers to frequently asked questions. Course document section includes a variety of learning media. Includes course content delivered through media such as: PowerPoint presentations; Short lectures in audio or video format; links to resources on websites; CD-ROM materials.

• Lectures – Notes and audio to highlight key concepts of course content Caution: For face-to-face classes with web-enhancement, faculty may wish to include required assignments, even if minor, for extra points to be turned in at the scheduled class times or other incentives to maintain class attendance.

• Communication Tools – Areas for sending and receiving e-mail, participating in group or class discussions about particular issues, keeping electronic journals, completing "dry or simulated lab" exercises to prepare for "wet or real lab" experiences, or engaging in chat sessions.

• Student Tools – Areas for using a digital drop box to send and receive completed papers, homepages, or personal profiles of students, and access to grades.

• Assessment Tools– Areas for quizzes, exams, and surveys; online grade books; and assessment statistics. Course assignments are designed to be interactive and require students to interact with: each other and their instructor via e-mail, chat room, and/or discussion board.

4 Using the Moodle Platform in Class

Moodle is a tool which enables instructors to create a website environment for your class with online activities such as forums and quizzes. "Moodle is a Course Management System (CMS), also known as a Learning Management System (LMS) or a Virtual Learning Environment (VLE). It is a free web application that educators can use to create effective online learning sites." (http://moodle.org/)

The web application was designed for a course entitled "Fundamental of electrical circuits (FEC)" which was a core module offered to engineering students. The front webpage provides the overall course content of the FEC module with the names of the chapters, followed by the activities in a drop-down list for each chapter. The activities involved in each chapter include: course materials, additional materials, quizzes, open forum/chat and latest news message/calendar (Zhang and Sun, 2017).

Teaching electrical engineering laboratory procedures by means of a virtual laboratory on a personal computer will be much welcome by educational institutions for whom maintaining a hands-on electric engineering lab is not viable due to various reasons. Instructional laboratory simulations can be incorporated in the virtual laboratory resources where students are free to make the decisions they would confront in an actual laboratory setting (Aradoaei et al., 2005; Beetham and Sharpe, 2013).

There are a total of four chapters in FET with different topics. Each of these chapters has plenty of information and activities related to the topic. This includes the course materials in the form of PowerPoint slides and Acrobat PDF documents, which are the duplicates of hand-outs that the students received in class. It is important to provide a softcopy to the students, as it is coloured compared to their hardcopy and helps better in comprehending complex figures or diagrams.

Nowadays students are very much visual learners (Ng et al., 2017). The majority of the students expressed the strongest preference to visual learning style compared to other learning style dimensions. This implies that engineering students are strongly depending on visual learning environment. Video is clearly a valuable additional learning activity that provides a sensory experience that allows concepts and ideas to actually become alive and connected. It has the option to rewind and review a particular section of the video to ensure students understand the key concept. Thus, free educational video sharing websites that explained the FET theories were uploaded in the webpage. In addition to this were video links from YouTube.

Apart from this, problems and solutions as well as simplified diagrams explaining complex concepts, taken from textbooks or take-home questions which were not discussed in class, were made available online for students. In each of these adapted materials, references were stated clearly in order to allow students to seek the original sources if the need arises, apart from avoiding copyright infringement (Svoboda, Špaldonová, and Guzan, 2006).

4.1 Learning Process

Before Attending Class:

- Explore the Overviews & Theory, Examples, Applications, and Simulations sections for the Lessons to be covered in the Classroom Activities, Figure 1. (See Schedule).
- Complete Language Quizzes for Lessons to be discussed in class.

Classroom Activities:

- Attend class!
- Be prepared to contribute!
- Active learning environment with team-based problems solving.
- Web ready solutions from each team are due by the end of the week (Friday at 5 pm.)

After Attending Class:

- Complete team-based analysis and design problems assigned in the classroom activities.
- Optional analysis and design problems are available on the website.
- Complete the Integration Quizzes for Lessons covered in class.

Quizzes were incorporated in each chapter for students who were keen to self-test their knowledge and learning after the revision of a chapter. Short quizzes in the form of true/false, multiple choice, short answers or numerical questions were assigned, depending on the chapter content. The majority of the questions were of problem solving type that involved calculation with pre-determined specific units and significant figures of the numerical answers. Positive responses were provided if the students were successful in answering the questions. However, there was no time limit to answer each question as the students were given sufficient time to read and understand the questions, and to answer calmly at their own pace.

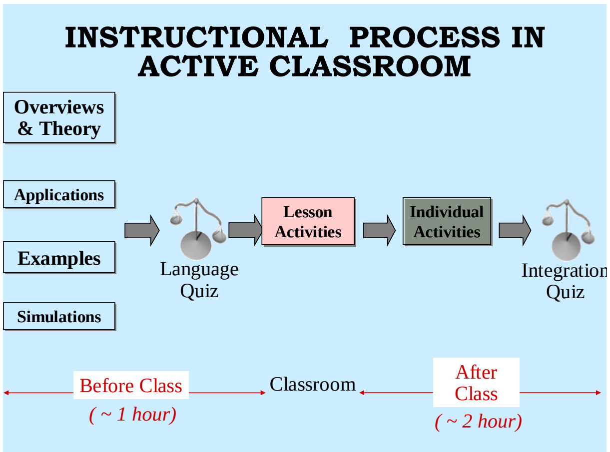

Fig. 2. Instructional process in Blended Learning Environment.

Since the quizzes were not part of the students’ assessment, it was considered as an independent study at the students’ own will. Hence, the quizzes were designed with a due date of two weeks, in order to encourage the students to have a constant revision and to avoid last-minute cramming before examination.

Open forum serves the purpose of allowing a student to post his/her questions or doubts and can be viewed by their fellow peers. This allows the lecturer to disseminate the answered questions to the whole class without repeating in the classroom. Hence, each of the chapters was constructed with their very own Open Forum. Students were also encouraged to use the chat function that facilitated live discussion and interaction with their instructors and peers.

Another interesting feature of Moodle is the function on the right of the webpage which allows the lecturers to post any new messages. It also comes with the list of recent activities so that students can keep-track with any updates. General announcements such as due date of assignments, examination dates and venues, replacement classes etc. were posted at this section and these were linked to the students' email accounts, so that they were notified of every update studies.

4.2 Learning scenario for Course "Fundamental of Electrical Circuits, FEC"

The course was organized in blended mode with support of e-learning environment Moodle. The scenario for course "FEC", Table 1 are stressed on the use of SCORM compatible interactive and simulation learning objects combined with practical problem solving in "face to face" mode and development of assignments in online mode.

Table 1. *Learning scenario schema of the course "E-Learning technologies"*

Face to face activities	**Online activities and resources**
Workshop – Topic 1 (2 hours) • Demonstrations by the tutor • Solving Tasks with resources prepared in advance and published in the online course (all task are implemented in the e-learning environment)	Home work (1) • Preparing home work – solving tasks in their own Learning Project • Using of SCORM compatible simulations. • Discussion
Workshop – Topic 2 (2 hours) • Discussions about home work from previous session • Demonstrations by the tutor • Solving Tasks with resources prepared in advance and published in the online course (all task are implemented in the e-learning environment)	Home work (2) • Preparing home work – solving tasks in their Learning • Using of SCORM compatible simulations. • Discussion
Workshop – Topic 7 (2 hours) • Discussions about home work from previous session • Demonstrations by the tutor • Solving Tasks with resources prepared in advance and published in the online course (all task are implemented in the Moodle platform)	Home work (7) • Preparing home work – solving tasks in their own course • Using of SCORM compatible simulations. • Discussion
Assessment: 1. Developed individual assignments; 2. Performance of the assignments in front of all students	

The course was organized in blended mode with support of e-learning environment Moodle.

The students had 14 hours lectures and 7 hours exercises in "face to face" mode and around 30 hours for development of own e-learning course in Moodle. During the lectures they learned mentioned above topics of the course. During the face to face exercises the students mastered basic techniques for solving problems and performing virtual experiments. They worked under supervising of the tutor with resource files, prepared in advance by lecturer and used on-line simulations and demonstrations. To master basic skills for development of e-learning course all students followed common tasks.

The tasks were related to: 1. Using learning resources - web page, link to file or external web resource, label; 2. Using and management of learning activities –assignment, lesson, test, forum, blog, wiki; 3. Questionnaire etc.; 4. Management of students – grouping, assigning students to activities and resources.

The students were grouped approximately 5 students per group. Each group was assigned to one common e-learning course activity. During the face to face exercises students used resource materials offered by the teacher to learn basic techniques and functionalities of the e-learning electrical engineering environment. Also they had a possibility to use SCORM based e learning demonstrations and simulations. Each student in role of “teacher” could assign another student in her/his course like “a student”. In this way another students have a possibility to be enrolled in the course with student rights and could observe work of their colleagues.

5 Effectiveness of e-learning within Universities

This paper describes a methodological framework consisting of factors necessary for assessing the effectiveness of e-learning within Universities.

An e-learning framework comprises eight dimensions namely: pedagogical, technological, interface design, evaluation, management, institutional, resource support, and ethical.

Effectiveness of blended e-learning can be determined by evaluating four main dimensions, namely: E-learning Readiness, E-learning Course Delivery Strategies, Quality E-learning Systems and Effects of Blended E-learning.

E-learning Readiness (in terms of costing and budgeting, policies, support, cultural awareness, and infrastructure) have an influence on the quality of elearning systems and e-learning course delivery strategies, which in turn have an impact on the effectiveness of blended e-learning.

To ensure effective blended elearning, that review paper propose a framework that focuses on having a well balanced mix of effective pedagogy in elearning course design and delivery, relevant institutional readiness for e-learning and use of quality e-learning systems to meet institutional and student learning goals.

Conclusions

This paper presents e-learning instruction materials to develop on the Virtual Learning Environment http://moodle.ee.tuiasi.ro/. Processes of: design, development and implementation of interactive educational modules are presented, for the topic of electrical engineering.

The modulus is divided into a number of teaching and learning units which can be studied autonomously (or independent). Fundamental of Electrical Circuits (FEC) discipline model is a new approach to learning electrical technology-one that presents concepts in the customary logically developed order but illustrates them with exemplars that reflect the applications students are interested in (http://www.walter-fendt.de/ph14ro, accesed 2018; http://electronics.wisc-online.com/, accesed 2018). eLearning modules are using visualization of electrical engineering concepts. These principles focus on a few specific pedagogical pointers: 1) providing multiple representations and descriptions; 2) making linked referential connections visible; 3) presenting the dynamic and interactive nature of electrical engineering; 4) promoting the transformation between 2D and 3D; and 5) reducing cognitive load by making information explicit and integrating information for students (https://www.wisc-online.com/learn/technical, accesed 2018).

This paper is a synthesis that presents how use Moodle Virtual Learning Environment for the development courses which mainly contains materials in order to educate the Engineering Students. There exists a greater acceptance of the online mode of instruction as an adjunct to learning. Their positive attitude was observed towards the model of blended learning approach, and Moodle platform did create a positive impact on students' learning experiences in terms of the accessibility of learning materials and the support of online assessment activities.

Although the students agreed that the hybrid learning provided them with the needed assistance, one of the drawbacks observed was that this method of delivery was prone to become a one-way communication. Communication tools such as forum discussion and online chat room have the features that create interaction with instructors and among the peers. However, most students are likely to participate in the learning practices only if the activities are considered as part of the evaluation of their academic performance. It is therefore necessary to assign grading procedure in e-learning activities to increase students' participation. With the improvements at these loose ends, Moodle application in Electrical Engineering will be an invaluable and imperative tool for the instructors as well as for the students (http://phet.colorado.edu/en/ simulations/translated/en, accesed 2018; http://moodle.ee.tuiasi.ro, accesed 2018).

The development of courseware materials for student engineers in Romania will have an increasing impact on the national scene of Engineering Education, and the development of online materials devoted to the development of human resources and human potential will accelerate the process of transfer of up-to-date technology.

Acknowledgment

We wish to address our thanks to all authors and institutions for the value of their ideas, concepts and information that we used in our project design. All sources are cited in the bibliography.

References

Aradoaei S., Hanganu S., Donciu C.,Socotar D., Olariu M. (2005): Prototype architecture of a remote teaching laboratory, In *Proceedings of The 4th International Conference on Management of Technological Changes,* Chania, Greece, 179-182.

Adascalitei, A. A. (2006, July). Courseware structure for online electromagnetic compatibility. *Industrial Electronics, 2006 IEEE International Symposium on* (Vol. 4, pp. 3210-3213).

Aguti, B., Wills, G. B., & Walters, R. J. (2014, November). An evaluation of the factors that impact on the effectiveness of blended e-learning within universities. *Information Society (i-Society), 2014 International Conference on* (pp. 117-121). IEEE.

Beetham H., Sharpe R., (2013): *Rethinking pedagogy for a digital age: Designing for 21st century learning.* Routledge; 2nd edition.

Christiansen M. A., Weber J. M., (2017): *Teaching and the internet: The application of web apps, networking, and online tech for chemistry education* Chapter 10, American Chemical Society, pp 171–186.

Jiménez-Castañeda R., Cipri K., Clavijo-Blanco J. A., Moreno-Ruiz J., (2018): *The support of European programmes in the Internalization process of engineering courses*: DIEGO project — Development of high quality courses on renewable technologies and energy efficiency, IEEE Global Engineering Education Conference (EDUCON), 196 - 201.

Ng R. Y. K., Lam R. Y. S., Ng K. K., Lai I. K. W., (2017): A study of vocational and professional education and training (VPET) students and teachers' preferred support for technology based blended learning in educational technology, *International Symposium on Educational Technology* (ISET), 268-271.

Svoboda J.A., The Electronic Teaching Assistant: the Circuit Design Lab, Interactive Illustrations and Electric Circuit Study Applets. http://people.clarkson.edu/~jsvoboda/eta/

Zhang W., Sun Y., (2017): The Study on the Support of Online Learning Resource in Blended Learning Based on Learning Process, *International Conference of Educational Innovation through Technology* (EITT), 242-243.

Winterstein, T., Greiner, F., Schlaak, H. F., & Pullich, L. (2012, July). A blended-learning concept for basic lectures in electrical engineering: A practical report. In *Education and e-Learning Innovations (ICEELI), 2012 International Conference on* (pp. 1-4). IEEE.

http://www.walter-fendt.de/ph14ro, accesed 2018, JAVA Applets for Electrodynamics,

http://electronics.wisc-online.com/;

http://phet.colorado.edu/en/simulations/translated/en

http://moodle.ee.tuiasi.ro/ Moodle elearning, Electrical Engineering Faculty, Technical University "Gh. Asachi" Iași, România

http://ec.europa.eu/dgs/education_culture/repository/education/library/reports/modernisation-universities_en.pdf, Report to The European Commission on: New modes of learning and teaching in higher education, October 2014

BULETINUL INSTITUTULUI POLITEHNIC DIN IAŞI
Publicat de
Universitatea Tehnică „Gheorghe Asachi” din Iaşi
Volumul 65 (69), Numărul 1, 2019
Secţia
ELECTROTEHNICĂ. ENERGETICĂ. ELECTRONICĂ

CONSIDERATIONS REGARDING IMPROVING PERFORMANCE of the SERVO MOTORS

BY

VASILE BAHRIN* and SEBASTIAN ARĂDOAEI

“Gheorghe Asachi” Technical University of Iaşi,
Faculty of Electrical Engineering

Received: February 21, 2019
Accepted for publication: March 28, 2019

Abstract. This paper highlights the possibility of improving the performance of electric servo motors by using insulating materials in class H (limit temperature 180°C). The constructive and functional particularities of the SRD 191 C servo motor, as well as its advantages over a classical servo motor, are specified. The stages of the experimental determination of electromechanical characteristics and parameters of the SRD 191 C servo motor are presented. Using the MATLAB software package, the characteristics of the SRD 191 C: $E = f(n)$, $M_0 = f(n)$, $M_u = f(I)$ and $n = f(M)$ servo motors were plotted.

Keywords: servo motor; performance; insulating materials.

1. Introduction

Special electric machines have a range of performances defined for them, as well as a number of features that can only be appreciated from the point of view of the performances of the system they belong to (Simion, 1993; Shen & Tsai, 2014); Classical electric machines operate on the basis of the

* Corresponding author; *e-mail*: vasilebahrin@yahoo.com

electromechanical conversion of energy (Dobrea & Cociu, 2014), and in the case of special electrical machines the operation is based on other phenomena (magnetic hysteresis, single pole induction, form anisotropy) (Biro *et al*., 2015). The use of permanent magnets to excite servo motors has determined the disappearance of some thermal and mechanical restrictions (Basu *et al*., 2005); the absence of excitation windings, access terminals and power supplies of these windings has led to the elimination of excitation losses, resulting reduction of heating. In the operation of these servo motors, there is no danger of permanent magnets becoming out of operation due to overload. Also have some disadvantages, as the collector, the switching phenomenon and the loud noise.

Direct current servo motors performs continuous speed control within wide limits, have mechanical and linear adjustment characteristics, specific couples and high starting couples, high overload capability, lack of self-propulsion, low moment of inertia, and low electromechanical time constants (Kim, 2019). These servo motors are used in applications requiring continuous adjustment speed when the load is variable and has frequent shocks (Akar & Temiz, 2007).

The operating performance of direct current servo motors excited with low-power permanent magnets become comparable to those of relatively higher power electromagnetic excitation servomotors (Măgureanu &Vasile, 1990).

Construction of direct current servo motors excited with permanent magnets is similar constructive to the direct current classical machine, variety being a consequence of the diversity of characteristics of the magnetic materials used (Bahrin, 2006; Cojocaru-Filipiuc, 2001). The dimensions and powers of these servo motors are dictated by specific applications; the improvement of the construction-operation characteristics resulted from the use of high-performance magnetic materials for a high level of induction of the inductor, or through choosing of new technological solutions to obtain inductor, such as the cylindrical rotor, the glass shape rotor, the disc rotor, the winding rotor without a metal support, etc..

If it is compare insulation materials from class F (high temperature limit at 155°C) with insulating materials from H class (high temperature limit 180°C) it is noticed that H class materials offer a better performance of the servo motors characterized by high value of power/volume ratios. The SRD 191 C servo motor is equipped with a disc rotor which has a temperature limit of 175°C and, compared to SRD 1000 servo motors, develops a rated power with 30% higher under the same mass and gauge conditions. The SRD 1000 servo motor uses impregnated insulation with class E epoxy resins, by modifying the rotor insulation has been obtained the SRD 191 C 1300 servo motor, where the symbol has the following meanings: SRD servo motor with disc rotor, 191 outer diameter of the rotor, the C-version of the servo motor having H class insulation, and 1300 is the rated power of 1300W.

The SRD 191 C 1300 servo motor has a insulation based on glass fiber impregnated in bismaleimide rasin with H class insulation, pressed for 30 minutes at temperature 170°C. The servo motor rotor is made from stamped copper, the blades are hot-glued (due to the glass fiber impregnated with bismaleimide rasin) and then welded with the electron beam; the rotor has a high mechanical rigidity (the glass fiber impregnated with bismaleimide rasin is not sufficiently flexible) and a lower dielectric strength compare with the epoxy resin rotor. The SRD 191 C servo motor can be subjected to reversals load and has reduced mechanical and electromagnetic inertia, linearity of the characteristics, possibility of variation in wide speed limits; the servo motor meets the requirements of industrial robots and can be used in reversible drives with acceleration and braking transient modes (Celik & Gor,2019).

At the servo motors operation mode is accompanied by frequent variations in speed and load (Vasile & Slaiher, 2003). In these conditions a tolerable range of operating (S1) is defined as well as the extension of the transient regime (TR) in speed-torque coordinates, Fig. 1.

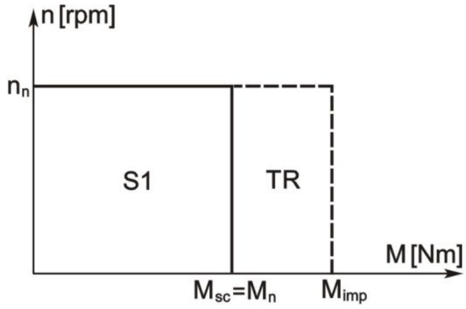

Fig. 1 − Operating range of servo motors.

2. Experimental Part

2.1. Determination of Rated Parameters

The couplings and speeds of the SRD 191 C servo motor are defined in direct current in the conditions of continuous operating (S1). The maximum impulse current, I_{imp}, refers to the permissible limit for the preservation of the mechanical, magnetic and thermal characteristics, and the prescribed value corresponds to the thermal equivalent of the allowed current over the cycle, Fig. 2.

Stabilization of permanent magnets is accomplished by running the servo motor for one hour at the speed variation after the cycle presented in Fig. 2 (the maximum pulse application rate is 9.76 s). The rated voltage U_n and the rated current I_n was determined at the rated speed n_n, the rated output P_n and the rated torque M_n:

$$M_n = \frac{60}{2\pi}\cdot\frac{P_n}{n_n} = 413.8\times10^{-2}\,\text{Nm}\cdot \tag{1}$$

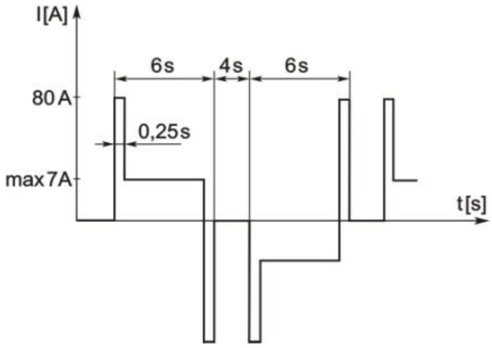

Fig. 2 – Characteristic $I = f(t)$.

The servo motor was powered from a direct curent generator and is loaded by coupling with a servo motor operating in the generator mode. For dragging the SRD 191 C servo motor, the rated current is calculated with the relation:

$$I_n = \frac{P_n}{E} + I_0 = 20.3 \text{ A}, \tag{2}$$

where: P_n is the rated power, E – electromotive voltage at rated speed (n_n = = 3,000 rpm), and I_0 is the absorbed current at idle speed at rated speed.

By varying the load resistance of the generator servo motor circuit, the rated current (calculated with the formula (2)) is fixed in the SRD 191 C servo motor circuit and also the rated speed in the group is establish by changing the supply voltage of the servo motor; for the SRD 191 C servo motor loaded at a load of 412×10^{-2} Nm and rated speed of 3000 rpm, the measured voltage resulted is 81.5 V and the absorbed current is 20.4 A.

Certification of the rated power of the servo motor is achieved by checking the maximum permissible overheat on the. The servo motor, loaded, will operate (at the calculated rated current at rated speed and rated voltage) until the temperature on the housing is stabilized. The servo motor was switched off and the temperature measurement of the rotor disk collector with a thermocouple probe (at least 5 measurements during cooling, graphically extracting the temperature when the actuator is switched off) was carried out in maximum 30 seconds. The rotor disc collector was obtained for an overheat υ_{rot} = 126°C (maximum admitted is 135°C). Measurements shall be made with measuring instruments (precision class 0.2) which determines the mean values of the measurements.

2.2. Check Current at Slow Speed

The current al the slow speed was checked by conducting a heating test until the temperature of the housing is stabilized, for the rotor current I_{sc} = 18 A;

measure the overheat of the rotor (collector) by thermocouple probe.

Powered the rotor with the I_{sc} = 18 A current at a slow speed of 50,...,100 rpm, the overheat value υ_{rot} = 128°C value was obtained for the rotor disk collector and for the torque value:

$$M_{sc} = K_T I_{sc} = 417.6 \times 10^{-2}\,\text{Nm}, \tag{3}$$

where K_T is torque on amp and it has value $K_T = 23.2 \times 10^{-2}$ Nm/A.

2.3. Determination of electromotive voltage

The electromotive voltage, K_E, at the speed of 1,000 rpm was determined by the characteristic electromotive voltage versus speed, $E = f(n)$, Fig. 3. The servo motor was running as an empty generator at different speeds and it was measure the voltage at terminals.

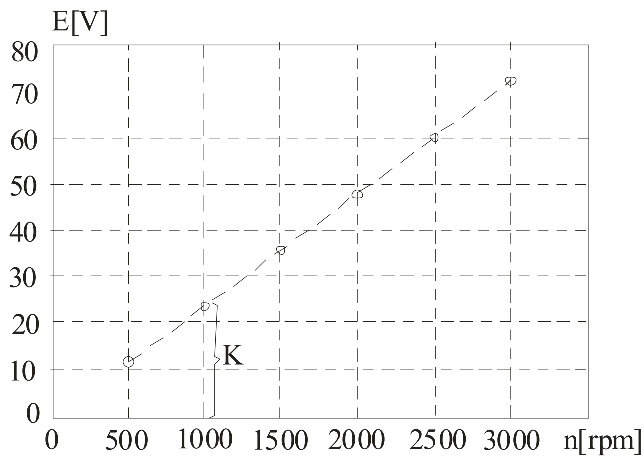

Fig. 3 – Characteristic E=f(n).

2.4. Determination of Electrical Resistance at Servo Motor Terminals

The electrical resistance at the servo motor terminals, R_b [Ω], at 25°C, was determined on the cold-state by the voltmeter method, with the rotor locked. The measurements have been accomplish in nine positions corresponding to a single axis rotation and the mean value of the resistance was calculated at R_b = 0.4 Ω.

2.5. Determination of Inductance of the Rotor

The inductance of the rotor, L [µH], was determined by a measurement bridge and it was obtained values for inductance L = 42 µH at f = 800 Hz.

2.6. Determination of the Electromechanical Time Constant

The electromechanical time constant τ_m, [ms], was determined with the relation:

$$\tau_m = \frac{J}{K_E} \cdot \frac{R_b}{K_T} \times 10^2 = 9.5\,\text{ms}. \tag{4}$$

2.7. Determination of Torque and Maximum Impulse Current

The maximum impulse torque M_{imp}, [Nm], and the maximum impulse current I_{imp}, [A], are defined as the maximum amplitudes of the useful torque or the corresponding short-time current absorbed in acceleration and braking processes so that the servo motor resists at mechanically and thermally stress, and not to be phenomena of diminishing E.M.V. as a result of the demagnetization of permanent magnets.

The servo motor was powered from a current limiting converter to I_{imp} by performing 10 accelerations and brakes over a minimum of 10 seconds with a transient process lower than that shown in Fig. 2, and each time measuring the I_{imp} value. The test was accomplish after stabilizing the permanent magnets.

Impulse torque is calculated with:

$$M_{\text{imp}} = K_T I_{\text{imp}} = 2{,}320\ \text{Ncm}. \tag{5}$$

The servo motor has resisted at mechanically and thermally stress and there was no reduction of E.M.V.

2.8. Maximum Speed Test

The maximum speed test, $n_{\max}$, [rpm], was performed for 2 minutes. with the servo motor, in the hot state, powered by a motor-generator group. After performing the test, the idling current was determined, I_0 [A]. The servo motor was running for 2 minutes at $n_{\max}$ = 5,000 rpm, and at n = 3,000 rpm the idling current was measured I_0 = 1.82 A.

2.9. Determination of Viscous Friction Torque

To determine the viscous friction torque, the characteristic $M_0 = f(n)$ is plotted, Fig. 4. The torque loss M_0 was determined with the relationship:

$$M_0 = M_F + nK_D 10^{-3} = \frac{60}{2\pi} \cdot \frac{p_{\text{mec}}}{n}. \tag{6}$$

where: $p_{mec}=EI_0$, [W], are the mechanical losses of the servomotor, and M_F, [Nm], is the viscous friction torque (value of the ordinate in origin of $M_0 = f(n)$).

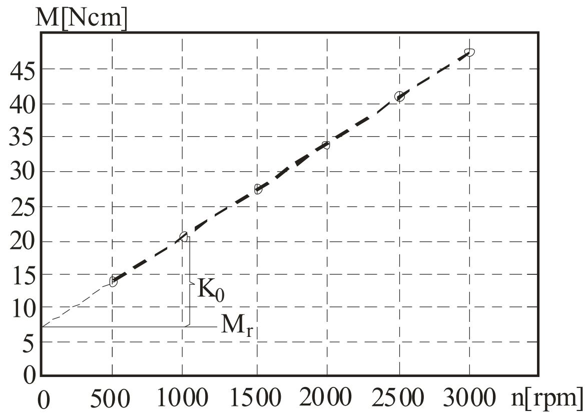

Fig. 4 − Characteristic $M_0 = f(n)$.

2.10. Determination of Torque Loss

The torque loss constant, K_D, was determined from the variation of the mechanical torque corresponding to the speed variation from 0 to 1,000 rpm on the characteristic $M_0 = f(n)$; the $K_D = 13.4 \cdot 10^{-2}$ Nm was obtained.

2.11. Determining the Torque on the amp

The servomotor was powered with the voltage $U = U_n$ = const. and by variation of the load the characteristic torque-current was plotted, $M_u = f(I)$, Fig. 5. The voltage was set at $U = 81.5$ V = const..

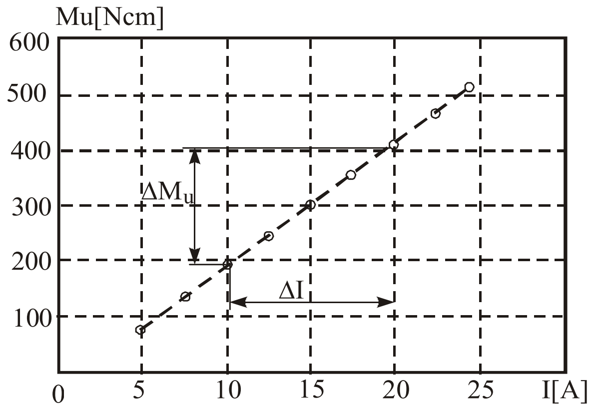

Fig. 5 − Characteristic M_u=$f(n)$.

The torque on the ampere is determined by the torque variation on the $M_u = f(I)$ characteristic corresponding to a 1 A variation of the current:

$$K_T = \frac{\Delta M_u}{\Delta I} = \frac{230}{10} = 23\times10^{-2}\,\frac{\text{Nm}}{\text{A}}. \tag{7}$$

2.12. Determination of Load Speed Decrease

The servo motor with the voltage $U = U_n$ = const. was powered, and by load variation the speed-torque characteristic was plotted, $n = f(M)$, Fig. 6, at the voltage U = 81.5 V = const..

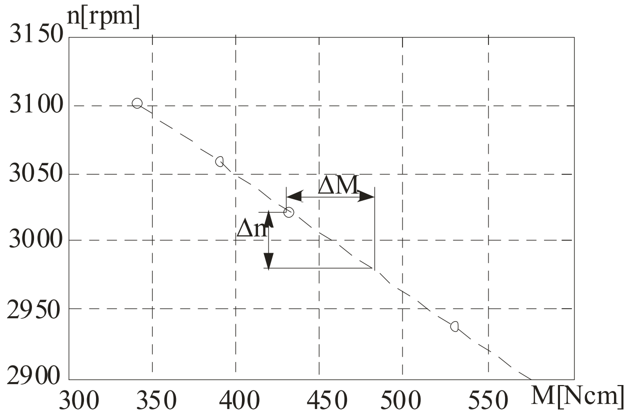

Fig. 6 − Characteristic $n = f(M)$.

The load speed decrease K_N, was determined as the variation of the speed (on the characteristic $n = f(M)$) corresponding to a torque variation of 1×10^2 Nm:

$$K_N = \frac{\Delta n}{\Delta M} = 1\times10^{2}\,\frac{\text{rpm}}{\text{Nm}}. \tag{8}$$

2.13. Determination of Idle Current

The idle current, I_0, [A], defined at rated speed, is determined by performing the idling test of the servo motor resulting the value I_0 = 1.98 A.

2.14. Determination of Idle Current

Determination of insulation resistance of windings to the servo motor housing was accomplish by measurement with 500 V megohmeter, for two distinct cases:

– for cold-dry state (before running under normal environmental conditions) 70 MΩ was obtained;

– for the hot-dry state (the servo motor running and reaches the operating temperature), 10 MΩ were obtained.

2.15. Dielectric Strength of the Insulation Against the Servo Motor Housnig

This was accomplish by applying a sinusoidal alternative voltage between $500 + 2U_n = 665$ V and 50 Hz frequency for 1 minute between the rotor winding terminals and the servo motor body. The insulation of the servo motor tested has not been bypassed or broken.

In Table 1 are presented standard electromechanical parameters of the 190 SRD servomotor and for the SRD 191 C servomotor, the standard parameters and the experimental results (Bahrin, 2006).

Table 1

Electromechanical Parameters of the 190 SRD Servomotor and for the SRD 191 C

Parameters	Symbol	UM	190 SRD	SRD 191 C	
				Standard	Experimental
Rated power	P_n	W	1,000	1,300	1,300
Rated torque	M_n	Nm	320×10^{-2}	413×10^{-2}	413.8
Rated speed	n_n	rpm	3,000	3,000	3,000
Rated voltage	U_n	V	82	82	81.5
Rated current	I_n	A	15	20	20.4
Maximum current at low speed	I_{sc}	A	16.5	18	18
E.M.V. at 1000 rpm	K_E	V	25	24.3	23.9
Terminal resistance at 20°C	R_b	Ω	0.45	0.45	0.4
Self inductance of rotor	L	μH	100	100	42
The inertia moment of rotor	J	Kg.m^2	12×10^{-4}	12×10^{-4}	11.98
Mechanical time constant	τ_m	ms	11	12.5	9.5
Maximum impulse torque	M_{imp}	Nm	$2{,}440\times10^{-2}$	$2{,}670\times10^{-2}$	2,320
Maximum impulse current	I_{imp}	A	100	100	100
Maximum speed	$n_{\max}$	rpm	5,000	5,000	5,000
Viscous friction torque at 1000 rpm	M_F	Nm	15×10^{-2}	15×10^{-2}	7
The constant of the losses couple in idle	K_D	Nm	15×10^{-2}	15.3×10^{-2}	13.4
Torque per amp	K_T	Nm/A	24.2×10^{-2}	23.2×10^{-2}	23
Load speed decrease for constant voltage	K_N	rpm/Nm	0.88×10^{2}	1×10^{2}	1
Idle current	I_0	A	2	2.5	1.98

3. Conclusions

This paper present the possibility of improving the performance of electric servo motors by using a different class of insulation material. The experimental results present that:

– using of Class H insulating materials has led to improvements in 190 SRD servo motor performance;

– high match between the standard parameters and those determined experimentally for the SRD 191 C servo motor.

The $M = f(I)$ and $n = f(I)$ characteristics of permanent magnet exciting servo motors are linear, which is a great advantage (because the elevation of these features involves the determination of only two points).

The characteristics $M = f(n)$, $M_u = f(I)$ and $n = f(M)$ of the SRD 191 C servo motor were determined with the MATLAB software.

REFERENCES

Akar M., Temiz I., *Motion Controller Design for the Speed Control of DC Servo Motor*, International Journal of Applied Mathematics and Informatics, **1**, *4*, 131-137 (2007).

Bahrin V., *Servomotoare electrice excitate cu magneţi permanenţi*, Ed. Performantica, Iaşi, 2006.

Basu A., Moosavian S.A., Morandini R., *Mechanical Optimization of Servo Motor*, Journal of Mechanical Design, **127**, *1*, 58-61 (2005).

Biro K.A., Viorel I.A., Szabo L., Henneberger G., *Maşini electrice speciale*, Ed. Mediamira, Cluj-Napoca, 2005.

Celik E., Gor H., *Enhanced Speed Control of a DC Servo System Using PI Plus DF Controller Tuned by Stochastic Fractal Search Technique*, Journal of the Franklin Institute-Engineering And Applied Mathematics, **356**, *3*, 1333-1359 (2019).

Cojocaru-Filipiuc C., *Micromaşini electrice sincrone şi de curent continuu*, Ed. ”Gh. Asachi”, Iaşi, 2001.

Dobrea V., Cociu R., *Maşini electrice*, Ed. Pontos, Chişinău, R. Moldova, 2014.

Kim S., *Moment of Inertia and Friction Torque Coefficient Identification in a Servo Drive System*, IEEE Transactions on Industrial Electronics, **66**, *1*, 60-70 (2019).

Măgureanu R., Vasile N., *Servomotoare fără perii tip sincron*, Ed. Tehnică, Bucureşti, seria Maşini şi aparate electrice, 1990.

Shen B.H., Tsai M.C., *Robust Dynamic Stiffness Design of Linear Servomotor Drives*, Control Engineering Practice, *14*, 1325-1336 (2006).

Simion Al., *Maşini electrice speciale pentru automatizări*, Ed. Universitas Chişinău, R. Moldova, 1993.

Vasile N., Slaiher S., *Servomotoare electrice*, Vol. **II**, Ed. Electra, Bucureşti, 2003.

CONSIDERAŢII PRIVIND AMELIORAREA PERFORMANŢELOR SERVOMOTORELOR ELECTRICE

(Rezumat)

În această lucrare se evidenţiază posibilitatea ameliorării performanţelor servomotoarelor electrice prin utilizarea materialelor izolante din clasa H (temperatura limită 180°C).

Sunt precizate particularităţile constructive şi funcţionale ale servomotorului SRD 191 C, precum şi avantajele acestuia faţă de un servomotor în construcţie clasică.

Sunt prezentate etapele determinării experimentale ale caracteristicilor şi parametrilor electromecanici ai servomotorului SRD 191 C.

Cu datele obţinute s-au trasat, utilizând pachetul de programe MATLAB, caracteristicile servomotorului SRD 191 C: $E = f(n)$, $M_0 = f(n)$, $M_u = f(I)$ şi $n = f(M)$.

Key Engineering Materials Vol. 543 (2013) pp 154-158
Online: 2013-03-11

doi:10.4028/www.scientific.net/KEM.543.154

THERMALLY STIMULATED DISCHARGE CURRENTS OF POLY(ACRYLONITRILE-CO-ACRYLIC ACID)-POLYPYRROLE COMPOSITES

S. CETINER[1], M. OLARIU[2], N.U. KAYA[3] and S. ARADOAEI[2]

[1]Kahramanmaras Sutcu Imam University, Department of Textile Engineering, Kahramanmaras, TURKEY
[2]Technical University , Electrical Measurements and Materials
[3]Istanbul Technical University, Department of Polymer Science and Technology, Istanbul, TURKEY

Keywords: Thermally Stimulated Discharge Currents, conductive composite, dielectric properties

Abstract.
Thermally Stimulated Discharge Currents, one of the oldest destructive method widely used for studying the mechanisms of polarization and depolarization within the dielectrics was employed for determining information related to trapped and/or detrapped charges and activation energy (Ea) within P(AN-co-AA)-PPy composite films. Two peaks or two relaxation regions could be noticed on the TSDC spectra for each material under test: one at a temperature around 323.15K (50°C), attributed to decomposition due to DMF removal as presented in our previous studies, and a second one at 363.15K (90°C), attributed to glass transition temperature. An increased of detrapped charges was observed when the PPy quantity within the P(AN-co-AA) matrix was increased. The same time, both relaxations appeared at very close temperatures for all three samples under test. Complementary measurements for an in-depth electrical analysis were performed with the help of Broadband Dielectric Spectroscopy (BDS), while further information regarding conductive composites structures was obtained through FTIR-ATR analysis.

Introduction

Conducting polymers exhibit excellent electrical, electrochemical and optical properties with an delocalization of p-electrons conjugated network opening the way to new applications in the fields of energy storage, microelectronics, textiles, sensors, electroluminescence and electromagnetic interference (EMI) shielding [1]. On the other hand, broadband dielectric spectroscopy provides a powerful tool for investigating a variety of dielectric processes for both electrical and non-electrical applications. The measurement separates molecular process on the basis of response time, providing a unique relaxation frequency along with a signature variation with frequency.[2, 3]

Principle of Thermally Stimulated Discharge Currents

The Thermally Stimulated Discharge/Depolarization Currents (TSDC), or at a glance, Thermally Stimulated Currents (TSC) is one of the oldest destructive methods used for studying the mechanisms of polarization and depolarization within the dielectrics. It was firstly developed by Bucci and Fieschi [4] in 1964 while trying to obtain information related to dipolar relaxation and punctual defects in ionic crystals. The principle of the method is simple, encompassing the following steps:

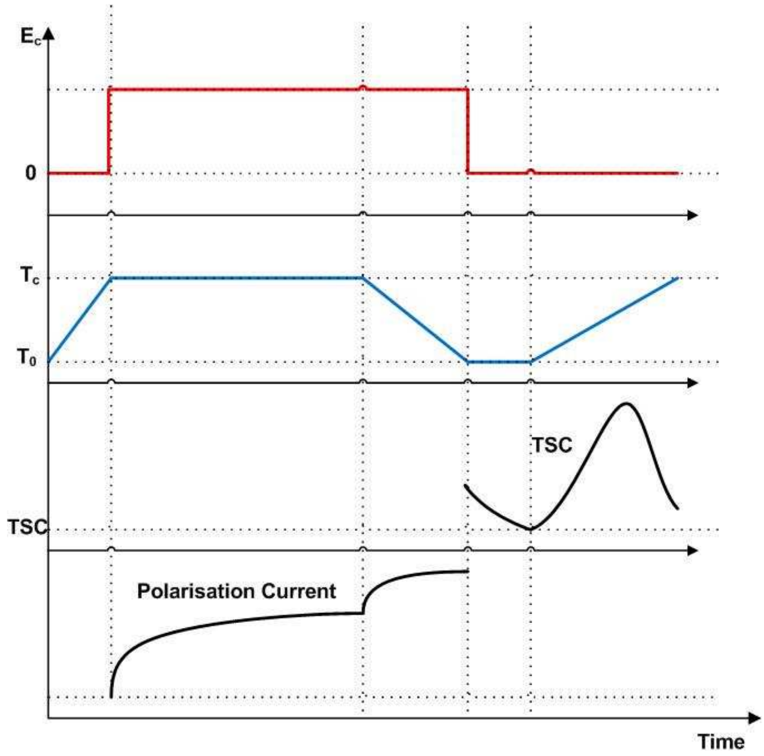

Figure 1 – TSDC's/TSC's principle

- The sample is sandwiched between two plated electrodes and than electrically conditioned at a fixed temperature, T_c, during a period of time t_c with the help of an electric field E_c; During this process different carriers are trapped;
- Under the presence of the electric field the sample is cooled down and short-circuited a certain time in order to freeze the polarized entities;
- Holding the sample in short-circuit, the temperature is increased linearly till a higher value;
- By heating the sample, the carriers in the bulk of the material are excited and thus the electrometer will measure the thermally stimulated current (TSC);
- The spectrum of the TSC is plotted against the temperature; the TSC curve may exhibit one or more peaks which are due to carriers detrapping; the movement direction of carriers towards the electrometer and their quantity is determining the TSC's polarity and intensity; The peaks may me less or more pronounced depending on phenomena's complexity;

The interpretation of the TSC curve allows the determination of a series of information related to relaxation time (τ), total quantity of detrapped charges and activation energy (E_a).

Materials and Method

Materials

The Cerium Ammonium (IV) Nitrate (CAN) and dimethylformamide (DMF) were all Merck reagents. Poly(Acrylonitrile-co-Acrylic Acid) [P(AN-co-AA)] (synthesized in the laboratory). Pyrrole (Py) was Aldrich reagent.

Preparation of Composites

P(AN-co-AA) was dissolved in dimethyl formamide (DMF). Conductive monomer (Py) [(i.e., 0.72, 1.44, 2.16, 2.88, 3.6 mmoles) was oxidatively polymerized on P(AN-co-AA) matrix in the presence of oxidant [Ce(IV)] to obtain conductive composite solutions. Then solvent casting process was applied to obtain composite films.

Results and Discussion
FTIR-ATR Analysis

The FTIR-ATR characterization of P(AN-co-AA)-PPy composite films was presented in Figure 1. Sequentially 2939 cm^{-1}, 2243 cm^{-1}, 1452 cm^{-1} and 1720 cm^{-1} peaks were related with CH bending, C≡N stretching and CH stretching of PAN and carboxyl (C=O) stretching of PAA. Furthermore, C=O stretching, the characteristic peak of DMF at 1660 cm^{-1} shifted to 1663 cm^{-1}. Moreover, C=O stretching of PAA segments shifted from 1720cm^{-1} to 1715cm^{-1} with the addition of rising PPy content into the composite films.

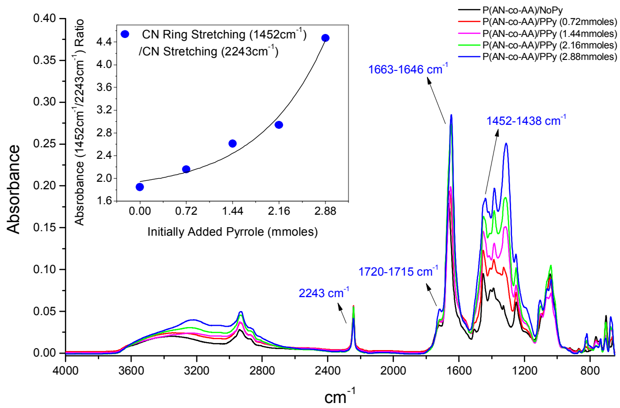

Figure 2. FTIR-ATR spectra of P(AN-co-AA)-PPy composite films

Furthermore, CN stretching vibration of PPy at 1452 cm^{-1} was observed in composite films. The results were consistent with the literature [4]. The ratio of the absorbance values of CN stretching of PPy to C≡N stretching of PAN segments was increasing as initially added Py was rising up. Thus, intermolecular interaction between PPy, P(AN-co-AA) and DMF could be seen form FTIR results (Figure 2).

Analysis of Thermally Stimulated Discharge/Depolarization Currents
The measuring protocol consisted in heating the sample at 323.15K (50°C). At this temperature, for 45 minutes, the sample was polarized at 250 V. While holding the sample under polarization field, the temperature was decreased at room temperature. The material was then short-circuited for 20 minutes, a period sufficient for freezing the polarized entities. Afterwards, the temperature in the oven was increased constantly from 312.15K (39°C) up to 393.15K (120°C) in order to measure the thermally stimulated discharge current [TSDC].

On the TSDC spectrum (Figure 3) two peaks, or relaxation regions, can be noticed. One at around 323.15K (50°C) and a second one at 363.15k (90°C). As it can be seen, the variation of the filler concentration in the polymeric matrix is not inducing a peak's shift neither for the lower temperatures nor for the higher ones. The TSDC currents are higher when increasing the quantity of conductive monomer (PPy), as presented in the Preparation of Composites section from 0.72 mmoles up to 3.16 mmoles. .

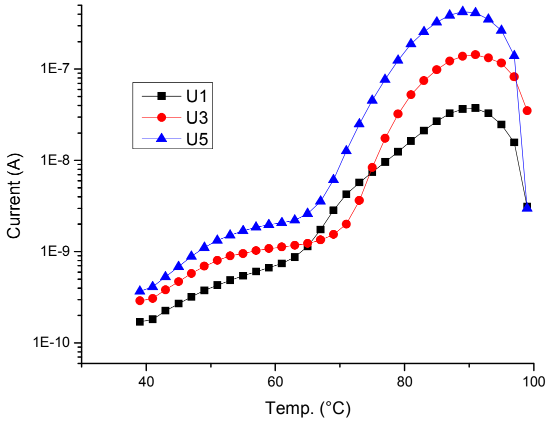

Figure 3. Thermally Stimulated Discharge/Depolarization Currents (TSDC) spectrum

We assumed that the first peak, at 323.15K (50°C), appeared due to the charges that were injected at the bulk of the material during the polarization and which are now detrapped when varying the temperature. The peaks at 323.15K (50°C) are appearing due to DMF solvent removal. As it can be observed on the TGA results, the composite films exhibit the decomposition peak at around 323.15K-333.15K (50-60 ^{o}C) due to the DMF removing as presented in our previous studies.[3] On the other hand, the second peak, at 363.15K (90°C), has material structural origins (practically, being observed when the glass transition temperature (Tg) is reached. As determined, the sampled employed in the study did show Tg at around 363.15K-378.15K (90-105 ^{o}C).

When referring to a classical insulating polymer, for sample PET, on the TSDC spectra one can also notice two peaks: one at temperatures around 323.15K (50°C), the other one at temperatures between 363.15K (90°C),and 373.15K (100°C), [5,6]. The first peak is due to the charges which were injected during the polarization, the second peak is assumed to appear when the glass transition temperature is reached. Practically, the difference between the insulators and the ICPs in relation to TSDC is a change of the temperature when the peak formed due to detrapped charges is appearing, and it is normal that in case of an ICP to be at lower temperatures. Practically, the charge carriers injected in case of the conducting materials need lower energies for being detrapped. If one is considering the energy band theory, for the conducting polymer the bandgap or the energy gap is more narrowed that in case of an insulator, and thus is easier for the polarized states to “jump” from the valency band up to conduction band.

Conclusions

FTIR-ATR spectroscopy results of composites showed the presence of PPy in the P(AN-co-AA) matrix indicating the successful reaction and dispersion of PPy particles on matrix by the use of Ce(IV). On the other side, the two peaks appearing on the TSDC spectra have different origins: space charge formation due to carriers injection during poling and structural origin and thus, it can be conclure that the charges injected have activation energies lower than the ones of charges existing in the bulk of the material during processing. More than that, the appearance of two peaks confirms the fact that we succeded in detrapping the most important part of charge carriers.

Acknowledgement: This paper was supported by the project PERFORM-ERA "Postdoctoral Performance for Integration in the European Research Area" (ID-57649), financed by the European Social Fund and the Romanian Government.

References

[1] Dhawan, S.K.; Singh, N.; Venkatachalam, S.: Shielding behaviour of conducting polymer-coated fabrics in X-band, W-band and radio frequency range, *Synthetic Metals*, **Vol.** 129 (2002), No., 3, pp. 261-267, (2002).

[2] Youngs, J. Lawrence, C.R., Treen, A.S., Stickland, T. Miah, M., Broadband dielectric spectroscopy of conducting polyaniline, 10.1049/ip-smt:19982102;

[3] Suat Cetiner, Marius Olariu, A.Sezai Sarac, Polymerization of Pyrrole Derivatives on Polyacrylonitrile Matrix, FTIR-ATR and Dielectric Spectroscopic Characterization of Composite Thin Films, Synthetic Metals, (2010), doi:10.1016/j.synthmet.2010.03.007

[4] Vanderschueren, J.: L'effet thermoélectret et les phénomènes de relaxation dans les polymères à l'état solide, Thèse de doctorat de l'Université – 1974.

[5] Olariu M. et. Al, Advanced composites from recycled polyethylene: Technology optimization via thermal step method, Management of Technological Changes, book 1, pages: 287-290, published: 2005;

[6] Olariu M. Et al, Space charge study via thermal step method and applications in new materials quality, Management of Technological Changes, book 1, pages: 291-296, published: 2005.

Materials and Applications for Sensors and Transducers II

10.4028/www.scientific.net/KEM.543

Thermally Stimulated Discharge Currents of Poly(acrylonitrile-co-acrylic Acid)-Polypyrrole Composites

10.4028/www.scientific.net/KEM.543.154

A New PSpice Implementation of a Three-Phase Induction Machine Model

Plopa Olga, Aradoaei Sebastian-Teodor, Ursan George-Andrei
Faculty of Electrical Engineering
“Gheorghe Asachi” Technical University of Iasi
Iasi, Romania
oplopa@tuiasi.ro, arsete@tuiasi.ro, agursan@tuiasi.ro

***Abstract*— The paper shows a new version of a three-phase model of the induction machine which can be implemented in PSpice program. The voltage equations and the flux expressions in the three-phase mathematical model are rewritten in a convenient form. After the analyzing of the previous implementations in PSpice, a simplified version of the equivalent electrical scheme was proposed. The computing capacity of the type E voltage sources was intensively used in order to reduce the number of nodes of the equivalent circuit. The proposed implementation can be designed as a subcircuit. The main program can call this subcircuit when needed. The proposed implementation proved to be fast and easy to use. No convergence issues were reported. It is extremely useful in a wide range of special situations which requires the use of three-phase model.**

Keywords—ac machine; bidirectional separator circuit; Park transformation

I. INTRODUCTION

In 2000, 1. 1929 - Fortescue’s paper on *Symmertical Components* [1]; and 2. 1929 - Park’ paper on *dq Transformation* (or Park transformation) [2] were voted the most important papers of the last 100 years [3].

The Park transformation had a special impact in the analysis of the three-phase electrical networks, but also of the AC machines, both asynchronous and synchronous.

In analysis of three-phase induction and synchronous machines, the Park transformation transfers three-phase stator and rotor quantities into a single rotating reference frame to eliminate the effect of time varying inductances. At the same time the number of equations that describe the machine's function is significantly reduced. The *d-q* model (two-phase model) is mainly used in steady state and transient conditions because it is simpler, more easily to implement and includes less equations. Using the *d-q* model is clearly advantageous especially if three-phase balanced voltage supply and machine parameters are identical for all three phases. The two-phase model is widely used in the analysis of AC machines [4] - [8], many authors even omit to specify this. The Matlab program (SimPowerSystem module) uses the *d-q* model in the analysis of electrical circuits containing AC machines.

978-1-7281-4011-7/19/$31.00 ©2019 IEEE

Although widespread, the two-phase model should be used with restraint in some cases. If the three-phase asynchronous machine is powered by a non-sinusoidal, unbalanced or asymmetrical three-phase system, the use of the *d-q* model in a classical manner is no longer possible. In these cases, [9] suggests the use of Park bidirectional transformation, which allows simultaneous both direct and reverse transformations of voltage and current through a single processing circuit. But the advantages of using the *d-q* model are diminished.

The three-phase model can be used without restrictions and can be considered a reference standard model for the other analysis methods.

In the case of an asymmetrical three-phase power supply or an asymmetrical machine (in the case of a defect), the three-phase model can be easily used. In these situations, the only model that leads to correct results is the natural model of the three-phase asynchronous machine, the three-phase model.

The three-phase model is a natural mathematical model that takes into account the phenomena in each phase and the interactions between stator and rotor phases as well. The number of equations is high, the parameters which characterize phases interactions are variable in time and the equation system is nonlinear. All these disadvantages led to an unpopular model, difficult to implement. However, in some circumstances using this model is mandatory.

The three-phase model allows the analysis of the operation of the three-phase asynchronous machine having the stator windings done in a star (with or without bound) or triangle connection. This is not possible in the two-phase system.

II. THREE-PHASE MODEL EQUATIONS

Lets consider the system of stator and rotor windings presented in Fig. 1. The complete notations of the quantities of interest (voltages, currents, flows) were presented only for the *a* stator winding (*sa*). The stator (m_{ss}), rotor (m_{rr}) and stator-rotor (m_{sr}=m_{rs}) mutual inductivities were also exemplified. We assume a stationary reference frame for the stator quantities and a rotating reference frame for the rotor quantities. The voltage equations of induction machine, expressed in a matrix form, are presented in (1):

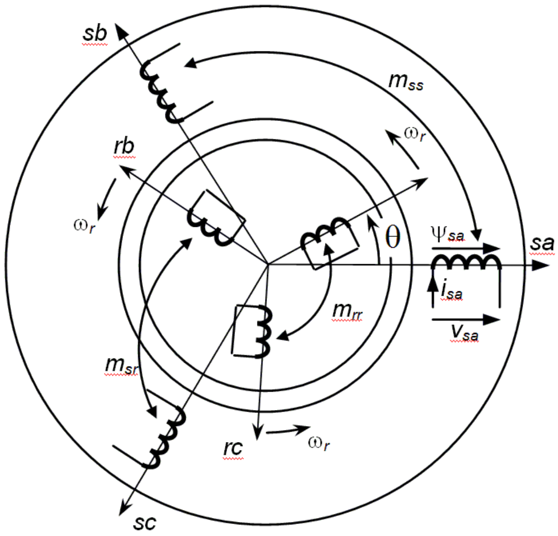

Fig. 1. Induction machine windings

$$[v]=[R][i]+\frac{\mathrm{d}}{\mathrm{d}t}\{[L][i]\} \tag{1}$$

where the inductance matrix is:

$$[L]=\begin{bmatrix}[L_{ss}] & [M_{sr}]\\ [M_{rs}] & [L_{rr}]\end{bmatrix} \tag{2}$$

We consider the rotor parameters related to the stator. Thus we have:

$$L_{os}=L_{or}=M_{sr}=M_{rs}=L_o \tag{3}$$

and the stator and rotor inductance matrices become:

$$[L_{ss}]=\begin{bmatrix} L_{\sigma s}+L_o & \frac{-L_o}{2} & \frac{-L_o}{2}\\ \frac{-L_o}{2} & L_{\sigma s}+L_o & \frac{-L_o}{2}\\ \frac{-L_o}{2} & \frac{-L_o}{2} & L_{\sigma s}+L_o \end{bmatrix} \tag{4}$$

$$[L_{rr}]=\begin{bmatrix} L_{\sigma r}+L_o & \frac{-L_o}{2} & \frac{-L_o}{2}\\ \frac{-L_o}{2} & L_{\sigma r}+L_o & \frac{-L_o}{2}\\ \frac{-L_o}{2} & \frac{-L_o}{2} & L_{\sigma r}+L_o \end{bmatrix} \tag{5}$$

and also, the mutual inductance matrices depending on angular position θ is:

$$[M_{sr}]=[M_{sr}]^T= L_o\cdot\begin{bmatrix} \cos\theta & \cos\left(\theta+\frac{2\pi}{3}\right) & \cos\left(\theta-\frac{2\pi}{3}\right)\\ \cos\left(\theta-\frac{2\pi}{3}\right) & \cos\theta & \cos\left(\theta+\frac{2\pi}{3}\right)\\ \cos\left(\theta+\frac{2\pi}{3}\right) & \cos\left(\theta-\frac{2\pi}{3}\right) & \cos\theta \end{bmatrix} \tag{6}$$

The voltage equations that characterize the stator windings have the form presented in (7):

$$\begin{aligned} v_{sa}&=R_s i_{sa}+L_{\sigma s}\frac{di_{sa}}{dt}+\frac{d\psi_{sa}}{dt}\\ v_{sb}&=R_s i_{sb}+L_{\sigma s}\frac{di_{sb}}{dt}+\frac{d\psi_{sa}}{dt}\\ v_{sc}&=R_s i_{sc}+L_{\sigma s}\frac{di_{sc}}{dt}+\frac{d\psi_{sa}}{dt} \end{aligned} \tag{7}$$

The derivative of the stator flow represents an induced voltage noted like in (8):

$$\frac{d\psi_{sa}}{dt}=v_{i\,sa}\,;\ \frac{d\psi_{sb}}{dt}=v_{i\,sb}\,;\ \frac{d\psi_{sc}}{dt}=v_{i\,sc} \tag{8}$$

so that voltage equations become:

$$\begin{aligned} v_{sa}&=R_s i_{sa}+L_{\sigma s}\frac{di_{sa}}{dt}+v_{i\,sa}\\ v_{sb}&=R_s i_{sb}+L_{\sigma s}\frac{di_{sb}}{dt}+v_{i\,sb}\\ v_{sc}&=R_s i_{sc}+L_{\sigma s}\frac{di_{sc}}{dt}+v_{i\,sc} \end{aligned} \tag{9}$$

The induced voltage expressions $v_{i\,sx}$, are intricate because the windings interaction is strongly dependent on the angular position θ:

$$\begin{aligned} v_{i\,sa}&=L_0\frac{d}{dt}\Big[i_{sa}-\frac{1}{2}i_{sb}-\frac{1}{2}i_{sc}+\cos\theta i_{ra}+\\ &\quad+\cos(\theta+\frac{2\pi}{3})i_{rb}+\cos(\theta-\frac{2\pi}{3})i_{rc}\Big]\\ v_{i\,sa}&=L_0\frac{di_{sa}}{dt}+L_0\frac{d}{dt}\Big[-\frac{1}{2}i_{sb}-\frac{1}{2}i_{sc}+\cos\theta i_{ra}+\\ &\quad+\cos(\theta+\frac{2\pi}{3})i_{rb}+\cos(\theta-\frac{2\pi}{3})i_{rc}\Big] \end{aligned}$$

$$v_{i\,sa}=L_0\frac{di_{sa}}{dt}+L_0\frac{d}{dt}\sum i^*_{sa} \tag{10}$$

$$v_{i\,sb} = L_0 \frac{d}{dt}\left[-\frac{1}{2}i_{sa} + i_{sb} - \frac{1}{2}i_{sc} + \cos(\theta - \frac{2\pi}{3})i_{ra} + \right.$$
$$\left. + \cos\theta i_{rb} + \cos(\theta + \frac{2\pi}{3})i_{rc}\right]$$
$$v_{i\,sb} = L_0 \frac{di_{sb}}{dt} + L_0 \frac{d}{dt}\left[-\frac{1}{2}i_{sa} - \frac{1}{2}i_{sc} + \right.$$
$$\left. \cos(\theta - \frac{2\pi}{3})i_{ra} + \cos\theta i_{rb} + \cos(\theta + \frac{2\pi}{3})i_{rc}\right]$$

$$v_{i\,sb} = L_0 \frac{di_{sb}}{dt} + L_0 \frac{d}{dt}\sum i_{sb}^{*} \tag{11}$$

$$v_{i\,sc} = L_0 \frac{d}{dt}\left[-\frac{1}{2}i_{sa} - \frac{1}{2}i_{sb} + i_{sc} + \right.$$
$$\left. + \cos(\theta + \frac{2\pi}{3})i_{ra} + \cos(\theta - \frac{2\pi}{3})i_{rb} + \cos\theta i_{rc}\right]$$
$$v_{i\,sc} = L_0 \frac{di_{sc}}{dt} + L_0 \frac{d}{dt}\left[-\frac{1}{2}i_{sa} - \frac{1}{2}i_{sb} + \right.$$
$$\left. + \cos(\theta + \frac{2\pi}{3})i_{ra} + + \cos(\theta - \frac{2\pi}{3})i_{rb} + \cos\theta i_{rc}\right]$$

$$v_{i\,sc} = L_0 \frac{di_{sc}}{dt} + L_0 \frac{d}{dt}\sum i_{sc}^{*} \tag{12}$$

Similarly, for the rotor quantities we can write:

$$\begin{aligned} v_{ra} &= R_r i_{ra} + L_{\sigma r}\frac{di_{ra}}{dt} + v_{i\,ra} \\ v_{rb} &= R_r i_{rb} + L_{\sigma r}\frac{di_{rb}}{dt} + v_{i\,rb} \\ v_{rc} &= R_r i_{rc} + L_{\sigma r}\frac{di_{rc}}{dt} + v_{i\,rc} \end{aligned} \tag{13}$$

$$v_{i\,ra} = L_0 \frac{d}{dt}\left[i_{ra} - \frac{1}{2}i_{rb} - \frac{1}{2}i_{rc} + \cos\theta i_{sa} + \right.$$
$$\left. + \cos(\theta - \frac{2\pi}{3})i_{sb} + \cos(\theta + \frac{2\pi}{3})i_{sc}\right]$$
$$v_{i\,ra} = L_0 \frac{di_{ra}}{dt} + L_0 \frac{d}{dt}\left[-\frac{1}{2}i_{rb} - \frac{1}{2}i_{rc} + \cos\theta i_{sa} + \right.$$
$$\left. + \cos(\theta - \frac{2\pi}{3})i_{sb} + \cos(\theta + \frac{2\pi}{3})i_{sc}\right]$$

$$v_{i\,ra} = L_0 \frac{di_{ra}}{dt} + L_0 \frac{d}{dt}\sum i_{ra}^{*} \tag{14}$$

$$v_{i\,rb} = L_0 \frac{d}{dt}\left[-\frac{1}{2}i_{ra} + i_{rb} - \frac{1}{2}i_{rc} + \right.$$
$$\left. + \cos(\theta + \frac{2\pi}{3})i_{sa} + \cos\theta i_{sb} + \cos(\theta - \frac{2\pi}{3})i_{sc}\right]$$
$$v_{i\,rb} = L_0 \frac{di_{rb}}{dt} + L_0 \frac{d}{dt}\left[-\frac{1}{2}i_{ra} - \frac{1}{2}i_{rc} + \right.$$
$$\left. + \cos(\theta + \frac{2\pi}{3})i_{sa} + \cos\theta i_{sb} + \cos(\theta - \frac{2\pi}{3})i_{sc}\right]$$

$$v_{i\,rb} = L_0 \frac{di_{rb}}{dt} + L_0 \frac{d}{dt}\sum i_{rb}^{*} \tag{15}$$

$$v_{i\,rc} = L_0 \frac{d}{dt}\left[-\frac{1}{2}i_{ra} - \frac{1}{2}i_{rb} + i_{rc} + \right.$$
$$\left. \cos(\theta - \frac{2\pi}{3})i_{sa} + \cos(\theta + \frac{2\pi}{3})i_{sb} + \cos\theta i_{sc}\right]$$
$$v_{i\,rc} = L_0 \frac{di_{rc}}{dt} + L_0 \frac{d}{dt}\left[-\frac{1}{2}i_{ra} - \frac{1}{2}i_{rb} + \right.$$
$$\left. \cos(\theta - \frac{2\pi}{3})i_{sa} + \cos(\theta + \frac{2\pi}{3})i_{sb} + \cos\theta i_{sc}\right]$$

$$v_{i\,rc} = L_0 \frac{di_{rc}}{dt} + L_0 \frac{d}{dt}\sum i_{rc}^{*} \tag{16}$$

III. PSPICE IMPLEMENTATION ANALIZE

Since the PSpice program analyzes the electrical circuits, the first step for implementing the voltage equations is to establish the equivalent electrical circuit for these equations. Voltage equations (9) and (13) are easy to implement in PSpice using ordinary circuit elements, a resistor and a coil.

In [9] an E type controlled voltage source E_{sx} or E_{rx} is added corresponding to the induced voltage $v_{i\,sx}$, $v_{i\,rx}$. Its value is calculated separately because the current flowing through L_0 is made of six components. The G type controlled current source G_{sx}, performs the weighted sum of the six currents. The only meaning of the E_{sx} source is to copy the voltage value obtained at the L_0 inductance terminals. Two distinct circuits are highlighted:

- a circuit equivalent to the voltage equation comprising a resistor, a coil and a voltage controlled source;
- an additional circuit for calculating of the voltage induced by the six currents in the considered winding.

This paper proposes a simplification of the equivalent electrical scheme. Analyzing the circulation of currents presented in Fig. 2, the structure presented in [9] can be simplified, reaching a single equivalent circuit as presented in Fig. 3.

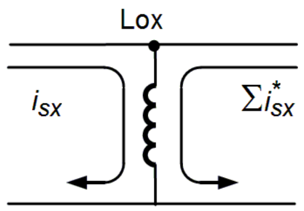

Fig. 2. The currents' circulation through mutual inductance

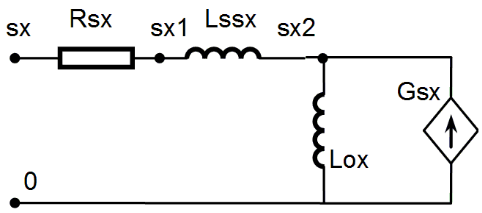

Fig. 3. Stator voltage equation equivalent circuit

The current-controlled current source *Gsx* calculates the weighted sum of the five currents that cross the other windings of the AC machine. The advantages of this structure are:

- by the disappearance of the second circuit, we have one less node for each phase;
- the voltage controlled source which copies the voltage value obtained at the L_0 inductance terminals disappears.
- the volume of calculation realized by the current-controlled current source *Gsx* is reduced.

The correspondence between the electrical quantities in the equations and the quantities calculated by PSpice is presented in (17).

$$\begin{array}{lcl} v_{sx} & \leftrightarrow & \mathrm{V(sx)} \\ i_{sx} & \leftrightarrow & \mathrm{I(Rsx)} \\ v_{i\,sx} & \leftrightarrow & \mathrm{V(sx2)} \end{array} \tag{17}$$

A characteristic three-phase implementation of the model is a more complex expression of electromagnetic torque. The calculations are carried out by the controlled current source *Gte*. In addition, the angular position of the rotor θ has to be calculated like in [9]:

$$\theta(t) = \theta_0 + \int_0^t \omega_r \mathrm{d}t \tag{18}$$

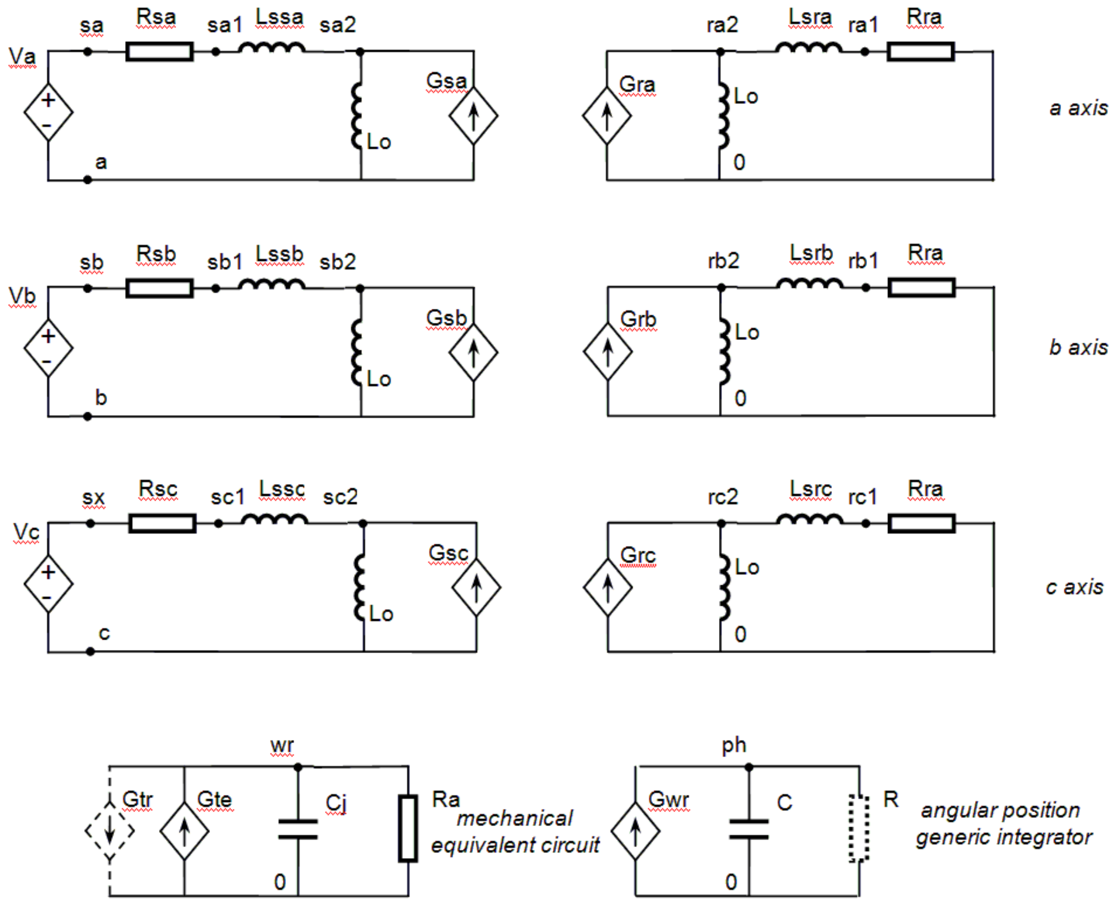

Fig. 4. Equivalent circuits for PSpice implementation.

where the corresponding generic integrator is shown in Fig. 4 together with the other equivalent circuits [10].

The correspondence between the mechanical quantities and the quantities calculated by PSpice is:

$$\begin{array}{lllllll} t_e & \leftrightarrow & \mathrm{I(Gte)} & \omega_r & \leftrightarrow & \mathrm{V(wr)} \\ t_r & \leftrightarrow & \mathrm{I(Gtr)} & \theta & \leftrightarrow & \mathrm{V(ph)} \end{array} \quad (19)$$

IV. SIMULATATION RESULTS

In order to verify the correctness of the obtained in this paper results, the proposed modified model was used to simulate the operation of a three-phase asynchronous machine having a nominal power of 5 kW, connected to the power network in the star connection. The machine is characterized by the following parameters:

$$\begin{array}{lll} P_n = 5\,\mathrm{kW} & p = 1 & \\ U_1 = 380\ \mathrm{V} & f_1 = 50\ Hz & \mathrm{Y}\ conn. \\ R_s = 1.5\,\Omega & R_r^{'} = 1.3\,\Omega & \\ L_0 = 100\ \mathrm{mH} & L_{\sigma s} = 8\ \mathrm{mH} & L_{\sigma r}^{'} = 7\ \mathrm{mH} \\ J = 25\mathrm{g}\cdot\mathrm{m}^2 & F_\alpha = 1\cdot 10^{-3}\ \mathrm{N}\cdot\mathrm{m}\cdot\mathrm{s/rad.}; & \end{array}$$

The simulation was performed using PSpice 16.0 ver. running on a computer with following characteristics: CPU - Intel Pentium E2180, RAM - 2 GB, HDD - 180 GB.

First it was considered the symmetrical power supply of the machine with the voltages $U_{1a\,m} = 311\mathrm{V}$; $U_{1b\,m} = 311\mathrm{V}$; $U_{1c\,m} = 311\mathrm{V}$.

The starting operation regime was taken into the consideration because it is the most complex transient mode of the induction machine. As can be seen in Fig. 5, the start ends after approx. 0.45 s. After that follows the steady state (up to 1s). There have been shown two representative parameter variations: angular rotor speed versus time in Fig. 5 and rotor currents versus time in Fig. 6.

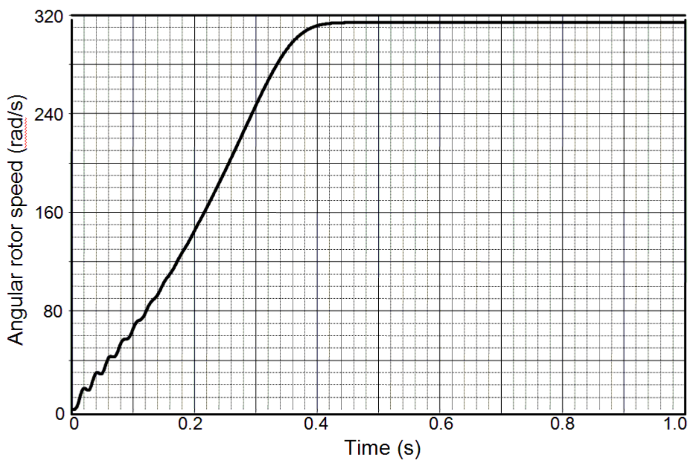

Fig. 5. Angular rotor speed in starting operation - symmetrical power supply.

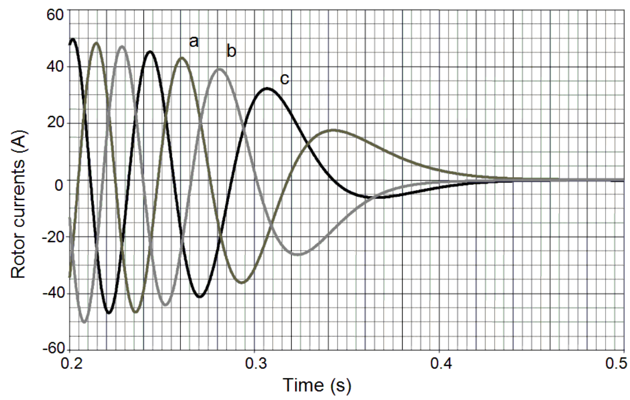

Fig. 6. Rotor currents in starting operation - symmetrical power supply.

The obtained results are identical (in the smallest de-tails) to those obtained using the model from [9]. The comparative synthetic results are presented below:

The old model [9]:

- Step time – 0.1 ms;
- Total job time – 8.19 s;
- Data file – 6329 kB.

The proposed model:

- Step time – 0.1 ms;
- Total job time – 6.88 s;
- Data file – 4685 kB.

Although the working conditions are the same, the new model is proven to be superior by the shorter simulation time and the smaller size of the data file.

Further it has been considered asymmetrical power supply of the machine with the voltages $U_{1a\,m} = 155\mathrm{V}$; $U_{1b\,m} = 311\mathrm{V}$; $U_{1c\,m} = 311\mathrm{V}$.

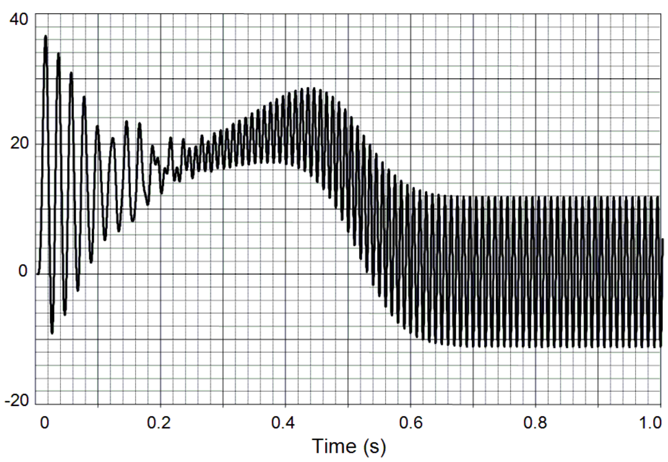

Fig. 7. Electromagnetic torque in starting operation - asymmetrical power supply.

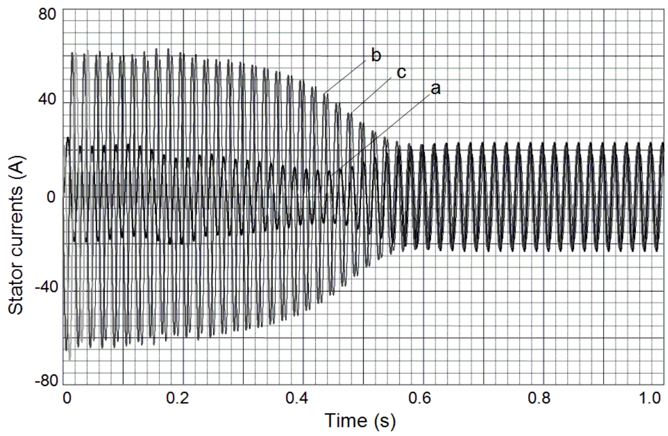

Fig. 8. Rotor currents in starting operation - asymmetrical power supply.

There have been shown two representative parameter variations: electromagnetic torque versus time in Fig. 7 and rotor currents versus time in Fig. 8. The obtained results are also identical to those obtained using the mod-el from [9]. The comparative synthetic results are presented below:

The old model [9]:

- Step time – 0.1 ms;
- Total job time – 8.14 s;
- Data file – 6329 kB.

The proposed model:

- Step time – 0.1 ms;
- Total job time – 6.97 s;
- Data file – 4685 kB.

The same observations as for the symmetrical power supply of the machine can be applied.

V. Conclusions

This paper proposes a simplification of the equivalent electrical circuit used for the implementation in PSpice. By analyzing the flow of currents, the structure presented in [9] can be simplified, reaching a single equivalent circuit for a phase and an armature.

Only one current-controlled source *Gsx* is used to supply the mutual inductance L_0. It calculates the weighted sum of the five currents that cross the other windings of the AC machine.

The advantages of this structure are multiple: by the disappearance of the second circuit, one node is saved for each phase and armature, in total six nodes; the voltage controlled source which copies the voltage value obtained at the L_0 inductance terminals disappears; the volume of calculations performed by the current-controlled source *Gsx* is reduced; the duration of the simulation process decreases.

References

[1] C.L. Fortescue, Method of Symmetrical Coordinates Applied to the Solution of Polyphase Networks, Trans. AIEE, pt. II, vol. 37, pp. 1027–1140, 1929

[2] R. Park, “Two reaction theory of synchronous machines,” Transactions of the AIEE, v. 48, p. 716-730, 1929

[3] G. Heydt, S. Venkata, and N. Balijepalli, “High impact papers in power engineering, 1900-1999, NAPS, 2000.

[4] Tripti Rai, Prashant Debre, Generalized Modeling Model of Three Phase Induction Motor, 2016 International Conference on Energy Efficient Technologies for Sustainability (ICEETS), 7-8 April 2016, Nagercoil, India

[5] L. Cociu, C.G. Haba, V.R. Cociu, Particularities of Park Transformationin Special Cases, Proceedings of the 7th International Symposium Advanced Topics in Electrical Engineering, 12-14 May 2011 Bucharest, Romania, p.455-460

[6] L. Punit Ratnani, A.G. Thosar, Mathematical Modelling of an 3 Phase Induction Motor Using MATLAB/Simulink, International Journal Of Modern Engineering Research (IJMER), Vol. 4 | Iss. 6| June. 2014 pp 62-67

[7] L. Cociu, V.R. Cociu, “On the Park Transform in Case of Induction Machine Nonsinusoidal Supply” 7th International Conference on Electromechanical and Power Systems SIELMEN 2009, Iasi, vol 2, pp. 299-303, oct. 2009.

[8] V.R. Cociu and L. Cociu, “Symmetrical Components Method in Induction Machine Behavior Analisis”. Bul. Inst. Politehnic, Iasi, LX(LXIV), 4, Electrot., Energ., Electron., 23-38 (2014).

[9] L. Cociu, V.R. Cociu, An Optimized Pspice Implementation of the Three+Phase Induction Machine Model, Bul.Inst.Polit. Iaşi, Tom LVII(LXI), fasc. 3, (Electrotehnică, Energetică, Electronică), pp.(103-112), 2011

[10] O. Justus, “Dynamisches Verhalten elektrischer Maschinen. Eine Einfuhrung in die numerische Modellierung mit PSPICE”, Vieweg & Sohn Verlagsgesellschaft, Braunschweig/Wiesbaden, 1993.